THE ASTRONOMICAL JOURNAL

PUBLISHED BY THE AMERICAN INSTITUTE OF PHYSICS
FOR THE AMERICAN ASTRONOMICAL SOCIETY

VOLUME 65 1960 February ~ No. 1276 NUMBER 1

H-Line Profiles at High Galactic Latitudes*

W. C. Erickson, *Carnegie Institution of Washington, Washington, D. C., and Convair Scientific Research Laboratory, San Diego, California*

AND

H. L. Helfer, *Carnegie Institution of Washington, Washington, D. C., and University of Rochester, Rochester, New York*

(Received November 18, 1959)

As a convenience for other *H*-line observers, we are presenting data on the *H*-line profiles at high galactic latitudes. These are profiles of moderate accuracy obtained in a survey of high-latitude hydrogen. A map of the distribution of galactic hydrogen is presented.

INTRODUCTION

OBSERVATIONS of neutral hydrogen have been obtained with the 54 channel *H*-line receiver and the Wurzburg antenna of the Carnegie Institution of Washington. This system has been described previously (Helfer and Tatel 1955; Tatel *et al.* 1956–57). *H*-line profiles have been observed at 10°-longitude intervals along the ±20°, ±30° and ±40° parallels of galactic latitude; at 20°-intervals along the ±50° and +60° parallels; at 40°-intervals along the ±70° and ±80° parallels, and at the poles. In addition, the $l^{\mathrm{I}}=150°$–$330°$ meridian has been observed at 10°-intervals. Approximately two dozen observations have been taken at points near the galactic plane in order to correlate these observations with the Leiden survey (Muller and Westerhout 1957). The beam width of the Wurzburg antenna was about 2°. The observations were taken in two series, one series during the summer of 1957, and other series during January, 1958. The video frequency bandwidth of the receiver is 12 kc/sec. The profiles consist of averages of from two to 18 scans with integration times from 4.8 to 7.5 minutes.

ACCURACY OF DATA

The accuracy obtainable with the Carnegie multichannel receiver is quite optional and can be changed to suit the observer's needs. Most of the profiles given in this paper were obtained with only moderate accuracy. When interesting features were found, higher accuracy profiles were obtained. The input noise of the receiver was approximately 1000°K during these observations. The output fluctuation level has been studied, and is entirely consistent with the input noise, the integration time, and the bandwidth. This output fluctuation level is approximately ±2°K if a time constant of 4.8 minutes is employed. Our results are thus of comparable accuracy to those obtained by any other observer undertaking a large observational program. Signals greater than 4°K and of moderately narrow bandwidth are reliably detected. Our base line varies from time to time by several degrees K. This is due primarily to differences in the matching of the antenna feed under conditions of dew or frost. Therefore, we cannot confirm or dispute the existence of the broad, low-intensity *H*-line wings reported by the Leiden group (van de Hulst 1958; van Woerden *et al.* 1957).† Fortunately, this situation is improving, and profiles obtained by the Carnegie group more recently are not subject to this difficulty. Other sources of base line unsteadiness may be local interference or possible side lobes of the antenna pattern in the direction of large aggregations

---

* This research has been supported in part by funds from the Air Force Office of Scientific Research.

† Helfer, Savedoff and Burke have recently provisionally confirmed the existence of the broad 2°K features suggested by the profiles at $l^{\mathrm{I}}=90°$, $b=+70°$ and $l^{\mathrm{I}}=150°$, $b=+70°$. They have observed the *H*-line profile over a frequency range of 2 mc/sec near H_0 with an accuracy of approximately ±0.5°K. They find some evidence for a signal of 2°K intensity about 40–50 km/sec wide.

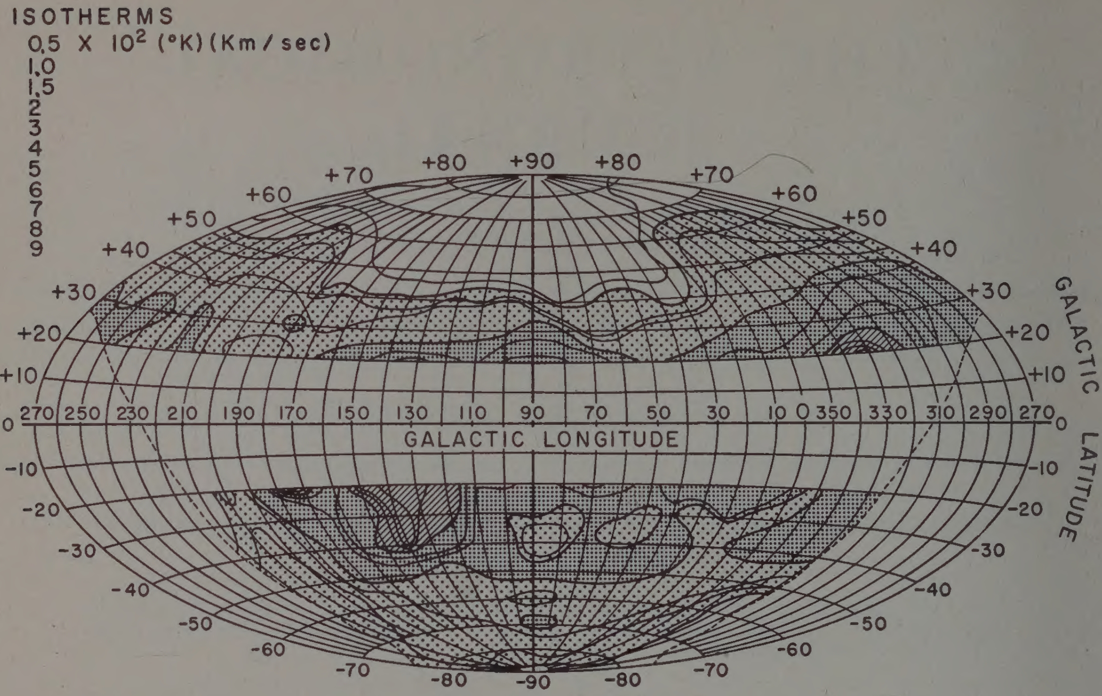

FIG. 1. Total amount of neutral hydrogen. The units (°K) (km/sec) may be converted to number of H atoms per cm² through multiplication by approximately 2×10^{18}.

of hydrogen near the galactic plane. However, our profiles have been examined for traces of signals at frequencies corresponding to the maxima of profiles obtained at adjacent points near the galactic plane. No signals at these frequencies have been found. In this respect it should be noted that the Wurzburg is a deep dish and very conservatively illuminated. Its side-lobe levels are too low to be easily measured.

The frequency width of our profiles is about 1 Mc/sec or 200 km/sec. Profiles are scanned with channel settings 4 km/sec apart. The operating frequencies are then modified, and intermediate points are interwoven. Therefore, alternate points given in the following graphs are entirely independent, having been obtained during different scans. Our method of data reduction was improved during this work. During some of the early observations, the data were not completely reduced for the entire width of the scan. However, we have examined original data at frequencies beyond those given in the accompanying graphs.

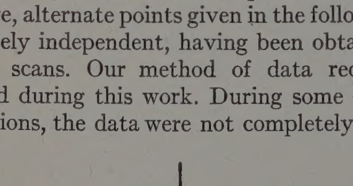

FIG. 2. The intensity and velocity scales for Fig. 3.

The observing frequency was determined by three independent methods. First, the frequencies of each of the local oscillators and the IF channels were determined and the observing frequency was calculated; Second, a crystal controlled auxiliary oscillator was constructed at a frequency which could be compared with WWV. This oscillator, having a harmonic near 1420 Mc/sec, was turned on periodically in order to broadcast a narrow-band signal to the dish. The output corresponding to this well-determined frequency was then recorded. Third, many accurate profiles taken near the galactic plane were compared with the Leiden survey (Muller and Westerhout 1957). Reduction of the profiles to the local standard of rest was made by use of the Lund Observatory Tables (1956).

During the course of the work the receiver was greatly improved. During 1957 there was some frequency modulation of the local oscillator which caused a sharp gradient of antenna temperature vs frequency to be blurred. We attempted to repeat all sharp features in 1958, after the defect had been corrected. In comparing 1958 to 1957 data, we often notice that peaks are slightly sharper and higher in the 1958 records. Otherwise, in almost all cases re-run features have reproduced very well. A few exceptions to this are noted

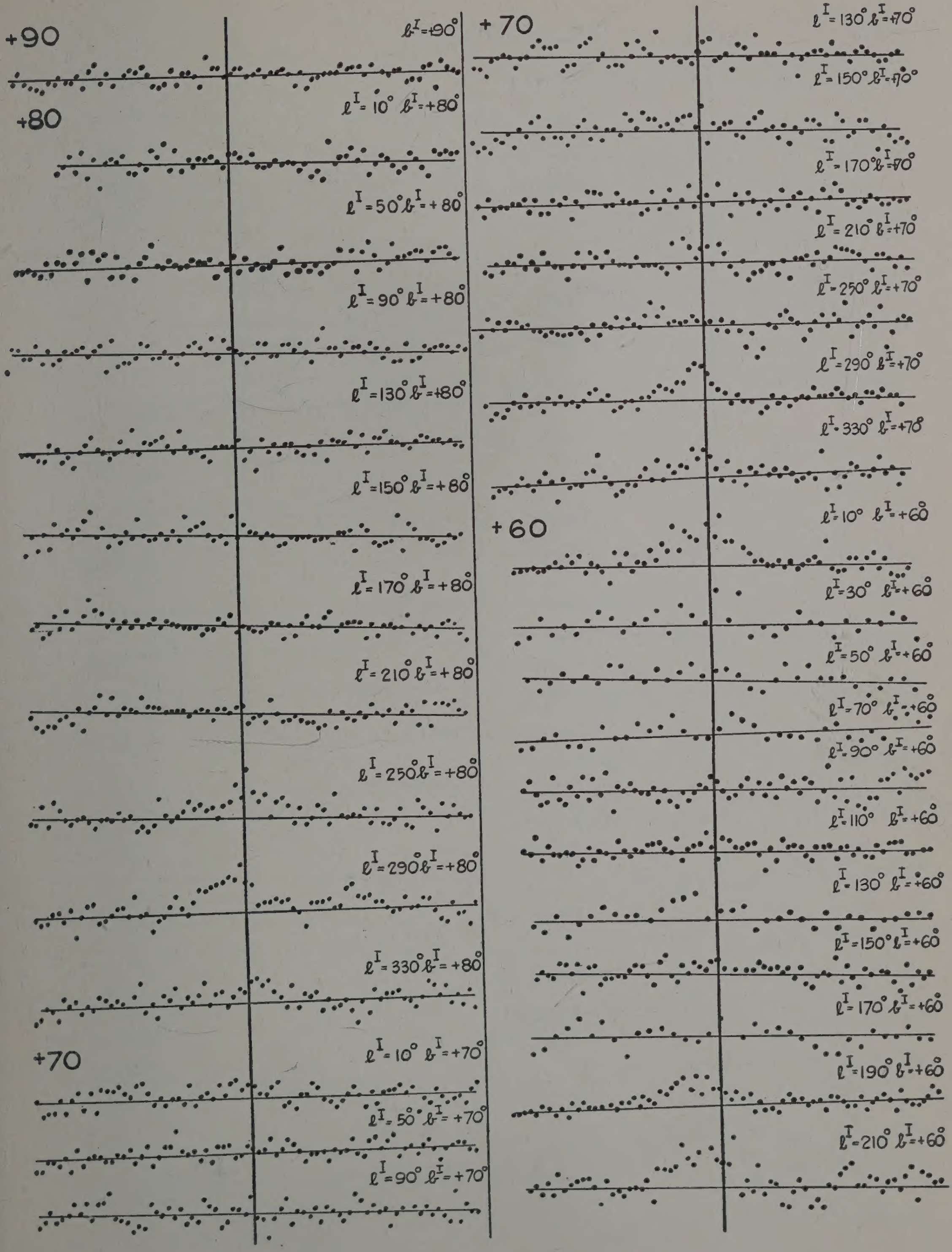

(a)

FIG. 3. The observed *H*-line profiles [parts (*b*)–(*l*) on following pages].

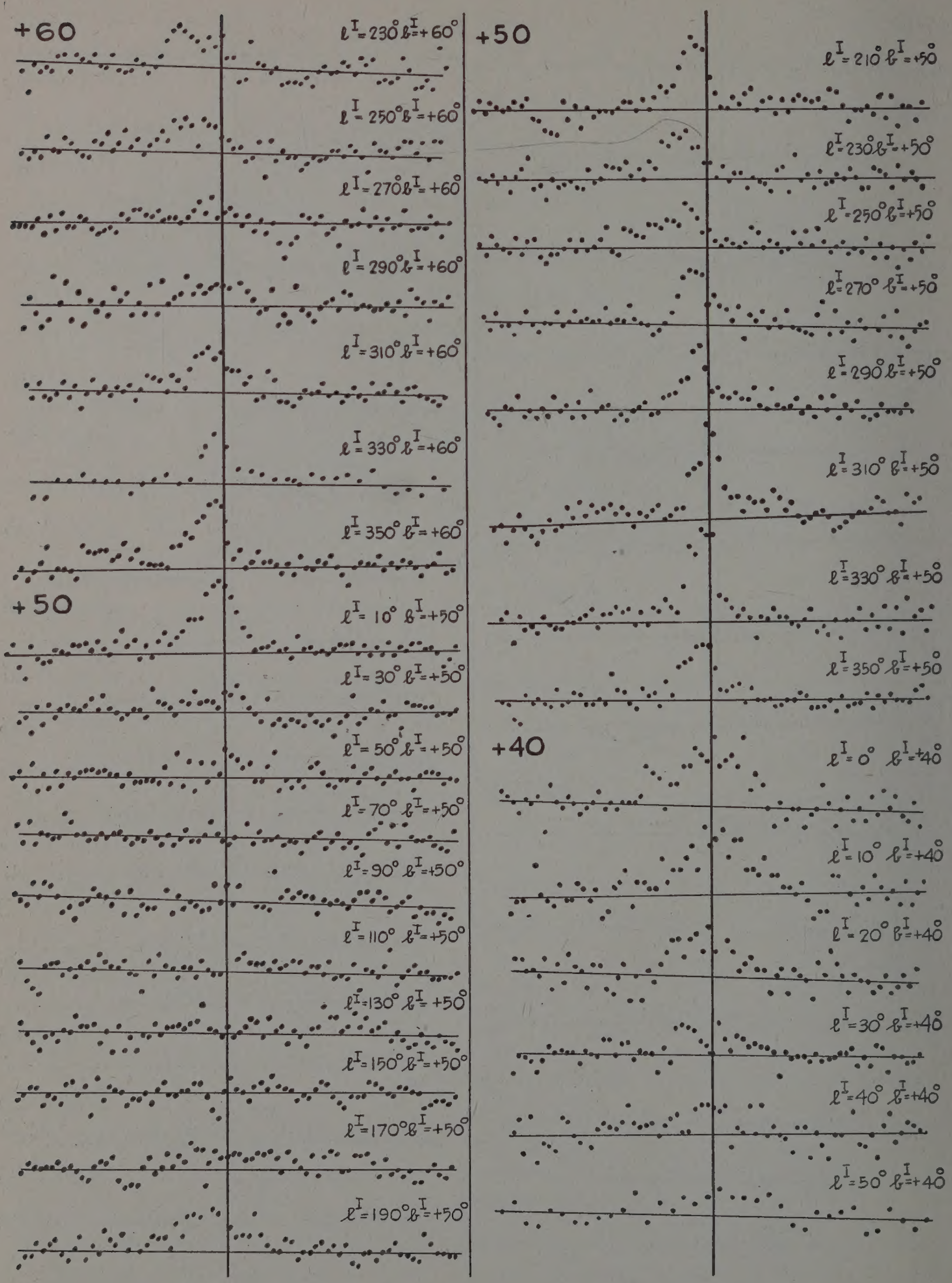
+60
lI = 230° bI = +60°
lI = 250° bI = +60°
lI = 270° bI = +60°
lI = 290° bI = +60°
lI = 310° bI = +60°
lI = 330° bI = +60°
lI = 350° bI = +60°
+50
lI = 10° bI = +50°
lI = 30° bI = +50°
lI = 50° bI = +50°
lI = 70° bI = +50°
lI = 90° bI = +50°
lI = 110° bI = +50°
lI = 130° bI = +50°
lI = 150° bI = +50°
lI = 170° bI = +50°
lI = 190° bI = +50°
+50
lI = 210° bI = +50°
lI = 230° bI = +50°
lI = 250° bI = +50°
lI = 270° bI = +50°
lI = 290° bI = +50°
lI = 310° bI = +50°
lI = 330° bI = +50°
lI = 350° bI = +50°
+40
lI = 0° bI = +40°
lI = 10° bI = +40°
lI = 20° bI = +40°
lI = 30° bI = +40°
lI = 40° bI = +40°
lI = 50° bI = +40°

(b)

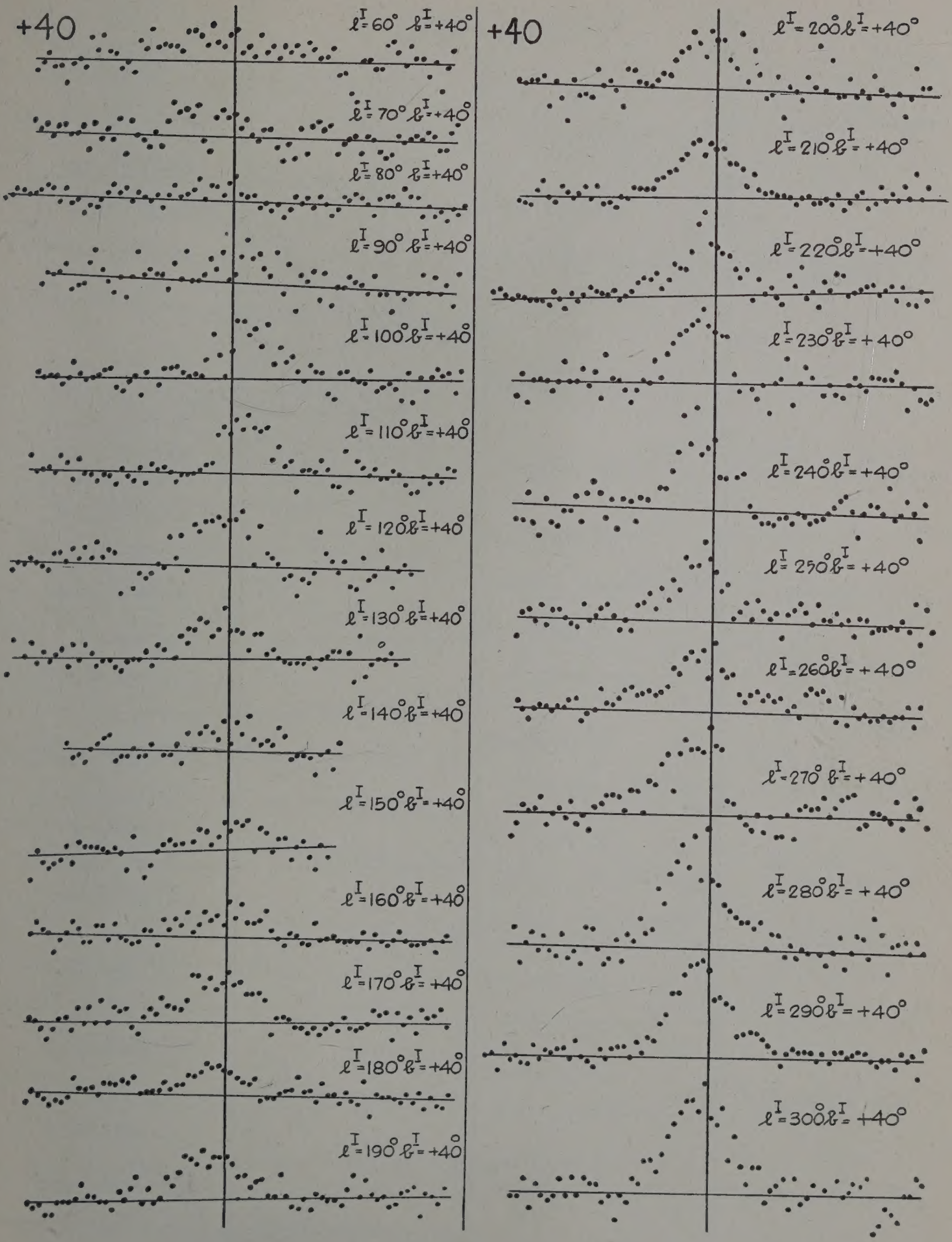
+40
lI = 60° bI = +40°
lI = 70° bI = +40°
lI = 80° bI = +40°
lI = 90° bI = +40°
lI = 100° bI = +40°
lI = 110° bI = +40°
lI = 120° bI = +40°
lI = 130° bI = +40°
lI = 140° bI = +40°
lI = 150° bI = +40°
lI = 160° bI = +40°
lI = 170° bI = +40°
lI = 180° bI = +40°
lI = 190° bI = +40°
+40
lI = 200° bI = +40°
lI = 210° bI = +40°
lI = 220° bI = +40°
lI = 230° bI = +40°
lI = 240° bI = +40°
lI = 250° bI = +40°
lI = 260° bI = +40°
lI = 270° bI = +40°
lI = 280° bI = +40°
lI = 290° bI = +40°
lI = 300° bI = +40°

(c)

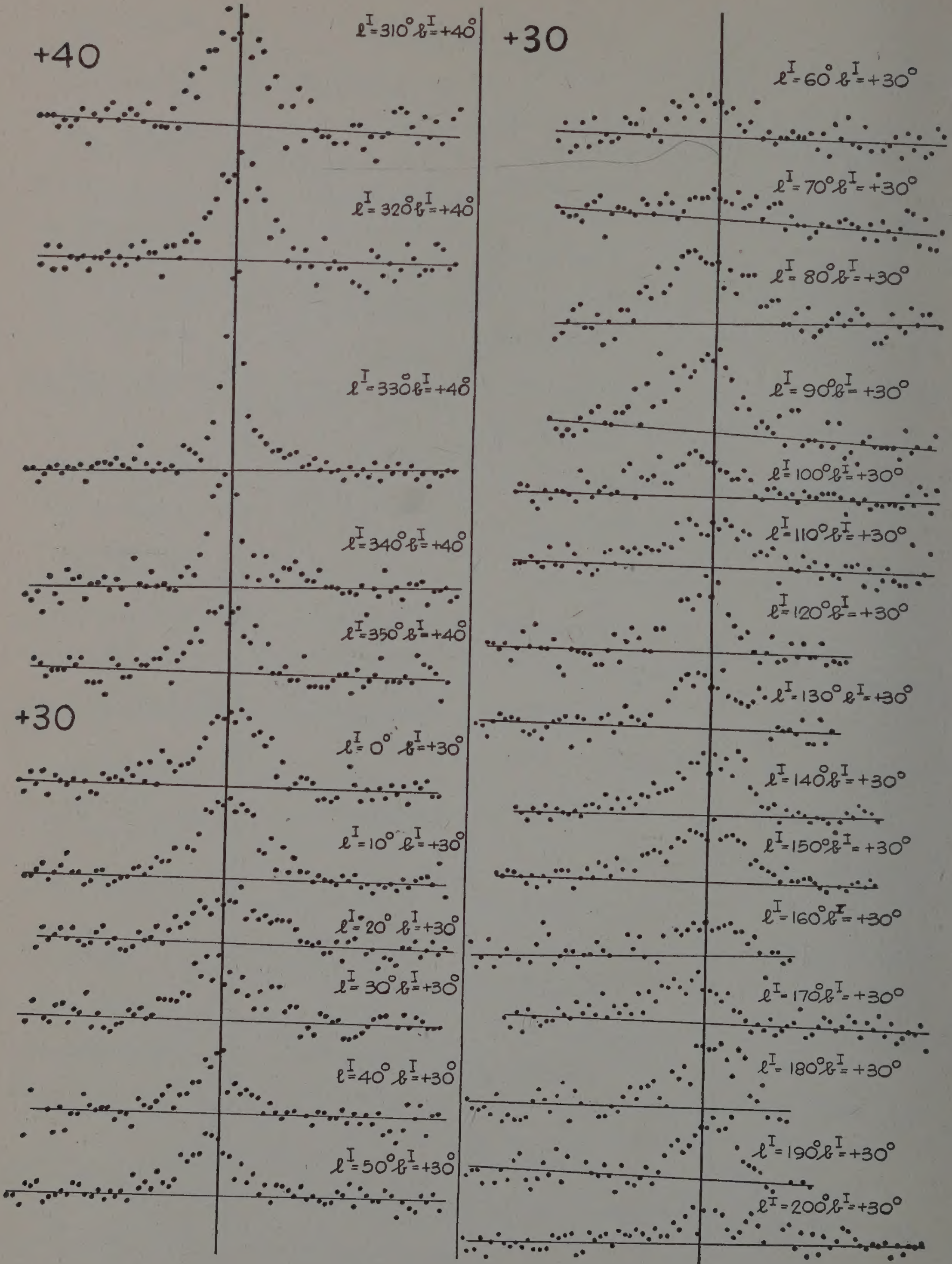
+40
l^{I}=310° b^{I}=+40°
l^{I}=320° b^{I}=+40°
l^{I}=330° b^{I}=+40°
l^{I}=340° b^{I}=+40°
l^{I}=350° b^{I}=+40°
+30
l^{I}=0° b^{I}=+30°
l^{I}=10° b^{I}=+30°
l^{I}=20° b^{I}=+30°
l^{I}=30° b^{I}=+30°
l^{I}=40° b^{I}=+30°
l^{I}=50° b^{I}=+30°
+30
l^{I}=60° b^{I}=+30°
l^{I}=70° b^{I}=+30°
l^{I}=80° b^{I}=+30°
l^{I}=90° b^{I}=+30°
l^{I}=100° b^{I}=+30°
l^{I}=110° b^{I}=+30°
l^{I}=120° b^{I}=+30°
l^{I}=130° b^{I}=+30°
l^{I}=140° b^{I}=+30°
l^{I}=150° b^{I}=+30°
l^{I}=160° b^{I}=+30°
l^{I}=170° b^{I}=+30°
l^{I}=180° b^{I}=+30°
l^{I}=190° b^{I}=+30°
l^{I}=200° b^{I}=+30°

(d)

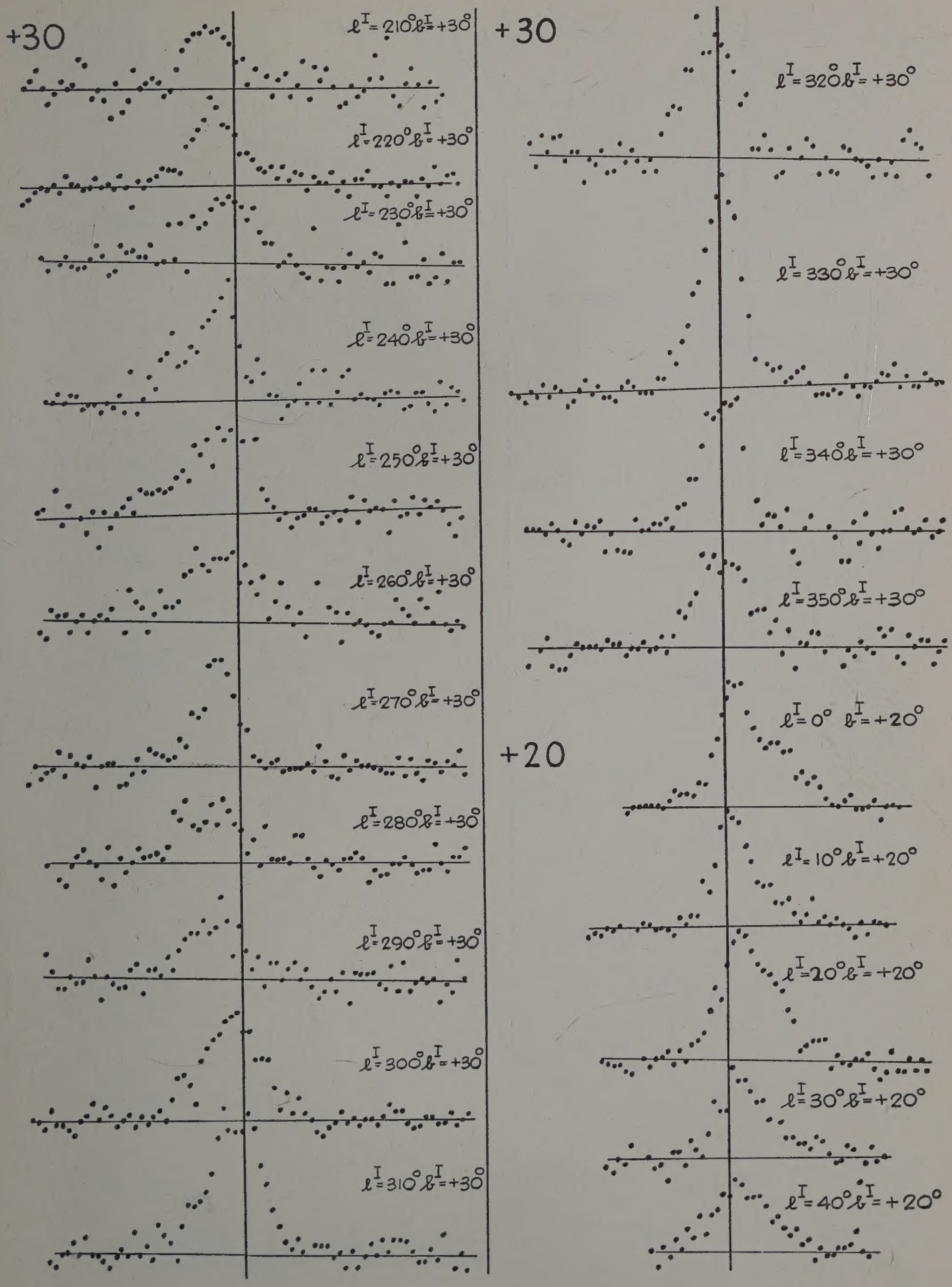
+30
$l^{I}=210^\circ$ $b^{I}=+30^\circ$
$l^{I}=220^\circ$ $b^{I}=+30^\circ$
$l^{I}=230^\circ$ $b^{I}=+30^\circ$
$l^{I}=240^\circ$ $b^{I}=+30^\circ$
$l^{I}=250^\circ$ $b^{I}=+30^\circ$
$l^{I}=260^\circ$ $b^{I}=+30^\circ$
$l^{I}=270^\circ$ $b^{I}=+30^\circ$
$l^{I}=280^\circ$ $b^{I}=+30^\circ$
$l^{I}=290^\circ$ $b^{I}=+30^\circ$
$l^{I}=300^\circ$ $b^{I}=+30^\circ$
$l^{I}=310^\circ$ $b^{I}=+30^\circ$
+30
$l^{I}=320^\circ$ $b^{I}=+30^\circ$
$l^{I}=330^\circ$ $b^{I}=+30^\circ$
$l^{I}=340^\circ$ $b^{I}=+30^\circ$
$l^{I}=350^\circ$ $b^{I}=+30^\circ$
+20
$l^{I}=0^\circ$ $b^{I}=+20^\circ$
$l^{I}=10^\circ$ $b^{I}=+20^\circ$
$l^{I}=20^\circ$ $b^{I}=+20^\circ$
$l^{I}=30^\circ$ $b^{I}=+20^\circ$
$l^{I}=40^\circ$ $b^{I}=+20^\circ$

(e)

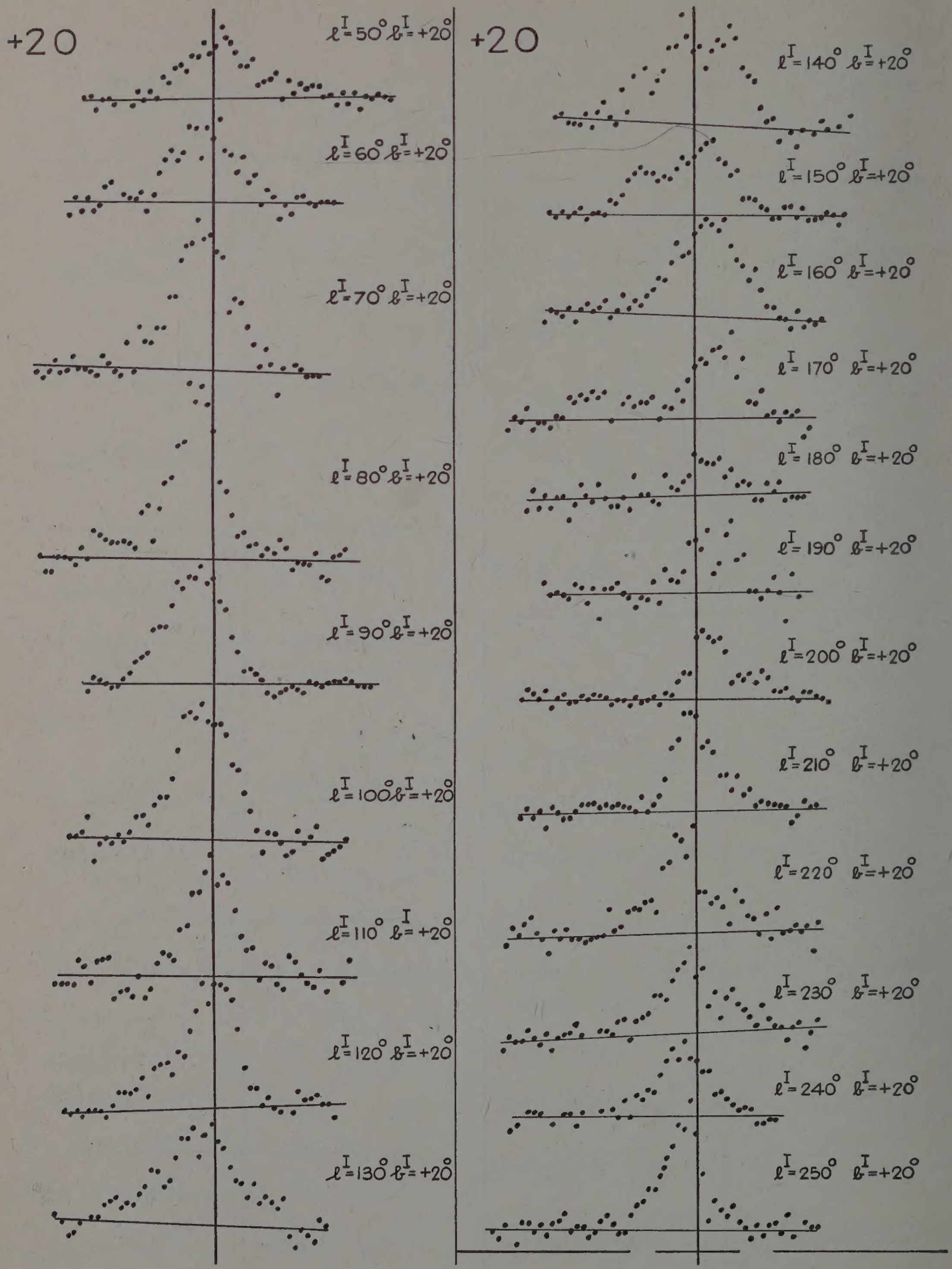
+20
$l^{I}=50^\circ$ $b^{I}=+20^\circ$
$l^{I}=60^\circ$ $b^{I}=+20^\circ$
$l^{I}=70^\circ$ $b^{I}=+20^\circ$
$l^{I}=80^\circ$ $b^{I}=+20^\circ$
$l^{I}=90^\circ$ $b^{I}=+20^\circ$
$l^{I}=100^\circ$ $b^{I}=+20^\circ$
$l^{I}=110^\circ$ $b^{I}=+20^\circ$
$l^{I}=120^\circ$ $b^{I}=+20^\circ$
$l^{I}=130^\circ$ $b^{I}=+20^\circ$
+20
$l^{I}=140^\circ$ $b^{I}=+20^\circ$
$l^{I}=150^\circ$ $b^{I}=+20^\circ$
$l^{I}=160^\circ$ $b^{I}=+20^\circ$
$l^{I}=170^\circ$ $b^{I}=+20^\circ$
$l^{I}=180^\circ$ $b^{I}=+20^\circ$
$l^{I}=190^\circ$ $b^{I}=+20^\circ$
$l^{I}=200^\circ$ $b^{I}=+20^\circ$
$l^{I}=210^\circ$ $b^{I}=+20^\circ$
$l^{I}=220^\circ$ $b^{I}=+20^\circ$
$l^{I}=230^\circ$ $b^{I}=+20^\circ$
$l^{I}=240^\circ$ $b^{I}=+20^\circ$
$l^{I}=250^\circ$ $b^{I}=+20^\circ$

(f)

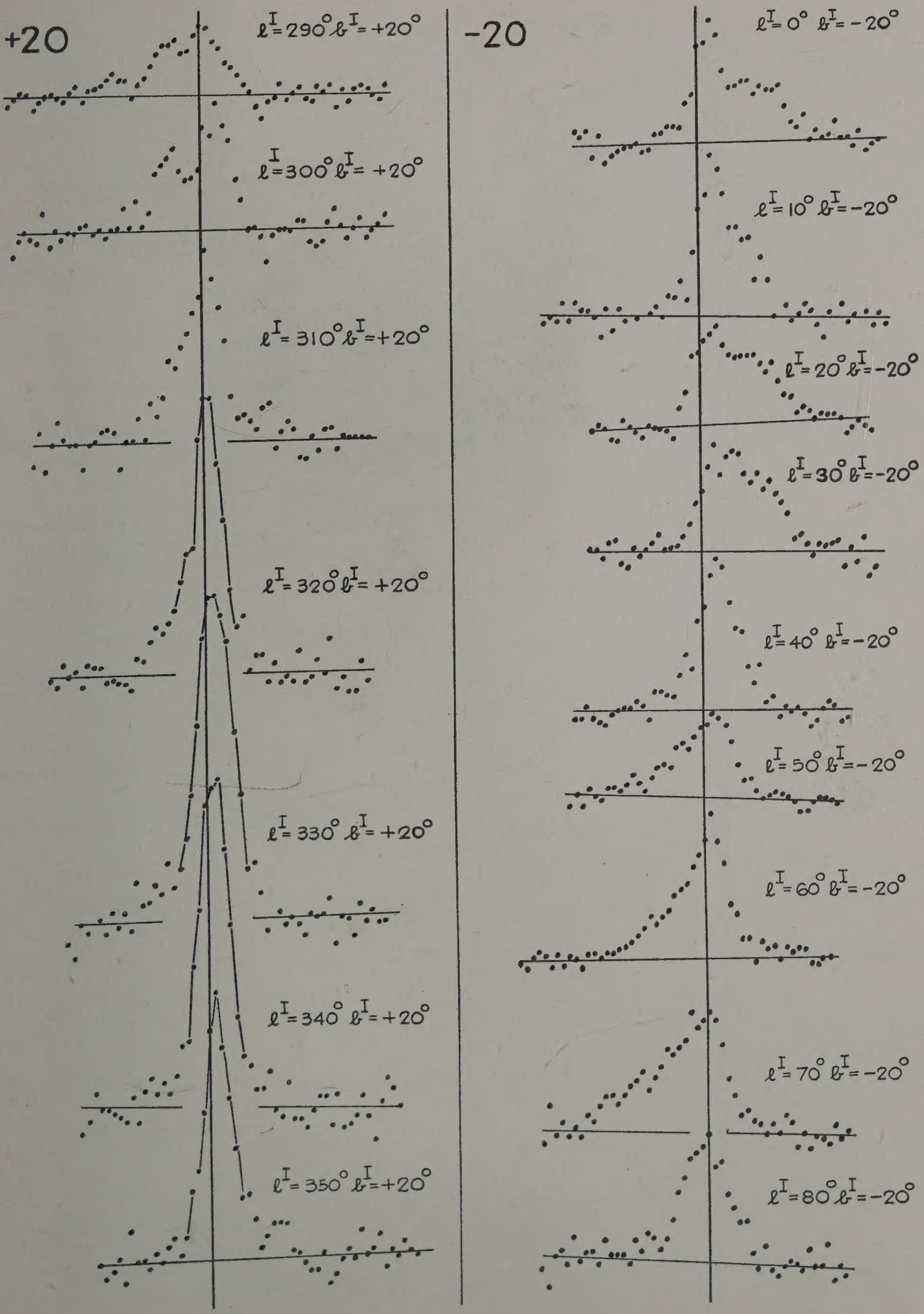
+20
ℓ^I=290° b^I=+20°
ℓ^I=300° b^I=+20°
ℓ^I=310° b^I=+20°
ℓ^I=320° b^I=+20°
ℓ^I=330° b^I=+20°
ℓ^I=340° b^I=+20°
ℓ^I=350° b^I=+20°
-20
ℓ^I=0° b^I=-20°
ℓ^I=10° b^I=-20°
ℓ^I=20° b^I=-20°
ℓ^I=30° b^I=-20°
ℓ^I=40° b^I=-20°
ℓ^I=50° b^I=-20°
ℓ^I=60° b^I=-20°
ℓ^I=70° b^I=-20°
ℓ^I=80° b^I=-20°

(g)

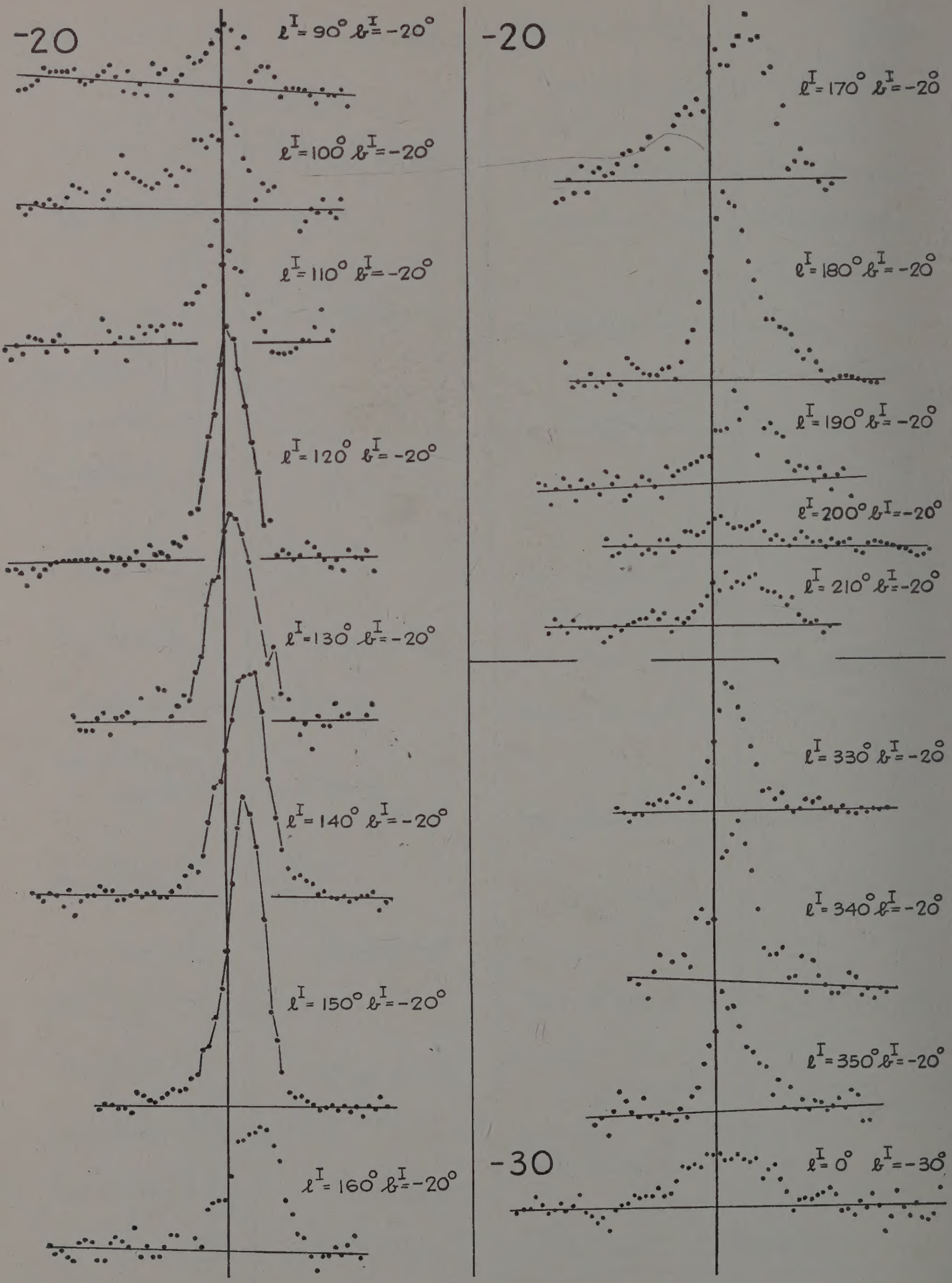
-20
$l^{I}=90^\circ$ $b^{I}=-20^\circ$
$l^{I}=100^\circ$ $b^{I}=-20^\circ$
$l^{I}=110^\circ$ $b^{I}=-20^\circ$
$l^{I}=120^\circ$ $b^{I}=-20^\circ$
$l^{I}=130^\circ$ $b^{I}=-20^\circ$
$l^{I}=140^\circ$ $b^{I}=-20^\circ$
$l^{I}=150^\circ$ $b^{I}=-20^\circ$
$l^{I}=160^\circ$ $b^{I}=-20^\circ$
-20
$l^{I}=170^\circ$ $b^{I}=-20^\circ$
$l^{I}=180^\circ$ $b^{I}=-20^\circ$
$l^{I}=190^\circ$ $b^{I}=-20^\circ$
$l^{I}=200^\circ$ $b^{I}=-20^\circ$
$l^{I}=210^\circ$ $b^{I}=-20^\circ$
$l^{I}=330^\circ$ $b^{I}=-20^\circ$
$l^{I}=340^\circ$ $b^{I}=-20^\circ$
$l^{I}=350^\circ$ $b^{I}=-20^\circ$
-30
$l^{I}=0^\circ$ $b^{I}=-30^\circ$

(h)

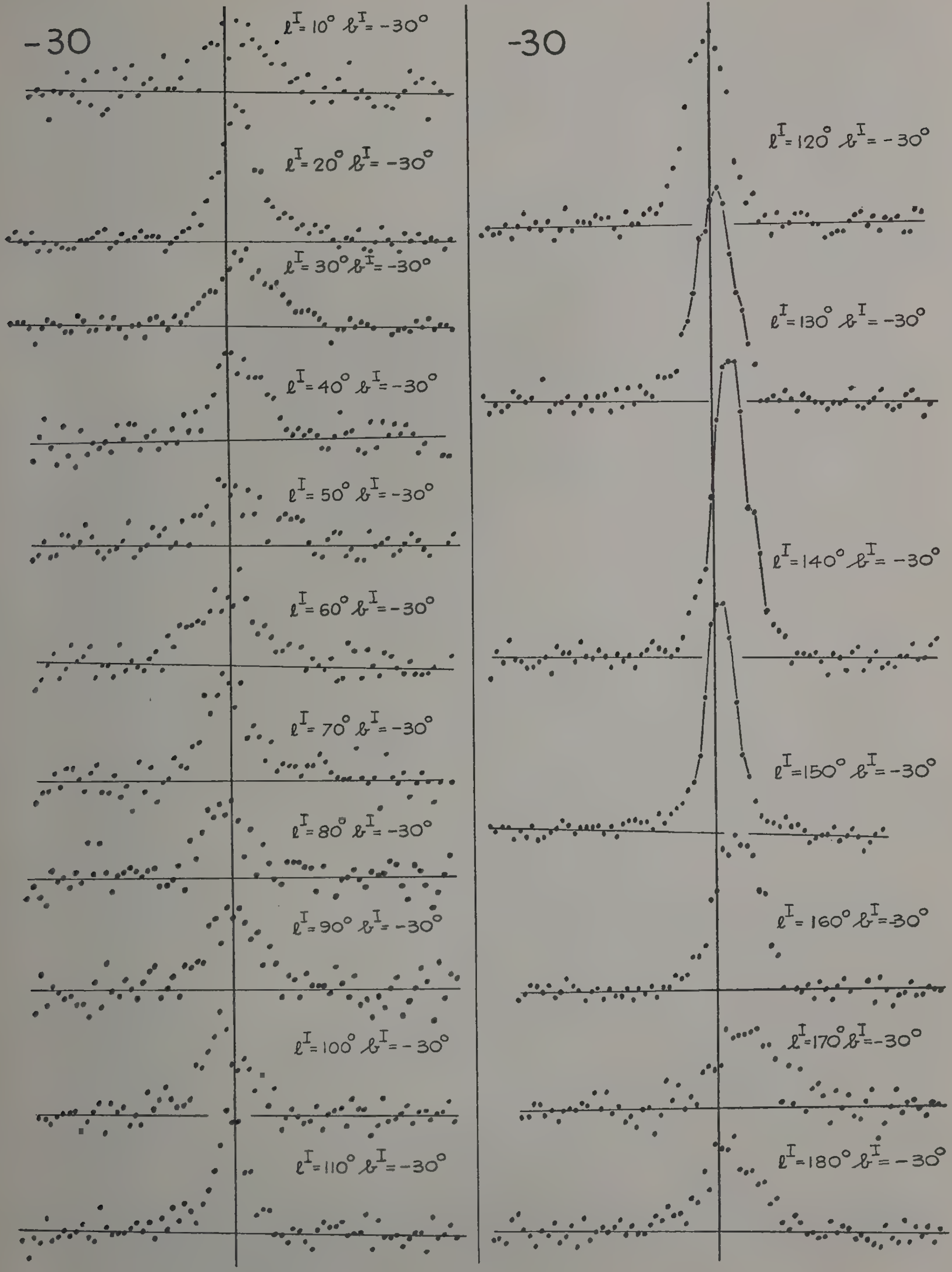
-30
l^I= 10° b^I= -30°
l^I= 20° b^I= -30°
l^I= 30° b^I= -30°
l^I= 40° b^I= -30°
l^I= 50° b^I= -30°
l^I= 60° b^I= -30°
l^I= 70° b^I= -30°
l^I= 80° b^I= -30°
l^I= 90° b^I= -30°
l^I= 100° b^I= -30°
l^I= 110° b^I= -30°
-30
l^I= 120° b^I= -30°
l^I= 130° b^I= -30°
l^I= 140° b^I= -30°
l^I= 150° b^I= -30°
l^I= 160° b^I= 30°
l^I= 170° b^I= -30°
l^I= 180° b^I= -30°

(i)

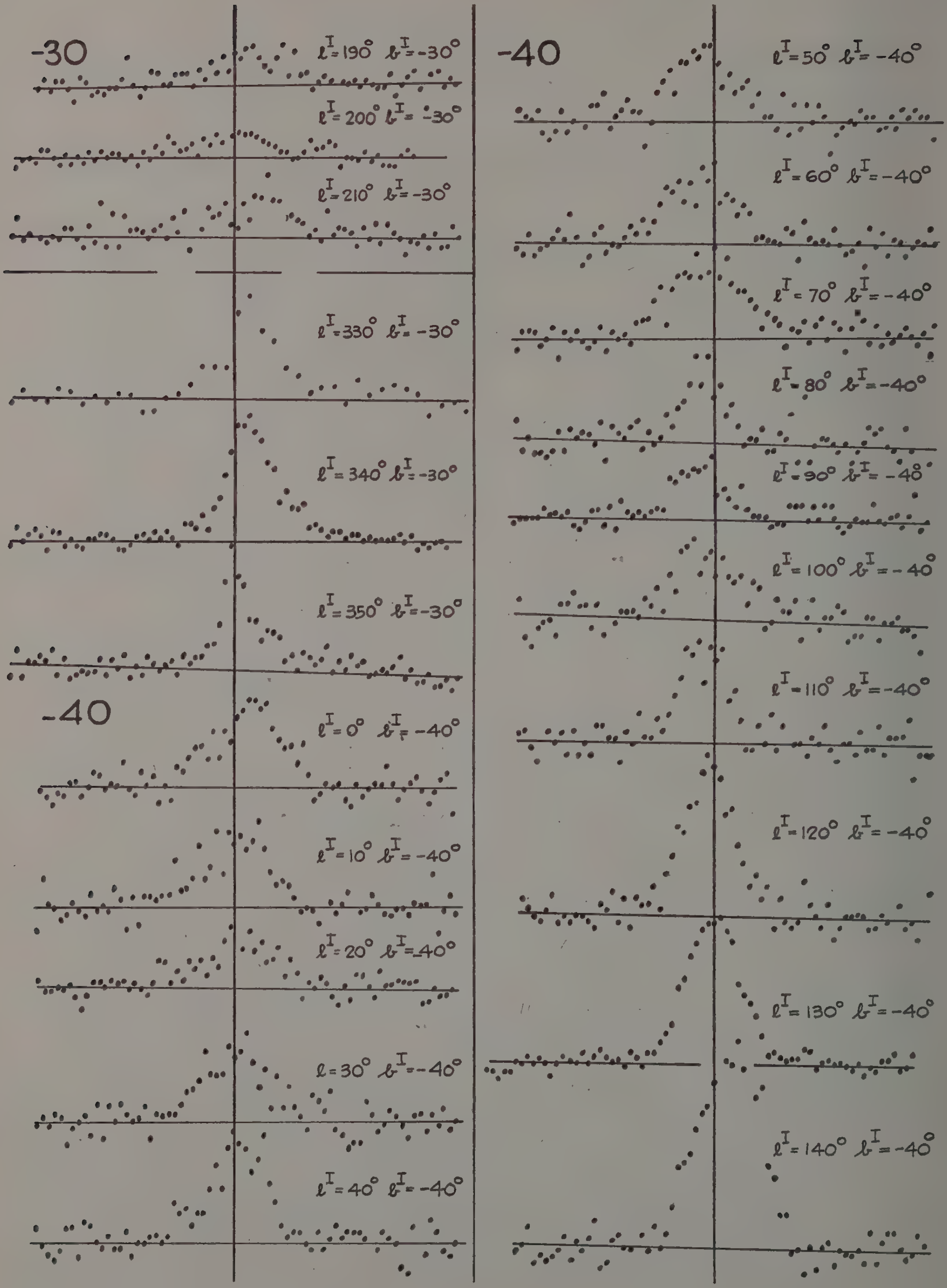
-30
lI=190° bI=-30°
lI=200° bI=-30°
lI=210° bI=-30°
lI=330° bI=-30°
lI=340° bI=-30°
lI=350° bI=-30°
-40
lI=0° bI=-40°
lI=10° bI=-40°
lI=20° bI=-40°
l=30° bI=-40°
lI=40° bI=-40°
-40
lI=50° bI=-40°
lI=60° bI=-40°
lI=70° bI=-40°
lI=80° bI=-40°
lI=90° bI=-48
lI=100° bI=-40
lI=110° bI=-40°
lI=120° bI=-40°
lI=130° bI=-40°
lI=140° bI=-40°

(j)

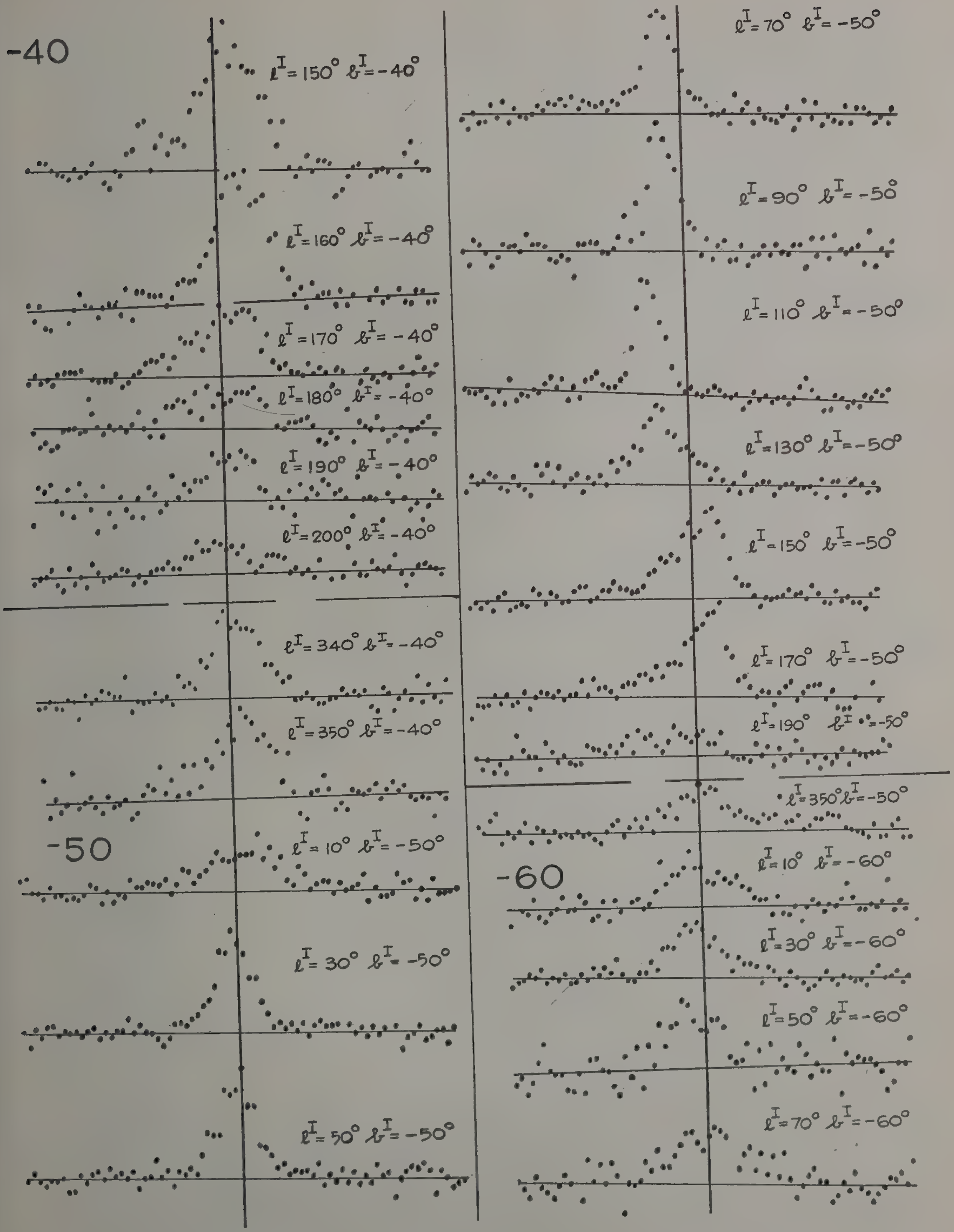
-40
l^I = 150° b^I = -40°
l^I = 160° b^I = -40°
l^I = 170° b^I = -40°
l^I = 180° b^I = -40°
l^I = 190° b^I = -40°
l^I = 200° b^I = -40°
l^I = 340° b^I = -40°
l^I = 350° b^I = -40°
-50
l^I = 10° b^I = -50°
l^I = 30° b^I = -50°
l^I = 50° b^I = -50°
l^I = 70° b^I = -50°
l^I = 90° b^I = -50°
l^I = 110° b^I = -50°
l^I = 130° b^I = -50°
l^I = 150° b^I = -50°
l^I = 170° b^I = -50°
l^I = 190° b^I = -50°
l^I = 350° b^I = -50°
-60
l^I = 10° b^I = -60°
l^I = 30° b^I = -60°
l^I = 50° b^I = -60°
l^I = 70° b^I = -60°

(k)

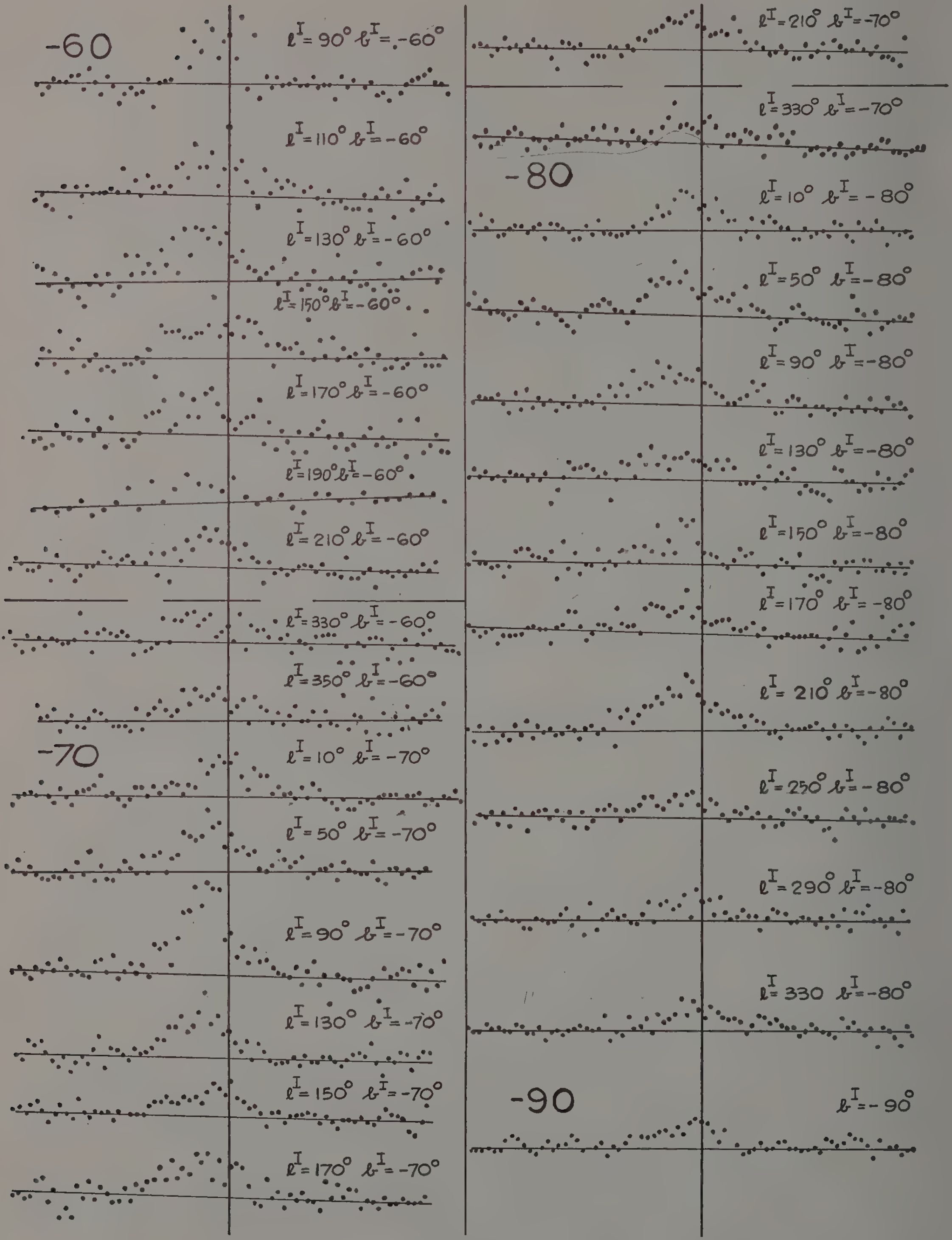
-60
$l^{I}=90^{\circ}$ $b^{I}=-60^{\circ}$
$l^{I}=110^{\circ}$ $b^{I}=-60^{\circ}$
$l^{I}=130^{\circ}$ $b^{I}=-60^{\circ}$
$l^{I}=150^{\circ}$ $b^{I}=-60^{\circ}$
$l^{I}=170^{\circ}$ $b^{I}=-60^{\circ}$
$l^{I}=190^{\circ}$ $b^{I}=-60^{\circ}$
$l^{I}=210^{\circ}$ $b^{I}=-60^{\circ}$
$l^{I}=330^{\circ}$ $b^{I}=-60^{\circ}$
$l^{I}=350^{\circ}$ $b^{I}=-60^{\circ}$
-70
$l^{I}=10^{\circ}$ $b^{I}=-70^{\circ}$
$l^{I}=50^{\circ}$ $b^{I}=-70^{\circ}$
$l^{I}=90^{\circ}$ $b^{I}=-70^{\circ}$
$l^{I}=130^{\circ}$ $b^{I}=-70^{\circ}$
$l^{I}=150^{\circ}$ $b^{I}=-70^{\circ}$
$l^{I}=170^{\circ}$ $b^{I}=-70^{\circ}$
$l^{I}=210^{\circ}$ $b^{I}=-70^{\circ}$
$l^{I}=330^{\circ}$ $b^{I}=-70^{\circ}$
-80
$l^{I}=10^{\circ}$ $b^{I}=-80^{\circ}$
$l^{I}=50^{\circ}$ $b^{I}=-80^{\circ}$
$l^{I}=90^{\circ}$ $b^{I}=-80^{\circ}$
$l^{I}=130^{\circ}$ $b^{I}=-80^{\circ}$
$l^{I}=150^{\circ}$ $b^{I}=-80^{\circ}$
$l^{I}=170^{\circ}$ $b^{I}=-80^{\circ}$
$l^{I}=210^{\circ}$ $b^{I}=-80^{\circ}$
$l^{I}=250^{\circ}$ $b^{I}=-80^{\circ}$
$l^{I}=290^{\circ}$ $b^{I}=-80^{\circ}$
$l^{I}=330$ $b^{I}=-80^{\circ}$
-90
$b^{I}=-90^{\circ}$

(1)

Table I. The observational parameters.

l	b	α	δ	Date	Time (EST)	Integration time	No. of scans	Remarks
				(a)				
	+90°	12$^{\text{h}}$ 43$^{\text{m}}$	27.7°	1/29/58	05:55	4.8$^{\text{m}}$	6	Profiles averaged
				7/27/57	16:31	4.5	4	
10°	+80	13 28	29.0	1/26/58	06:45	4.8	6	
50	+80	13 14	35.1	1/26/58	03:45	4.8	6	
90	+80	12 43	37.7	1/23/58	02:25	4.8	6	
130	+80	12 11	35.1	1/26/58	03:55	4.8	6	
150	+80	12 02	32.3	1/26/58	04:25	4.8	6	
170	+80	11 58	29.0	1/26/58	06:15	4.8	6	
210	+80	12 05	22.4	1/26/58	05:00	4.8	6	
250	+80	12 29	18.2	1/23/58	03:00	4.8	6	
290	+80	12 57	18.2	1/23/58	03:35	4.8	6	
330	+80	13 20	22.4	1/26/58	05:35	4.8	6	
10	+70	14 14	29.3	1/27/58	06:45	4.8	6	
50	+70	13 52	42.0	1/23/58	05:10	4.8	6	
90	+70	12 43	47.7	1/26/58	02:40	4.8	6	
130	+70	11 34	41.9	1/23/58	04:15	4.8	6	
150	+70	11 17	36.0	1/23/58	01:45	4.8	6	
170	+70	11 12	29.3	1/21/58	01:55	4.8	6	
210	+70	11 31	16.6	1/26/58	01:55	4.8	6	
250	+70	12 16	08.7	1/21/58	04:30	4.8	6	
290	+70	13 10	08.8	1/25/58	06:30	4.8	6	Profiles averaged
				1/29/58	05:25	4.8	6	
				(b)				
330°	+70°	13$^{\text{h}}$ 55$^{\text{m}}$	16.6°	1/27/58	05:03	4.8$^{\text{m}}$	6	
10	+60	14 59	28.7	7/28/57	20:48	7.5	4	
30	+60	14 57	38.6	7/28/57	20.28	7.5	2	
50	+60	14 37	47.9	7/28/57	20:51	7.5	2	
70	+60	13 52	54.9	7/28/57	21:15	7.5	4	
90	+60	12 43	57.7	7/31/57	13:08	4.5	4	
110	+60	11 33	54.9	7/31/57	12:22	4.5	4	
130	+60	10 48	47.8	7/29/57	13:40	4.5	4	
150	+60	10 28	38.6	7/27/57	13:08	4.5	4	
170	+60	10 26	28.6	7/27/57	14:15	4.5	4	
190	+60	10 37	19.0	7/27/57	14:35	4.5	4	Profiles averaged
				1/20/58	02:50	4.8	6	
210	+60	10 58	10.4	7/27/57	15:20	4.5	4	
230	+60	11 28	03.6	7/29/57	14:17	4.5	4	
250	+60	12 04	−00.8	7/29/57	15:00	4.5	4	
270	+60	12 43	−02.3	1/21/58	13:15	4.8	6	
290	+60	13 22	−00.8	7/29/57	15:39	4.5	4	
310	+60	13 58	03.6	7/31/57	14:22	4.5	4	
330	+60	14 27	10.4	7/31/57	15:37	4.5	3	
350	+60	14 48	19.0	1/25/58	07:05	4.8	6	
10	+50	15 44	27.1	1/25/58	07:45	4.8	6	Profiles averaged
				1/28/58	08:40	4.8	6	
30	+50	15 49	39.9	1/26/58	08:00	4.8	6	
50	+50	15 33	52.4	1/27/58	09:50	4.8	6	
70	+50	14 38	63.0	1/27/58	08:35	4.8	6	
90	+50	12 42	67.7	1/27/58	04:55	4.8	6	
110	+50	10 47	62.9	1/21/58	01:20	4.8	6	
130	+50	09 53	52.3	1/26/58	01:20	4.8	6	
150	+50	09 37	39.8	1/21/58	00:00	4.8	6	
170	+50	09 42	27.0	1/26/58	00.45	4.8	6	
				(c)				
190°	+50°	09$^{\text{h}}$ 59$^{\text{m}}$	14.9°	1/21/58	00:35	4.8$^{\text{m}}$	6	
210	+50	10 27	04.1	1/23/58	01:00	4.8	6	
230	+50	11 05	−04.6	1/22/58	02:00	4.8	6	
250	+50	11 51	−10.3	1/22/58	02:35	4.8	6	
270	+50	12 43	−12.3	1/22/58	04:05	4.8	6	
290	+50	13 35	−10.3	1/22/58	03:10	4.8	6	
310	+50	14 21	−04.6	1/27/58	06:10	4.8	6	
330	+50	14 59	04.1	1/26/58	07:25	4.8	6	
350	+50	15 27	14.9	1/27/58	08:00	4.8	6	
0	+40	16 16	17.4	7/25/57	19:38	7.5	2	
10	+40	16 27	24.7	7/25/57	20:03	7.5	2	
20	+40	16 35	32.1	7/25/57	20:28	7.5	2	
30	+40	16 41	39.7	7/28/57	21:57	7.5	4	

TABLE I. (Continued)

l	b	α	δ	Date	Time (EST)	Integration time	No. of scans	Remarks
40	+40	16 42	47.3	7/26/57	21:50	4.5	4	
50	+40	16 39	55.0	7/26/57	21:12	4.5	4	
60	+40	16 26	62.4	7/26/57	20:36	4.5	4	
70	+40	15 55	69.4	7/26/57	19:44	4.5	4	
80	+40	14 47	75.2	1/27/58	09:15	4.8	6	
90	+40	12 42	77.7	7/25/57	16:20	7.5	2	
100	+40	10 37	75.1	7/26/57	12:35	4.5	4	
110	+40	09 30	69.4	7/26/57	11:36	4.5	4	
120	+40	09 00	62.3	7/10/57	13:10	7.5	2	
130	+40	08 47	54.9	7/10/57	13:38	7.5	2	Profiles averaged
				7/26/57	13:19	4.5	4	
140	+40	08 43	47.2	7/10/57	14:03	7.5	4	
150	+40	08 45	39.6	7/10/57	15:03	7.5	4	
160	+40	08 50	32.0	7/17/57	11:10	5.0	6	
170	+40	08 59	24.6	7/17/57	12:06	5.0	6	
				(d)				
180°	+40°	09^{h} 09^{m}	17.3°	7/18/57	12:17	5.0^{m}	4	
190	+40	09 23	10.4	7/18/57	13:20	5.0	4	
200	+40	09 38	03.8	7/18/57	16:00	5.0	4	
210	+40	09 57	−02.4	7/18/57	14:10	5.0	4	Profiles averaged
				7/26/57	13:54	4.5	4	
220	+40	10 18	−07.9	1/20/58	02:15	4.8	6	
230	+40	10 42	−12.8	7/17/57	15:12	5.0	4	
240	+40	11 09	−16.8	7/17/57	14:44	5.0	4	
250	+40	11 38	−19.8	7/26/57	14:35	4.5	4	
260	+40	12 10	−21.1	7/26/57	15:15	4.5	4	
270	+40	12 43	−22.3	7/26/57	15:55	4.5	4	
280	+40	13 16	−21.7	7/29/57	16:19	4.5	4	
290	+40	13 48	−19.8	7/26/57	18:30	4.5	4	Profiles averaged. 1958 profile sharper than 1957 profile
				1/21/58	05:05	4.8	6	
300	+40	14 17	−16.8	7/25/57	16:57	7.5	2	
310	+40	14 44	−12.7	7/25/57	17:34	7.5	2	
320	+40	15 08	−07.9	7/27/57	18:00	7.5	2	Probably slightly smeared due to local oscillator unstability
330	+40	15 29	−02.3	1/25/58	08:20	4.8	6	Profiles averaged
				1/28/58	08:00	4.8	6	
340	+40	15 48	03.9	1/29/58	07:05	4.8	6	
350	+40	16 03	10.5	7/25/57	19:13	7.5	4	
0	+30	16 55	13.5	7/19/57	21:47	4.5	4	
10	+30	17 08	21.5	7/13/57	23:19	7.5	2	Profiles averaged
				7/19/57	22:30	4.5	4	
20	+30	17 21	29.7	7/20/57	19:37	4.5	4	
30	+30	17 31	38.1	7/20/57	20:18	4.5	4	
40	+30	17 41	46.5	7/20/57	21:04	4.5	4	
50	+30	17 49	55.1	7/20/57	21:47	4.5	4	Profiles averaged
				1/18/58	10:30	4.8	6	
				(e)				
60°	+30	17^{h} 54^{m}	63.8°	7/25/57	22:02	7.5^{m}	2	
70	+30	17 54	72.4	7/25/57	21:20	7.5	2	
80	+30	17 34	81.0	7/25/57	20:49	7.5	4	
90	+30	12 27	87.7	7/25/57	15:55	7.5	2	
100	+30	07 51	80.9	7/19/57	10:47	5.0	4	
110	+30	07 32	72.3	7/19/57	10:04	5.0	4	
120	+30	07 32	63.6	7/11/57	12:49	7.5	2	
130	+30	07 37	55.0	7/11/57	13:10	7.5	4	
140	+30	07 45	46.4	7/11/57	13:50	7.5	2	Profiles averaged
				7/19/57	11:30	5.0	4	
150	+30	07 54	38.0	7/11/57	14:17	7.5	2	Profiles averaged
				7/19/57	12:32	5.0	4	
160	+30	08 05	29.6	7/11/57	14:42	7.5	2	
170	+30	08 17	21.4	7/30/57	08:20	4.5	4	
180	+30	08 31	13.4	7/11/57	15:29	7.5	2	
190	+30	08 47	05.6	7/11/57	15:55	7.5	2	
200	+30	09 05	−01.8	1/20/58	01:00	4.8	6	
210	+30	09 26	−08.7	7/17/47	12:50	5.0	4	
220	+30	09 49	−15.2	7/17/57	13:15	5.0	4	Profiles averaged
				1/20/58	01:55	4.8	6	
230	+30	10 17	−20.8	7/17/57	13:45	5.0	4	
240	+30	10 48	−25.6	7/17/57	14:13	5.0	4	

TABLE I. (Continued)

l	b	α	δ	Date	Time (EST)	Integration time	No. of scans	Remarks
250	+30	11 24	−29.2	7/25/57	14:42	7.5	2	
260	+30	12 02	−31.5	7/25/57	15:28	7.5	2	
270	+30	12 43	−32.3	7/22/57	16:47	7.5	2	Profiles averaged
				1/21/58	03:50	4.8	6	
280	+30	13 24	−31.5	7/22/57	17:16	7.5	2	
290	+30	14 02	−29.2	7/22/57	17:51	7.5	3	
				(f)				
300°	+30°	14^{h} 38^{m}	−25.6°	7/22/57	18:19	7.5^{m}	2	Profiles averaged
				1/21/58	05:40	4.8	6	
310	+30	15 09	−20.8	7/19/57	19:25	4.5	4	
320	+30	15 37	−15.1	7/19/57	20:05	4.5	4	
330	+30	16 00	−08.7	7/19/57	21:30	4.5	4	Profiles averaged. 1958 profile was sharper and higher than 1957 profiles
				1/27/58	07:20	4.8	6	
340	+30	16 21	−01.7	7/19/57	20:55	4.5	4	
350	+30	16 39	05.7	7/19/57	21:23	4.5	4	
0	+20	17 32	09.2	6/15/57	00:30	7.5	2	Profiles averaged
				6/16/57	00:38	7.5	2	
				1/17/58	10:30	4.8	6	
10	+20	17 48	17.7	6/15/57	01:07	7.5	2	Profiles averaged
				1/17/58	11:45	4.8	6	
20	+20	18 04	26.4	6/15/57	01:33	7.5	2	Profiles averaged
				1/17/58		4.8	6	
30	+20	18 19	35.2	6/15/57	01:59	7.5	2	
40	+20	18 36	44.0	6/15/57	02:15	7.5	2	Profiles averaged
				1/17/58	13:20	4.8	6	
50	+20	18 55	52.9	6/15/57	02:54	7.5	2	Profiles averaged
				1/17/58	13:55	4.8	6	
60	+20	19 20	61.6	6/15/57	03.21	7.5	2	
70	+20	19 57	70.2	6/15/57	03:47	7.5	2	
80	+20	21 15	78.1	6/15/57	04:16	7.5	2	
90	+20	00 45	82.3	7/7/57	07:24	7.5	2	Profiles averaged
				1/12/58	18:50	4.8	6	
100	+20	04 12	78.0	7/10/57	09:32	7.5	2	
110	+20	05 29	70.1	7/9/57	12:18	7.5	2	
120	+20	06 07	61.5	7/9/57	12:50	7.5	3	
130	+20	06 31	52.7	7/9/57	13:28	7.5	3	
140	+20	06 50	43.9	6/11/57	14:56	7.5	2	
				(g)				
150°	+20°	07^{h} 07^{m}	35.0°	6/11/57	15:21	7.5^{m}	2	Profiles averaged
				1/19/58	21:55	4.8	6	
160	+20	07 23	26.3	6/11/57	15:46	7.5	2	
				6/12/57	14:39	7.5	2	
170	+20	07 38	17.6	6/11/57	16:11	7.5	2	
180	+20	07 55	09.1	6/11/57	16:46	7.5	2	
190	+20	08 12	00.8	6/12/57	15:06	7.5	2	
200	+20	08 32	−07.2	6/12/57	15:31	7.5	2	Profiles averaged
				1/19/58	23:45	4.8	6	
210	+20	08 54	−15.0	6/12/57	15:58	7.5	2	Profiles averaged
				1/20/58	00:20	4.8	6	
220	+20	09 19	−22.2	7/9/57	14:12	7.5	2	
230	+20	09 49	−28.6	7/9/57	14:38	7.5	4	
240	+20	10 25	−34.2	7/9/57	15:27	7.5	4	
250	+20	11 06	−38.6	1/21/58	02:30	4.8	6	
290	+20	14 20	−38.5	1/21/58	06:20	4.8	6	
300	+20	15 02	−34.1	1/21/58	06:55	4.8	6	
310	+20	15 34	−27.8	6/15/57	22:17	7.5	2	
320	+20	16 07	−22.0	6/15/57	22:49	7.5	2	
330	+20	16 32	−14.8	6/15/57	23:15	7.5	2	
340	+20	16 54	−07.2	6/15/57	23:41	7.5	2	
350	+20	17 14	00.9	6/16/57	00:06	7.5	2	
0	−20	19 54	−09.1	6/15/57	05:10	7.5	2	Profiles averaged
10	−20	20 12	−00.7	6/16/57	02:59	7.5	2	
20	−20	20 31	07.3	5/19/57	08:19	7.5	4	Profiles averaged
				1/19/58	14:45	4.8	6	
30	−20	20 54	15.0	6/15/57	05:38	7.5	2	
40	−20	21 19	22.1	5/19/57	08:55	7.5	2	Profiles averaged
				1/16/58	16:10	4.8	6	

TABLE I. (Continued)

l	*b*	*α*	*δ*	Date	Time (EST)	Integration time	No. of scans	Remarks
				(h)				
50°	−20°	21^h 49^m	28.6°	5/19/57	09:45	7.5	4	Profiles averaged
				1/16/58	17:00	4.8	6	
				1/19/58	15:25	4.8	6	
60	−20	22 24	34.2	7/7/57	05:49	7.5	2	Profiles averaged
				6/15/57	06:03	7.5	2	
				1/17/58	15:15	4.8	6	
70	−20	23 06	38.6	7/7/57	06:17	7.5	2	
80	−20	23 53	41.4	7/7/57	06:44	7.5	2	
90	−20	00 43	42.3	7/7/57	07:55	7.5	2	
100	−20	01 33	41.3	7/7/57	08:21	7.5	3	
110	−20	02 20	38.5	7/7/57	08:58	7.5	2	
120	−20	03 02	34.2	7/7/57	09:25	7.5	2	Profiles averaged
				1/18/58	21:45	4.8	6	
130	−20	03 37	28.6	7/9/57	10:14			
140	−20	04 07	22.0	7/9/57	10:40	7.5	4	Profiles averaged
				1/18/58	22:25	4.8	6	
150	−20	04 32	14.8	7/10/57	10:15	7.5	3	Profiles averaged
				1/18/58	23:20	4.8	6	
				1/19/58	19:15	4.8	6	
160	−20	04 54	07.2	7/10/57	12:28	7.5	2	
				7/11/57	09:35	7.5	3	
170	−20	05 14	−00.9	7/11/57	10:16	7.5	2	
180	−20	05 32	−09.2	7/11/57	10:47	7.5	2	Profiles averaged
				1/19/58	20:35	4.8	6	
190	−20	05 48	−17.7	7/11/57	11:20	7.5	3	
200	−20	06 04	−26.4	7/10/57	11:00	7.5	4	Profiles averaged
				1/19/58	21:15	4.8	6	
210	−20	06 19	−35.2	7/10/57	11:45	7.5	4	Profiles averaged
				1/20/58	21:35	4.8	6	
330	−20	19 06	−35.0	6/16/57	01:12	7.5	2	Profiles averaged
				1/27/58	10:30	4.8	6	
340	−20	19 22	−26.3	6/16/57	01:37	7.5	2	
350	−20	10 38	−17.6	6/15/57	04:43	7.5	2	
				6/16/57	02:02	7.5	2	
				(i)				
0°	−30°	20^h 31^m	−13.4°	7/28/57	23:15	7.5^m	4	
10	−30	20 47	−05.6	7/29/57	01:12	7.5	2	
20	−30	21 05	01.8	7/18/57	02:03	5.0	4	Profiles averaged
				1/16/58	15:00	4.8	6	
30	−30	21 26	08.7	7/18/57	02:31	5.0	4	Profiles averaged
				1/16/57	15:35	4.8	6	
40	−30	21 49	15.2	7/18/57	02:58	5.0	4	
50	−30	22 17	20.8	7/18/57	03:24	5.0	4	
60	−30	22 48	65.6	7/18/57	03:49	5.0	4	
70	−30	23 24	29.2	7/18/57	04:25	5.0	4	
80	−30	00 02	31.5	7/21/57	05:45	4.5	4	
90	−30	00 43	32.3	7/21/57	06:12	4.5	4	
100	−30	01 24	31.5	7/21/57	06:38	4.5	4	
110	−30	02 02	29.2	1/19/58	16:05	4.8	6	
120	−30	02 38	25.6	7/21/57	07:31	4.5	4	Profiles averaged
				1/19/58	16:45	4.8	6	
130	−30	03 09	20.8	7/21/57	07:58	4.5	4	Profiles averaged
				1/19/58	18:00	4.8	6	
140	−30	03 37	15.1	7/12/57	10:15	7.5	2	Profiles averaged
				1/19/58	18:35	4.8	6	
150	−30	04 00	08.7	1/12/58	20:15	4.8	6	Profiles averaged
				1/12/58	20:45	4.8	6	
160	−30	04 21	01.7	7/22/57	10:08	4.5	4	
170	−30	04 39	−05.7	7/26/57	09:48	4.5	4	
180	−30	04 55	−13.5	7/26/57	09:25	4.5	4	Profiles averaged. 1958 profile slightly sharper than 1957 profile
				1/12/58	21:30	4.8	6	
190	−30	05 08	−21.5	7/22/57	09:27	4.5	4	
200	−30	05 21	−29.7	7/18/57	09:47	5.0	4	Profiles averaged
				1/12/58	22:45	4.8	6	
				7/22/57	09:00	4.5	4	

TABLE I. (Continued)

l	b	α	δ	Date	Time (EST)	Integration time	No. of scans	Remarks
				(j)				
210°	−30°	05^{h} 31^{m}	−38.1°	1/20/58	20:55	4.8^{m}	6	
330	−30	19 54	−38.0	1/27/58	11:15	4.8	4	
340	−30	20 05	−29.6	7/14/57	00:37	7.5	4	
				1/27/58	11:50	4.8	6	
350	−30	20 17	−21.4	1/27/58	12:30	4.8	6	
0	−40	21 09	−17.3	7/29/57	00:45	7.5	2	
10	−40	21 23	−10.4	7/29/57	01:36	7.5	2	
20	−40	21 38	−03.8	7/29/57	02:01	7.5	4	
30	−40	21 57	02.4	7/29/57	02:42	7.5	2	
40	−40	22 18	07.9	7/19/57	05:23	5.0	4	
50	−40	22 42	12.8	7/19/57	05:49	5.0	4	
60	−40	23 09	26.8	7/19/57	06:14	5.0	4	Profiles averaged
				7/21/57	04:23	4.5	4	
70	−40	23 38	19.8	7/19/57	06:40	5.0	4	Profiles averaged
				7/21/57	04:51	4.5	4	
80	−40	00 10	21.7	7/19/57	07:06	5.0	4	
90	−40	00 43	22.3	7/19/57	08:00	5.0	4	Profiles averaged
				7/21/57	05:18	4.5	4	
100	−40	01 16	21.7	7/19/57	07:35	5.0	4	
110	−40	01 48	19.8	7/19/57	08:24	5.0	4	
120	−40	02 17	16.8	7/19/57	08:49	5.0	4	
130	−40	02 44	12.7	1/19/58	17:20	4.8	6	Profiles averaged
				7/19/57	09:14	5.0	4	
140	−40	03 08	07.9	7/19/57	09:38	5.0	4	
150	−40	03 29	02.3	7/22/57	06:03	4.5	4	
160	−40	03 48	−03.9	7/22/57	06:30	4.5	4	
170	−40	04 03	−10.5	7/22/57	06:54	4.5	4	
180	−40	04 16	−17.4	7/22/57	07:35	4.5	4	
190	−40	04 27	−24.7	7/18/57	09:03	5.0	4	
200	−40	04 35	−32.1	7/22/57	08:19	4.5	4	
				(k)				
340°	−40°	20^{h} 50^{m}	−32.0°	7/14/57	01:26	7.5^{m}	2	Profiles averaged
				7/29/57	23:56	7.5	2	
350	−40	20 59	−24.6	7/29/57	00:22	7.5	2	
10	−50	22 00	−14.3	1/27/58	13:45	4.8	6	
30	−50	22 27	−04.1	1/24/58	14:55	4.8	6	
50	−50	23 05	04.6	1/23/48	16:45	4.8	6	
70	−50	23 51	10.3	1/22/58	15:55	4.8	6	
90	−50	00 43	12.3	1/20/58	16:10	4.8	6	
110	−50	01 35	10.3	1/22/58	16:30	4.8	6	
130	−50	02 21	04.6	1/22/58	17:05	4.8	6	
150	−50	02 59	−04.1	1/24/58	18:35	4.8	6	Profiles averaged
				1/25/58	18:00	4.8	6	
170	−50	03 28	−14.9	1/23/58	17:25	4.8	6	
190	−50	03 44	−27.1	1/23/58	18:40	4.8	6	
350	−50	21 42	−27.0	1/27/58	13:05	4.8	6	
10	−60	22 37	−19.0	7/30/57	02:49	4.5	4	
30	−60	22 58	−10.4	7/30/57	03:39	4.5	4	Profiles averaged
				1/22/58	15:30	4.8	6	
50	−60	23 28	−03.6	7/30/57	04:43	4.5	4	
70	−60	00 04	00.8	7/30/57	05:05	4.5	4	
90	−60	00 43	02.3	7/30/57	05:31	4.5	4	
110	−60	01 22	00.8	7/30/57	06:44	4.5	4	
130	−60	01 58	−03.6	7/30/57	07:10	4.5	4	
150	−60	02 27	−10.4	7/30/57	07:35	4.5	4	
170	−60	02 48	−19.0	7/30/57	05:58	4.5	4	
190	−60	02 59	−28.7	7/30/57	06:22	4.5	4	
210	−60	02 57	−38.6	1/22/58	18:30	4.8	6	
330	−60	22 38	−38.6	1/24/58	14:10	4.8	6	
350	−60	22 26	−28.6	7/30/57	02:10	4.5	4	
				(l)				
10°	−70°	23^{h} 17^{m}	−22.6°	1/27/58	14:15	4.8^{m}	6	
50	−70	23 51	−11.8	1/25/58	16:20	4.8	6	
90	−70	00 43	−07.7	1/24/58	15:25	4.8	6	
130	−70	01 35	−11.8	1/25/58	16:40	4.8	6	
150	−70	01 55	−16.6	1/23/58	18:00	4.8	6	
170	−70	02 08	−22.6	1/24/48	18:00	4.8	6	

TABLE I. (Continued)

l	b	α	δ	Date	Time (EST)	Integration time	No. of scans	Remarks
210	−70	02 09	−36.0	1/24/58	17:20	4.8	6	Profiles averaged
				1/28/58	17:10	4.8	6	
330	−70	23 17	−36.0	1/28/58	15:50	4.8	6	
10	−80	23 59	−25.5	1/27/58	15:35	4.8	6	
50	−80	00 16	−19.9	1/24/58	16:00	4.8	6	
90	−80	00 43	−17.7	1/27/58	18:00	4.8	6	
130	−80	01 10	−19.9	1/24/58	16:35	4.8	6	
150	−80	01 20	−22.4	1/27/58	17:20	4.8	6	
170	−80	01 27	−25.5	1/25/58	17:15	4.8	6	
210	−80	01 24	−32.3	1/27/58	16:40	4.8	6	
250	−80	01 00	−37.0	1/20/58	17:15	4.8	6	Profiles averaged
				1/28/58	17:00	4.8	4	
290	−80	00 26	−37.0	1/20/58	16:45	4.8	6	Profiles averaged
				1/28/58	16:25	4.8	6	
330	−80	00 02	−32.3	1/29/58	16:10	4.8	6	
………	−90	00 43	−27.7	7/30/57	04:12	4.5	4	Profiles averaged
				2/4/58	16:00	4.8	6	

in Table I. When 1957 and 1958 records showed no appreciable difference, their average was taken in preparing this atlas.

DISCUSSION OF DATA

A brief discussion of the results was presented at the Paris Symposium on Radio Astronomy (Erickson *et al.* 1959) where an alternate representation of the radial velocity vs antenna temperature data was given. Further interpretation of these data is partially completed (Helfer 1959), and will be published shortly. For the sake of completeness we have reproduced in Fig. 1 a diagram of the total gas distribution.

We wish to encourage all *H*-line workers to observe the very sharp peak at $l^{\mathrm{I}}=330°, b^{\mathrm{I}}=+40°$; an interesting feature which should serve as a frequency, bandwidth, and intensity calibration for use in correlating the results of various surveys. It is near the celestial equator, and is visible from almost any part of the earth. The profile with sharp peak and long tail at $l^{\mathrm{I}}=60°, b^{\mathrm{I}}=-20°$, would also serve a similar purpose.

The interesting aggregation of gas along the $b^{\mathrm{I}}=-50°$ parallel near $l^{\mathrm{I}}=90°$ has been carefully observed. As one sweeps in galactic longitude, this feature under goes a rapid shift in velocity. Another gas aggregatio has been found in the region of $b^{\mathrm{I}}=70$–$80°$, $l^{\mathrm{I}}=$ 280–290°. Attempts to trace features such as thes both in galactic longitude and latitude are often quit successful.

Table I is our observing log, and describes the actua parameters employed in the individual observation given in Fig. 3. Figure 2 gives the intensity and velocit scales for Fig. 3, 10°K/cm and 20 km/sec/cm, re spectively. This work represents Part I of a forth coming Carnegie Atlas. Observations of the region fror $b^{\mathrm{I}}=+20°$ to $b^{\mathrm{I}}=-20°$ are now in progress.

REFERENCES

Erickson, W. C., H. L. Helfer, and H. E. Tatel, *Paris Symposiu on Radio Astronomy*, edited by R. N. Bracewell (Stanfor University Press, Stanford, California, 1959), p. 390.

Helfer, H. L., A. J. **64,** 128 (1959).

—— and H. E. Tatel, Astrophys. J. **121,** 585 (1955).

Muller, C. A. and G. Westerhout, Bull. Astron. Inst. Netherland **475,** 151 (1957).

Tatel, Helfer, and Tuve, *Carnegie Inst. of Washington Year Boo* **56,** 91 (1956–57), (note misprint, 7th line from bottom, 2n col. p. 91: "kc/sec" not "km/sec").

van de Hulst, H. C. Revs. Modern Phys. **30,** 913 (1958).

van Woerden, H., W. Rougoor, and J. Oort, Compt. rend. **24** 1691 (1957).

THE ASTRONOMICAL JOURNAL VOLUME 65, NUMBER 1276 FEBRUARY, 1960

Motion of Jupiter and Mass of Saturn*

G. M. Clemence
U. S. Naval Observatory, Washington, D. C.

(Received October 14, 1959)

The discrepancy between theory and observation in the longitude of Jupiter found by Krotkov and Dicke, which has coefficient of 0″.25 and a period of 4520 days, is removed by attributing mass 1/3499.7 to Saturn and adding two known corrections to the motion of the perihelion.

KROTKOV and Dicke (1959), in their study of the discrepancies between observations of the outer planets and the theory of their motions, as given by Eckert, Brouwer, and Clemence (1951), have found as their principal result, a periodic oscillation in the longitude of Jupiter which has a coefficient of 0″.25 and a period of 4520 days. They remark that the observations are also consistent with a positive increment to the motion of the perihelion amounting to 5″ per century; the short interval of 160 years covered by the observations does not permit a decision to be made between the two interpretations. My purpose here is to show that the discrepancy can be explained by conventional gravitational theory.

The motion of the perihelion, according to the calculations of Eckert, Brouwer, and Clemence, requires two separate positive corrections. One of them is due to the action of the four inner planets (Clemence 1954) neglected in the original calculations on account of the shortness of the periods involved; it amounts to 1″.6 per century. Secondly, Bessel's value 1/3501.6 for the mass of Saturn is known to be too small (van den Bosch 1927, Hertz 1953). It was used in the calculations only to preserve consistency in the whole body of theoretical work on the subject. From Hill's theory (1890) it is ascertained that a change in the mass from the value of Bessel to that of Hertz, 1/3497.6, corresponds to an increment of +0″.7 in the centennial motion of the perihelion of Jupiter. Thirdly, the observations have been reduced to a fixed equinox using Newcomb's value of the precession, which is known (Brouwer 1950, Morgan and Oort 1951) to require a correction of +0″.8 per century. The sum of the three corrections is 3″.1, which is not sufficient to explain the result of Krotkov and Dicke.

The effect of modifying the mass of Saturn is, however, imperfectly accounted for by changing the motion of the perihelion. The periodic perturbations of Jupiter by Saturn also require modification, and it turns out that the effects are important.

The procedure was as follows: The perturbations $n\delta z$ of Jupiter by Saturn given on pages 103–105 of Hill's theory, including those that express the motion of the perihelion, were evaluated for the sixty dates in the table of Krotkov and Dicke and multiplied by +0.00114, which gives the increment corresponding to Hertz's value of the mass of Saturn. To the result for each date was added the effect on the longitude of a motion of the perihelion of +2″.4 per century, corresponding to the action of the four inner planets and the correction to the precession. This sum was subtracted from the residual in the table of Krotkov and Dicke. The new residuals were used as the right-hand members of equations of condition, which were solved by least squares for four unknowns corresponding to initial conditions: a constant term, a term proportional to the time, and the coefficients of the sine and cosine of the mean anomaly of Jupiter. The mean square residual was reduced from 0.175 (before modifying the perturbations) to 0.097. The residuals are plotted in the middle portion of Fig. 1; the residuals used by Krotkov and Dicke are in the upper portion.

At this stage it was evident that the residuals were suitable for a new determination of the mass of Saturn, and the solution by least squares was repeated, introducing the perturbations of Jupiter by Saturn as coefficients of the fifth unknown, from which the mass of

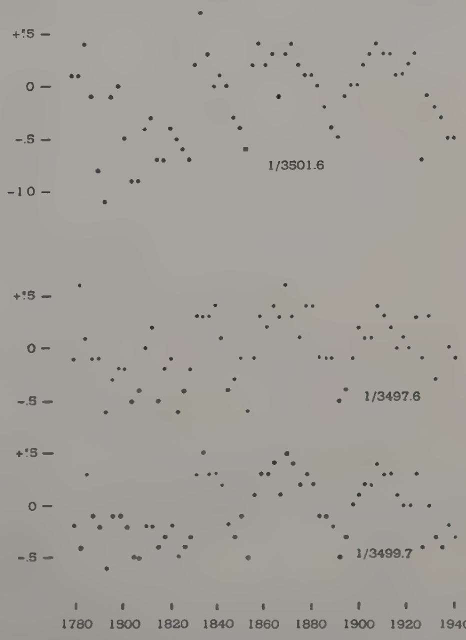

FIG. 1. Residuals in longitude corresponding to three values of the mass of Saturn.

---

* This work was supported by the Office of Naval Research.

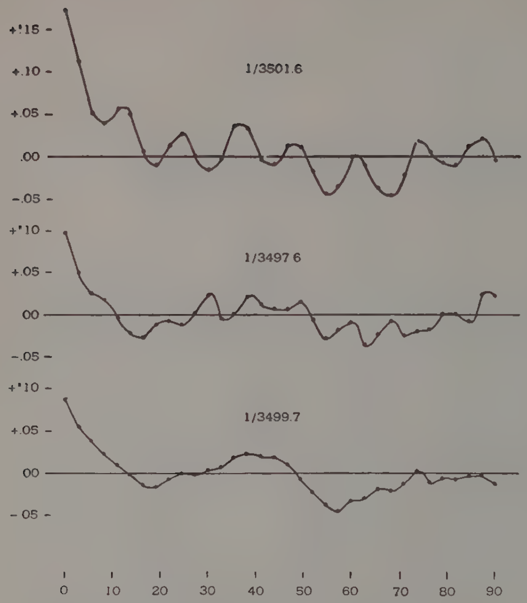

Fig. 2. Auto-covariance of residuals in Fig. 1.

Saturn is found to be 1/3499.7±0.4(pe); the mean square residual is 0.092, and the residuals are shown in the lower part of Fig. 1.

Fig. 2 shows the auto-covariance of the residuals in Fig. 1. The ordinate is the auto-covariance in squared seconds of arc; the abscissa, the lag in years. The upper curve is identical with that of Krotkov and Dicke. It will be noticed that the pronounced periodic wave in the upper curve is considerably modified by the introduction of Hertz's value of the mass of Saturn and the effects of the inner planets and the precession, while in the lower curve the wave virtually disappears, showing that it is fully accounted for by known causes.

The lower curve in Fig. 2 exhibits much the same features as Fig. 7 of Krotkov and Dicke, and they are discernible in Fig. 1, at least after 1840. What is equally remarkable is the preponderance of negative residuals before 1830. There is some evidence of a similar curve in the data of Krotkov and Dicke for Saturn. Since observations of Jupiter and Saturn are usually made at the same observatories using the same techniques, they are presumably affected by the same systematic errors, and perhaps those may be what is seen here. At least I have not been able to think of any conventional dynamical explanation.

Since I had conversations with Professor Dicke on the subject of his and Krotkov's article prior to publication, it may be in order to remark that the method of analysis used here did not occur to me until after their work was in print.

REFERENCES

Brouwer, D., Bull. Astron. **15**, 165 (1950).
Clemence, G. M., Astron. Papers Am. Ephemeris **13**, 387 (1954).
Eckert, Brouwer, and Clemence, Astron. Papers Am. Ephemeris **12**, (1951).
Hertz, H. G., Astron. Papers Am. Ephemeris **15**, 169 (1953).
Hill, G. W., Astron. Papers Am. Ephemeris **4**, 103 (1890).
Krotkov, R. and R. H. Dicke, Astron. J. **64**, 157 (1959).
Morgan, H. R. and J. H. Oort, Bull. Astron. Inst. Netherlands **11**, 379 (1951).
van den Bosch, C. A. *De Massa's van de Groote Planeten*, (Bakker, Baarn, 1927).

THE ASTRONOMICAL JOURNAL VOLUME 65, NUMBER 1276 FEBRUARY, 1960

The Eclipsing System, TZ Coronae-Austrinae

FRANK BRADSHAW WOOD

Flower and Cook Observatory, University of Pennsylvania, Philadelphia, Pennsylvania

(Received September 28, 1959)

New light, eclipse, and orbital elements are computed for the eclipsing system TZ CrA. They are based on two-color photoelectric observations obtained in 1957–58 at the Mount Stromlo Observatory. A brief discussion is given of the uncertainties involved in computed elements of eclipsing systems, and the limiting values for the present case are considered. A method of estimating the mass ratio from the light curve alone is described and applied to TZ CrA. The fainter component appears to be overluminous when compared to conventional mass-luminosity considerations. Since this is not uncommon in close double star systems, an attempt is made to explain it on theoretical grounds concerned with the evolution of close binaries. The assumptions differ from those usually made.

INTRODUCTION

THE light variation of TZ CrA (CoD−43°8543, 127.1910, HV 3200) was discovered by Miss Cannon (Pickering, 1910). No further observations were made until Gaposchkin (1953) and Mrs. Payne-Gaposchkin (1943, 1950) included it in their general study of eclipsing systems made by photographic estimates. They determined the nature of the light curve and gave ranges and light elements. The curve is Algol type, with a depth of primary minimum slightly greater than 0.7 mag and a secondary depth of about 0.1 mag. The eclipses are partial; the duration of each is 3.7 hr; the period is about 16.5 hr. Miss Cannon has classified the spectrum as A0 (Campbell, 1943).

OBSERVATIONS

The observations were made with the 30-in. Reynolds reflector of the Mount Stromlo Observatory and a 1P21 multiplier photocell refrigerated with dry ice. The photometer and filters have been described by Gascoigne and Burr (1956). The spectral ranges used correspond closely to the International *P* and *V* systems.

The observations are listed in Table I. Times are heliocentric measured from Greenwich mean noon; the magnitude differences are on the natural scale of the equipment. The comparison star was CoD−44° 12493. The observations on JD 2436039 were not used in the solution.

EPOCH AND PERIOD

The few available published times of minimum are listed in Table II, together with residuals from new light elements:

$$\text{Pr. min (hel)} = \text{JD } 2436080.034 + 0\overset{d}{.}68674954\, E.$$

The improbably large residual of the discovery minimum becomes reasonable if an error of one day in the published date is assumed. The published minima show no evidence of change of period, nor do unpublished minima kindly supplied by S. Gaposchkin. However, small period changes could easily have gone undetected.

ORBITAL AND ECLIPSE ELEMENTS

The solution was made with the aid of Merrill's nomographs and tables (Merrill, 1950, 1953), following in general the procedure summarized by Russell and Merrill (1952). In initial treatment, independent rectifications for the blue and yellow curves were carried out. Solutions found thus agreed reasonably well, but were not adopted for two reasons. First, the fit at the shoulders, while fairly close, was consistently above the observations; this could not be improved without causing similar departures elsewhere on the curve. Second, the coefficient of the cos2*θ* term, caused chiefly by the departure of the stars from spherical shape, was larger in the blue than in the yellow. This is contrary to what we expect from theory, and in this particular case led to a rectified depth of primary minimum in yellow slightly deeper than that in blue. This also is unrealistic, and while it probably could be explained by invoking a shell with specially chosen properties, it seems unwise to do this without further investigation of the conventional model.

Consideration of the uncertainties inherent in the rectifications showed a narrow range of values of the coefficients which fitted satisfactorily the observations in both wavelength regions. Since the effects are small, this does little violence to theoretical considerations. The values finally adopted in the usual relation,

$$I = A_0 + A_1 \cos\theta + A_2 \cos 2\theta,$$

were

$$A_0 = 0.970, \quad A_1 = -0.006, \quad A_2 = -0.025.$$

The maximum permissible variation in A_0 and A_2 is 0.003 and, in A_1, it is 0.002. Higher harmonics and sine terms were negligible; such evidence as does exist seems to be caused by minor fluctuations in brightness from night to night, rather than permanent harmonics in the curve.

With this rectification, in both blue and yellow the nomographs showed the depth line tangent to the shape line near the point represented by $k = 0.71$ and $p_0 = -0.81$. The principal eclipse is clearly a transit; thus

TABLE I.

JD (hel) 2436+	C−V	Phase	JD (hel) 2436+	C−V	Phase
Yellow Observations					
039.0568	$-0\overset{\mathrm{m}}{.}169$	$+0\overset{\mathrm{d}}{.}2278$	053.0817	$-0\overset{\mathrm{d}}{.}217$	$0\overset{\mathrm{m}}{.}5177$
.0603	−0.171	0.2313	.1057	−0.226	0.5417
.0828	−0.251	0.2538	.1103	−0.233	0.5463
.0864	−0.268	0.2574	.1241	−0.260	0.5601
.1063	−0.227	0.2773	.1296	−0.260	0.5656
.1092	−0.235	0.2802	.1462	−0.262	0.5822
.1172	−0.194	0.2882	.1508	−0.269	+0.5868
040.9330	−0.465	0.0437	.1741	−0.299	−0.0767
041.0482	−0.252	0.1589	.1796	−0.291	0.0712
.0683	−0.240	0.1790	.1922	−0.353	0.0586
.0896	−0.245	0.2003	.1971	−0.381	−0.0537
.0955	−0.233	0.2062	079.8793	−0.258	+0.5500
.1096	−0.244	0.2203	.9140	−0.252	0.5667
043.9194	−0.250	0.2831	.9255	−0.255	0.5782
.9255	−0.278	0.2892	.9302	−0.269	+0.5829
.9399	−0.282	0.3036	.9513	−0.277	−0.0827
.9475	−0.333	0.3112	.9548	−0.274	0.0792
.9628	−0.348	0.3265	.9591	−0.285	0.0749
.9749	−0.361	0.3386	.9732	−0.297	0.0608
.9904	−0.359	0.3541	.9749	−0.330	0.0591
.9954	−0.341	0.3591	.9789	−0.362	0.0551
045.9374	−0.239	0.2409	.9827	−0.400	0.0513
.9478	−0.228	0.2513	.9937	−0.509	0.0403
.9625	−0.232	0.2660	.9990	−0.566	0.0350
.9674	−0.245	0.2709	080.0029	−0.603	0.0311
.9850	−0.248	0.2885	.0163	−0.798	0.0177
.9971	−0.296	0.3006	.0209	−0.880	0.0131
046.0423	−0.339	0.3458	.0228	−0.896	0.0112
.0542	−0.338	0.3577	.0263	−0.932	−0.0077
.1457	−0.261	0.4492	.0385	−0.967	+0.0045
.1517	−0.263	0.4552	.0430	−0.947	0.0090
.1661	−0.245	0.4696	.0552	−0.760	0.0212
.1735	−0.245	0.4770	.0602	−0.674	0.0262
.8963	−0.234	0.5130	.0635	−0.627	0.0295
.9012	−0.221	0.5179	.0820	−0.397	0.0480
.9126	−0.225	0.5293	.0860	−0.378	0.0520
.9184	−0.241	0.5351	.0917	−0.356	0.0577
.9332	−0.240	0.5499	100.9128	−0.251	0.2763
.9402	−0.243	0.5569	.9225	−0.287	0.2860
.9450	−0.251	+0.5617	.9303	−0.290	0.2938
047.0342	−0.553	−0.0358	.9329	−0.307	0.2964
.0389	−0.633	0.0311	.9655	−0.355	0.3290
.0539	−0.840	0.0161	.9778	−0.359	+0.3413
.0591	−0.935	0.0109	.9802	−0.361	+0.3437
.0620	−0.954	−0.0080	101.0005	−0.359	+0.3640
.0720	−0.975	+0.0020	110.9003	−0.556	−0.0374
.0779	−0.945	0.0079	.9147	−0.747	0.0230
.0808	−0.941	0.0108	.9167	−0.787	0.0210
.0935	−0.748	0.0235	.9264	−0.919	0.0113
.0987	−0.669	0.0287	.9286	−0.949	0.0091
.1006	−0.602	0.0306	.9349	−0.978	0.0028
.1150	−0.474	0.0450	.9367	−0.973	−0.0010
.1207	−0.431	0.0507	.9450	−0.939	+0.0073
052.8862	−0.341	0.3222	.9488	−0.939	0.0111
.8920	−0.358	0.3280	.9522	−0.880	0.0145
.9024	−0.364	0.3384	.9628	−0.702	0.0251
.9075	−0.372	0.3435	.9661	−0.669	0.0284
.9221	−0.341	0.3581	.9705	−0.585	0.0328
.9267	−0.327	0.3627	.9946	−0.331	0.0569
.9378	−0.318	0.3738	.9973	−0.335	0.0596
.9419	−0.315	0.3779	293.2336	−0.324	0.3072
.9624	−0.290	0.3984	.2509	−0.354	0.3245
.9660	−0.285	0.4020	.2781	−0.357	0.3517
.9786	−0.269	0.4146	.2842	−0.355	+0.3578
.9831	−0.267	0.4191	294.2064	−0.249	−0.0935
.9966	−0.252	0.4326	.2225	−0.267	0.0774
053.0017	−0.250	0.4377	.2283	−0.279	0.0716
.0779	−0.223	0.5139	.2441	−0.377	0.0558

TABLE I. (Continued)

JD (hel) 2436+	C−V	Phase	JD (hel) 2436+	C−V	Phase
Yellow Observations					
294.2496	$-0^{\mathrm{m}}.412$	$0^{\mathrm{d}}.0503$	374.0339	$-0^{\mathrm{m}}.293$	$+0^{\mathrm{d}}.0711$
.2624	−0.562	0.0375	.0390	−0.283	0.0762
.2680	−0.632	0.0319	.0582	−0.244	0.0954
.2806	−0.816	0.0193	.0635	−0.244	0.1007
.2853	−0.884	−0.0146	.0754	−0.239	+0.1126
Blue Observations					
039.0578	$+0^{\mathrm{m}}.221$	$+0^{\mathrm{d}}.2288$	052.9978	$+0^{\mathrm{m}}.144$	$0^{\mathrm{d}}.4338$
.0610	+0.218	0.2320	053.0026	+0.141	0.4386
.0838	+0.151	0.2548	.0788	+0.156	0.5148
.0876	+0.133	0.2586	.0825	+0.151	0.5185
.1073	+0.177	0.2783	.1066	+0.180	0.5426
.1118	+0.148	0.2828	.1114	+0.155	0.5474
.1184	+0.191	0.2894	.1235	+0.154	0.5613
040.9341	−0.067	0.0448	.1307	+0.151	0.5667
041.0497	+0.155	0.1604	.1474	+0.138	+0.5834
.0700	+0.170	0.1807	.1518	+0.142	−0.0990
.0913	+0.165	0.2020	.1753	+0.093	0.0755
.0961	+0.159	0.2068	.1809	+0.107	0.0699
.1116	+0.144	0.2223	.1932	+0.015	0.0576
043.9209	+0.108	0.2846	.1981	+0.008	−0.0537
.9268	+0.094	0.2905	079.9034	+0.142	+0.5561
.9413	+0.105	0.3050	.9148	+0.154	0.5675
.9488	+0.091	0.3125	.9265	+0.145	0.5792
.9642	+0.052	0.3279	.9310	+0.144	+0.5837
.9740	+0.050	0.3377	.9520	+0.131	−0.0820
.9916	+0.046	0.3541	.9557	+0.113	0.0783
.9966	+0.042	0.3603	.9601	+0.114	0.0739
045.9390	+0.135	0.2425	.9614	+0.109	0.0726
.9490	+0.135	0.2525	.9756	+0.044	0.0584
.9635	+0.139	0.2670	.9700	+0.014	0.0541
.9685	+0.131	0.2720	.9834	−0.017	0.0506
.9862	+0.121	0.2897	.9947	−0.106	0.0393
.9990	+0.094	0.3025	080.0041	−0.228	0.0299
046.0430	+0.049	0.3465	.0173	−0.434	0.0167
.0552	+0.070	0.3587	.0218	−0.506	0.0122
.1471	+0.148	0.4506	.0235	−0.518	0.0105
.1533	+0.151	0.4568	.0271	−0.561	−0.0069
.1696	+0.140	0.4731	.0396	−0.575	+0.0056
.1746	+0.145	0.4781	.0434	−0.550	0.0094
.8975	+0.163	0.5142	.0568	−0.344	0.0228
.9028	+0.173	0.5195	.0595	−0.306	0.0255
.9138	+0.166	0.5305	.0644	−0.239	0.0304
.9197	+0.158	0.5364	.0829	−0.031	0.0489
.9413	+0.142	+0.5580	.0875	+0.022	0.0535
046.9461	+0.148	+0.5628	.0925	+0.016	0.0585
047.0353	−0.176	−0.0347	100.9135	+0.113	0.2770
.0399	−0.258	0.0301	.9232	+0.083	0.2867
.0550	−0.458	0.0150	.9309	+0.087	0.2944
.0599	−0.518	0.0101	.9335	+0.069	0.2970
.0631	−0.577	−0.0069	.9670	+0.066	0.3305
.0945	−0.346	+0.0245	.9784	+0.038	0.3419
.0994	−0.264	0.0294	.9806	+0.036	0.3441
.1016	−0.222	0.0316	101.0008	+0.048	+0.3643
.1162	−0.061	0.0462	110.9008	−0.135	−0.0369
.1216	−0.024	0.0516	.9152	−0.348	−0.0225
052.8874	+0.048	0.3234	.9174	−0.402	0.0203
.8929	+0.062	0.3289	.9270	−0.526	0.0107
.9035	+0.052	0.3395	.9293	−0.552	0.0084
.9112	+0.047	0.3472	.9354	−0.610	0.0023
.9232	+0.074	0.3592	.9372	−0.601	−0.0005
.9276	+0.075	0.3636	.9454	−0.572	+0.0077
.9388	+0.079	0.3748	.9494	−0.560	0.0117
.9432	+0.081	0.3792	.9528	−0.500	0.0151
.9635	+0.108	0.3995	.9633	−0.338	0.0256
.9668	+0.111	0.4028	.9666	−0.270	0.0289
.9795	+0.120	0.4155	.9714	−0.196	0.0337
.9840	+0.119	0.4200	.9952	+0.084	0.0575

TABLE I. (Continued)

JD (hel) 2436+	C−V	Phase	JD (hel) 2436+	C−V	Phase
Blue Observations					
110.9977	$+0\overset{\mathrm{m}}{.}068$	$0\overset{\mathrm{d}}{.}0600$	294.2654	$-0\overset{\mathrm{m}}{.}185$	$0\overset{\mathrm{d}}{.}0345$
293.2398	+0.077	0.3134	.2705	−0.258	0.0294
.2531	+0.057	0.3267	.2832	−0.453	0.0167
.2803	+0.042	0.3539	.2869	−0.505	−0.0130
.2857	+0.051	+0.3593	374.0367	+0.105	+0.0739
294.2103	+0.126	−0.0896	.0402	+0.097	0.0774
.2250	+0.135	0.0749	.0607	+0.122	0.0979
.2325	+0.109	0.0674	.0652	+0.142	0.1024
.2473	+0.019	0.0526	.0781	+0.158	+0.1143
.2524	−0.030	0.0475			

the hotter star is also the larger. The function α_0 (the fraction of light lost expressed in terms of light loss at internal tangency) is about 0.90. In both wavelength bands, solutions were tried for different assumed limb darkenings without altering these general conclusions. For the yellow curve, the fit to the observations with assumed limb darkening coefficient $x=0.6$ was slightly better than that for $x=0.4$; the difference is not large enough to be conclusive. For $x=0.8$, no satisfactory solution could be found. The best fit to the entire curve assumes $x=0.6$ for the hotter, and $x=0.8$ for the cooler star. For the blue curve, satisfactory solutions could be found with either $x=0.6$ or $x=0.8$ for the hotter component, and $x=0.8$ for the cooler. However, in order to find geometrical elements which will satisfy the yellow observations also, it is necessary to use the solution for darkening coefficient $x=0.6$ for the primary.

The elements as computed from the two curves were in rather close agreement. Since the geometrical elements such as the inclination and the ratio of the radii should have the same numerical values regardless of the wavelength in which they are observed, it is in order to try to find common values which will satisfy both curves; the relative brightnesses will of course be different in the two cases. Such a solution was found; the results are shown in Table III. The notation used is the standard one (Merrill 1950). Table IV gives the theoretical curve computed from this solution. For the entire curve, the probable error of an individual observation from the theoretical curve was $\pm 0\overset{\mathrm{m}}{.}009$ in both wavelength regions. Figure 1 shows the individual observations and the theoretical curve.

TABLE II. Minima of TZ CrA.

Obs. (hel) JD 24+	O—C	Epoch	Reference
17030.70	$-0\overset{\mathrm{d}}{.}28$	−27,738	Pickering, 1910 a, b
17684.80	+0.04	−26,786	Pickering, 1910 a, b
17728.72	−0.01	−26,722	Pickering, 1910 a, b
18145.57	0.00	−26,115	Pickering, 1910 a, b
24669.695	+0.005	−16,615	Payne-Gaposchkin, 1943
29115.018	−0.002	−10,142	Gaposchkin, 1953
36047.069	−0.001	−48	Wood
36080.034	0.000	0	Wood
36110.939	+0.001	+45	Wood

DETERMINACY OF THE ELEMENTS

It has been pointed out frequently that a solution is of limited value unless an idea is given of the precision with which the various elements are known. Because of the complexity of the functions involved, an attempt to do this merely by computing probable errors for the elements themselves is usually misleading. As Russell (1945) and others have emphasized, reliable information can best be conveyed by the publication of limiting values.

The possible sources of uncertainty are:

(1) The range of uncertainty in the rectification as determined by the precision and distribution of the observations, and by the presence and size of terms inexplicable by present theory.

(2) Uncertainty introduced by lack of knowledge of the precise degree of limb darkening.

(3) For any given limb darkening and rectification, uncertainties inherent in the solution; these depend on the precision and distribution of the observations and on the geometry of the eclipse.

TABLE III. Elements.

Epoch	JD 243 6080.034	
Period	$0\overset{\mathrm{d}}{.}68674954$	
k	0.708	
r_g	0.392	
r_s	0.278	
θ_e	$41\overset{\circ}{.}1$	
p_0	−0.810	
i	$80\overset{\circ}{.}4$	
z	0.042	
$\alpha_0{}^{oc}$	0.950	
$\alpha_0{}^{tr}$	0.902	
x	(assumed)	(0.6, 0.8)
	Yellow	Blue
$(1-l_0)^{tr}$	0.459	0.465
$(1-l_0)^{oc}$	0.070	0.058
L_g	0.926	0.939
L_s	0.074	0.061
J_g/J_s	5.8	7.1

(4) Failure of the model used to correspond to the real system. Probably the most serious danger here is the possibility of changes caused by the presence of streams or shells of gas surrounding the system, by bright or dark spots on the surface of the components, or by other intrinsic fluctuations in brightness.

In any particular case, each of these sources of error must be considered.

In the present case, the initial indication is that the uncertainty in rectification has but relatively small effect on the computed elements. The independent rectifications gave results contrary to theory, and there is only a narrow range of values of coefficients satisfactory to both colors. A more serious difficulty lies in the scarcity of observations near the quarter point between primary and secondary minima. This means, especially in the case of the coefficient of cos2θ, that the rectification is controlled chiefly by the observations in the maximum following secondary. If the system follows any conventional model this should make no difference, but there are many cases where differences at the quarter points do exist. A recent unpublished study by R. H. Koch of R Canis Majoris (A. J., in press) shows small but unmistakable differences; rectification by one gave a satisfactory solution while the other did not. It is clear, that because of the small values of the coefficients, no major changes in the elements will be caused by this uncertainty. The uncertainties in the computed radii of the components from this cause can scarcely be more than 0.01, and are probably less.

TABLE IV. Computed curve.

Phase	Yellow (C−V)	Blue (C−V)
$\pm 0^{d}.0000$	$-0^{m}.974$	$-0^{m}.586$
0.0092	−0.927	−0.548
0.0134	−0.882	−0.502
0.0195	−0.797	−0.415
0.0298	−0.645	−0.260
0.0349	−0.575	−0.189
0.0403	−0.509	−0.122
0.0525	−0.386	+0.003
0.0607	−0.330	+0.061
0.0773	−0.268	+0.122
0.0953	−0.259	+0.131
0.1145	−0.247	+0.143
0.1335	−0.239	+0.151
0.1526	−0.233	+0.157
0.1717	−0.229	+0.161
0.1908	−0.231	+0.159
0.2098	−0.235	+0.155
0.2289	−0.241	+0.149
0.2480	−0.250	+0.140
0.2661	−0.257	+0.132
0.2825	−0.273	+0.118
0.2900	−0.283	+0.110
0.3012	−0.303	+0.092
0.3064	−0.313	+0.084
0.3112	−0.322	+0.076
0.3217	−0.340	+0.061
0.3281	−0.349	+0.053
0.3325	−0.354	+0.049
0.3434	−0.359	+0.045

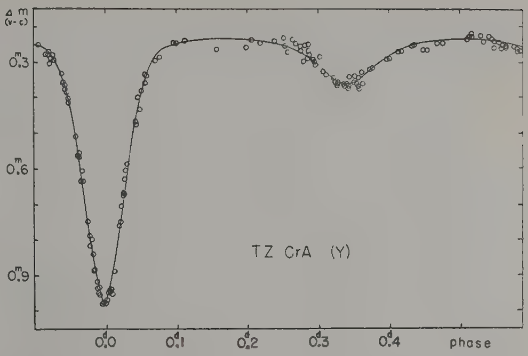

FIG. 1. Yellow observations and theoretical light curve.

From a partial eclipse of this nature, it is very difficult to derive a precise value of the limb darkening coefficient of either component, and values assumed from theoretical considerations must be used. The uncertainty introduced by lack of knowledge of the proper coefficient can be demonstrated by attempting solutions over a range of possible values, and determining what changes are thus introduced in the computed elements. In the case of the yellow curve, a solution assuming $x=0.4$ for the hotter, and 0.6 for the cooler component, gave $r_g=0.380$, $r_s=0.276$, and $i=80^{\circ}.8$; comparison with Table III shows that the maximum deviation in the computed radii is barely 3%. No satisfactory solution could be found with an assumed $x=0.8$; this is not surprising since both theory and reliable observed cases indicate lower values for a star of this color.

In the blue curve, an assumption of $x=0.8$ leads to a solution with computed values of $r_g=0.394$, $r_s=0.276$, and $i=80^{\circ}.3$. Again the differences are insignificant and it is clear that any conclusions on the general nature of the system will not be altered by uncertainty in the knowledge of the precise value of the limb darkening.

Even granted perfect rectification and precisely known limb darkening coefficient, the intrinsic scatter of even the best observations introduces uncertainty into the computed elements. This is clearly shown on the Merrill nomographs. Here the solution is found from the intersection of a line computed from the depths of minima and a curve determined by the shapes. In some cases two intersections occur and, especially in the case of shallow secondaries, real analytical indeterminacy may occur, and no method will distinguish between the two solutions. (An exception may occur when light curves in two colors are available; in this case, only one intersection, and hence one solution, may be common to both colors). The power of the nomographs lies in the fact that this situation is clearly and immediately shown; with the older methods, one solution may be found and labeled "the" solution, and the computer may remain unaware that the other possibility exists.

Because the observations are not infinitely accurate, we are not really dealing with lines, but rather with

TABLE V. L_1+L_2 as a function of k and p_0'
For this table $(1-l_0)^{oc}=0.072$, $(1-l_0)^{tr}=0.461$.

k	0.69	0.70	0.71	0.72	0.73
p_0					
−0.79	1.068	1.041	1.016	0.990	0.966
−0.80	1.062	1.035	1.009	0.983	0.959
−0.81	1.055	1.027	1.001	0.977	0.953
−0.82	1.048	1.021	0.995	0.970	0.946
−0.83	1.042	1.013	0.989	0.964	0.941

the intersection of two bands of finite width, and all that we can say is that the solutions lie within an area given by the intersection of the bands.

J. E. Merrill has suggested a method of demonstrating in tabular form the range of possibilities in any given case. From the observations we can determine limiting values for the shape curve and from the nomographs we can take limiting values of k and p_0. These in turn give definite values of α_0^{oc}, α_0^{tr}, and χ. With these and the observed depths we can compute L_s and L_g and tabulate their sum. But by definition the sum of these must be unity, and this condition enables us to see immediately from the table what the limiting values are. This is demonstrated in Table V where the values of depth used in Table III are used in conjunction with limiting values of k and p in the neighborhood of the intersection. As is easily seen, limiting values of k are 0.716 (for $p_0=-0.79$) and 0.705 (for $p_0=-0.83$); the value of k for any intermediate p_0 is easily read from the table. An objection to this method is that there is a finite uncertainty in the precision with which the depths are known. This is easily overcome by carrying out similar computations for the maximum and minimum depths permitted by the observations. The computations can be made rapidly, and demonstrate clearly the possible permitted ranges.

These are extreme limits and in many cases can be narrowed. Sometimes, certain values of the depths permitted by the observations will fall below the shape "band"—that is, below the largest value of χ permitted by the observations in the partial phases, and this will narrow the range of uncertainty. Furthermore, the shape functions depend chiefly on observations near two particular points, and it is entirely possible that the solution fit these and not be satisfactory elsewhere, particularly at the shoulders. The old and reliable criterion—the fit of the computed curve to the individual observations—must never be neglected, and this may well narrow further the permitted range. Finally, these elements must satisfy the observations in both wavelength bands, and also can narrow the range.

In the present case, consideration of the above gives limiting values of k and p_0. The largest and smallest values of the radii and inclination computed from these are

$$0.393>r_g>0.390; \qquad 0.279>r_s>0.277;$$
$$80\overset{\circ}{.}6>i>80\overset{\circ}{.}4.$$

These may be taken as limiting values inherent in the solution apart from questions of rectification and darkening. The extremely narrow limits arise from the fact that much of the range permitted by the yellow is ruled out by the blue and vice versa. This may be fortuitous but is more likely to be connected with the fact that any contribution to the light—or absorption of it—by circumstellar material or any intrinsic fluctuations, may not be precisely the same in two wavelengths.

Finally, we must consider the possibility that the actual systems may not correspond to the model adopted. Here the most serious danger is the addition of extra light by a faint companion, by bright nebular material in the field, or by a shell or stream of gas associated with the system itself, or by intrinsic changes in one of the components. Concerning the first two possibilities, all that can be said is that careful inspection on the best moonless nights showed no evidence of either; I estimate that under these conditions anything contributing as much as 1% to the total light would have been detected, unless it were an invisible companion too close to the variable to be separated. As for the latter possibilities, there is some evidence in the light curve which suggests that effects other than those included in eclipse theory may be operating.

Some of this is furnished by the observations on JD 2436039. Initially these lie well above the curve indicated by observations on other nights; then they descend to it, and finally increase again. The changes are of the order of a few hundredths of a magnitude and, on a smaller scale, resemble those occurring almost continuously in UX Mon. The tracings look good and give no reason for rejecting these observations. As added evidence, the latter half of the ascending branch of secondary, especially in the yellow, lies consistently below the computed curve; no theoretical curve consistent with the other observations can be made to fit these. This depends on observations on one night only; on this night the observations ran alternately below, above, and again below the theoretical curve. Something of this tendency is shown by other observations in secondary and in this part of the light curve, observations at the same phases on different nights do not agree precisely, especially in the yellow. The differences are small—of the general order of one or two hundredths of a magnitude—so it is not possible to reach a definite conclusion, but at least there is a possibility that a stream or shell of the same sort exists. In this case the asymmetry in secondary suggests that the stream is concentrated on the following side of the brighter component, and by absorption makes the egress longer than would be the case otherwise. On the other hand, the fact that satisfactory solutions with the same geometrical elements can be found in both blue and yellow suggests that any such complications are relatively minor.

An idea of just what uncertainties are introduced can be obtained by assuming an arbitrary amount of extra light and seeing what effect this has on the computed elements. The observations are "corrected" by the same method as that used when a faint companion has of necessity been included in the diaphragm. As an extreme case, I carried through a solution assuming that 5% of the total light of the system was introduced by an uneclipsed shell. Actually, I doubt very much if the contribution is nearly that great, but this will give a limit and illustrate the maximum size and the nature of the uncertainties thus introduced. Again, the nomographs rapidly illustrate the situation. The depth line slides upward and cuts the shape in two points. The value of r_g is almost the same in the two solutions (0.363 and 0.365), while in the first, $r_s=0.283$ and $i=79.^\circ9$. The second achieved almost the same effect in the light curve by a smaller secondary (0.256) and a higher inclination ($82.^\circ8$). However, while curves computed from these solutions of necessity fitted the observed curve at the two points on which the nomographs are based, the fit at the shoulders was very poor and could not be improved without causing similar departures elsewhere. The conclusion is that it is unlikely that the elements are altered in any significant manner by the existence of a shell at the epoch of observation.

The final conclusion, thus, is that the general nature of the system is rather precisely determined. Solutions using alternate rectifications and limb darkenings, indicate that r_g lies between 0.395 and 0.370, and r_s between 0.265 and 0.295. Actually, to find a really satisfactory fit to the observations at all phases, the limits must be even closer to the values listed in Table III.

DISCUSSION

We can now consider the nature of the system in so far as it can be deduced from observations made to date. The HD classification of A0 does not agree with that determined from color measures. Near the bottom of secondary, the smaller component contributes barely 1% of the total light, and the measured color is essentially that of the primary. Colors on the four nights when observations were made in this region give average values of $B-V$ (on the U, B, V system using conversion formulae determined by S. C. B. Gascoigne) of $+0.^m28$, $+0.^m27$, $+0.^m29$, and $+0.^m30$, respectively. The mean of these, $+0.^m285$, indicates a spectral class slightly earlier than F0 according to the table of Johnson and Morgan (1953). The extremely short period leaves little doubt that the luminosity class for each star is V. Pending further spectroscopic work, this classification will be adopted.

It is of course possible that the star is reddened by part or all of this amount. If reliable evidence later shows this to be the case, the following discussion can easily be repeated using a different mass and spectral class for the primary. That appreciable reddening is unlikely is indicated by a letter from A. R. Hogg, who states that John Whiteoak has inspected various Milky Way prints in the region and remarks, "it appears to be the same elsewhere along the ouside of the Milky Way proper in this general area," and adds that the region "looks very clear." The relative depths of the rectified minima can be used to estimate the spectrum of the fainter component using the method of Russell and Merrill. Essentially, this assumes gray-body theory, which "is probably as good a guide as is available" at present. In both colors, this leads to a spectrum of K0V, and this agreement increases confidence in the validity of the rectification.

In the absence of radial velocity measures, no measured values of the masses can be found. The light curve does give us, however, an indication of the mass ratio. From the coefficients of the rectification, the quantity z can be computed by any assumed limb darkening; z, the elipticity constant, is determined by the effect on the light curve caused by departure of the stars from spherical shape. It is found directly from the rectification after the influence of reflection, assumed limb darkening, and gravity effects are removed. In the case of TZ CrA, the rectification gives a value of $z=0.042$.

But if we knew in advance the shapes of the stars we could compute directly the numerical value of z. We do not know the shapes initially, but we do know that they depend on the sizes of the stars relative to their separation, on the mass ratio, and to a minor degree on the degree of central condensation (Russell 1948). The first of these quantities can easily be found from the solution for any given mass ratio. We can then assume different mass ratios, compute what the numerical value of z will be in each case, and compare these computed values with that determined from the light curve. The treatment is not absolutely rigorous, since the original determination of z from the rectification assumed similar ellipsoids, but for small coefficients the errors introduced are completely negligible.

The general trend can easily be predicted. For equal mass ratio, both components will be distorted with the larger component showing the greater distortion. With increasing mass ratio, the larger component will become more nearly spherical, and the less massive star will become more distorted. Because of the much greater contribution of the hotter star to the total light, the weighted mean z will decrease. Eventually, at very high ratios, the hotter star will have become so nearly spherical that assumed changes in mass ratio will no longer alter it appreciably, and z will increase for increases in mass ratio. Long before this point is reached, however, the secondary component will exceed its stability limits, so the case is of no practical value.

For TZ CrA, the computed values of z for various assumed mass ratios are

m_b/m_f	2	3	4	5
$\bar{z}$	0.080	0.062	0.051	0.039.

With the value of z computed from the light curve, this indicates a mass ratio of between 4.5 and 5.0. If both components were typical main sequence stars, according to Russell and Moore (1940), the radii should be proportional to the 0.70 power of the mass, and from the relative radii we compute a mass ratio of 1.6. From the mass-luminosity relation, using the appropriate bolometric corrections, we find $m_1/m_2=2.1$. The empirical values listed by Hynek (1951) lead to mass ratios of 1.9 using the computed magnitude difference from the solution and 2.1 from the relation between spectral class and mass using the spectral classes computed from the measured color and rectified depth of minima. These various determinations agree in indicating a mass ratio in the neighborhood of 2, and this is in sharp contrast with the value derived from the light curve.

It thus becomes important to examine the reliability of this value. The chief theoretical uncertainty is lack of knowledge of the precise value of the limb darkening. However, if this is assumed to be 0.8, the discrepancy becomes worse, whereas assumption of 0.4 leads to $z=0.051$ and a mass ratio which is still 4. Observationally, the weakest point is the lack of observations near first quarter. However, enough of these exist to show that the curve can scarcely be appreciably higher than at third quarter. Including all uncertainties, it seems that a mass ratio of less than 4 would call for a significantly larger coefficient of rectification, A_2, than is permitted by the observations.

We are thus left with a dilemma, but it is a familiar one. In many systems of what might well be called the R CMa type we find a secondary star much too bright for its mass. Frequently the primary is also overluminous; sometimes it is normal; in other systems the primary's mass is normal, but its radius is smaller than normal for its spectral type. (e.g., Struve 1948). It may be significant that in many cases the secondary is usually close to its stability limits. The same seems to be true here. For a mass ratio of 4, the radii of the fainter component are to first-order approximation $a_2=0.278$, $b_2=0.252$, $c_2=0.241$; for a mass ratio of 5 the values are $a_2=0.278$, $b_2=0.248$, $c_2=0.236$. If we consider the b axis, computation of the surface of zero relative velocity gives a limit of 0.257 for mass ratio 4, and 0.241 for mass ratio 5. Comparison of this with the b radius of the fainter component indicates instability would set in at mass ratio 4.5, or almost precisely the ratio to which we were led by consideration of the effects of the shapes of the stars on the light curves. To confirm this conclusion, a further check was made using the tables prepared by E. G. Reuning and J. E. Merrill. These treat the distorted star on the assumption of a polytropic model (rather than a point source) using the equilibrium considerations developed by Chandrasekhar (1933). These agree in showing the star within stability limits for a mass ratio of 4, but for a ratio of 5, equal or outside of them at the limits of the shorter equatorial and polar axes and at the Lagrangian point away from the hotter star.

In most systems of this type, the hotter component is not abnormal in mass for its spectral type. It is therefore in order to assume that this is the case for TZ CrA also, and see what further information can be gathered based on this assumption. We can also investigate the assumption that the primary component obeys the normal relation between luminosity and color.

The color measures, on Johnson and Morgan's standard main sequence diagram, lead to a value of $(M_v)_g=+2.5$. From the relative luminosities of the components in this spectral range, this leads to a value of $(M_v)_f=+5.2$. The color of this star cannot be measured directly, but the rectified minima correspond to a spectral class of K0 and thus to a color, $(B-V)=+0.82$. This and the M_v place the star slightly above the main sequence.

If the mass of the brighter component be taken as normal, Hynek's table indicates a mass of 1.9☉. With a mass ratio of 4.5, the fainter component would have a mass of only 0.42 solar masses—not an unusual value for this type of system. Then, from Kepler's third law, the distance between the centers may be computed as:

$$a=0.0202\ \text{a.u.}=4.34\text{R}_{\odot}.$$

The larger equatorial radius of the larger star is then 1.70☉, and of the smaller, 1.21☉. The densities are $\rho_b=0.38\odot$ and $\rho_f=0.24\odot$. With these radii, the visual, absolute magnitudes of the stars may be computed. In the case of the brighter component, using the effective temperature and bolometric correction indicated by the measured color, we get a value $M_v=+2.5$. This agrees with that taken from the color-magnitude diagram, and thus places the star on the main sequence.

If we use the depths of minima to compute spectral class and predicted color of secondary, and use its radius to compute its absolute magnitude, we get (as we should) agreement with that computed from the relative luminosities, +5.2. Using the computed color, we find this lies above the main sequence, and we have another case where the fainter component is overluminous for its mass.

Details of evolution of close binaries are as yet not completely understood. If the star formed initially as a normal K0 star, with the mass appropriate to this position in the main sequence, the mass ratio would have been approximately 2 and the star would have been within the stability surface. Even in this case, sufficiently violent ejection of material would eject it from the star and even from the system. The process might be very slow at first, but as the mass ratio increased the process would be accelerated. Thus the star could lose mass without awaiting slow evolutionary changes connected with hydrogen burning. Detailed calculations of the dynamics of the ejected material have been carried out by various authors (e.g., Gould, 1959); the only thing that concerns us here is that mass can be lost to the star.

The puzzling question is how it could do this without disturbing the balance in the interior. Huang (1956) has suggested that the star may eventually become a nova, but the details are not clear. One suggestion is that the process originally may have been very slow, but on nearing a critical limit accelerated rapidly so that the majority of the mass has been lost in a relatively short time. Shortly after this was written, D. C. Morton suggested at the 103rd meeting of the A.A.S. that mass transfer between the stars might happen fast enough so that there is a high probability that it would escape observation. A rough analogy is the loss of atmosphere by a planet where a relatively small change in the velocity of escape can have an extremely large effect on the length of time a planet can hold its atmosphere.

Various objections occur to the idea of a star's thus losing a relatively large portion of its mass, but we are still faced with the fact that we know of many close double star systems where the cooler component is definitely overluminous, and time after again in such systems this component is near the stability limit. In addition to spectrographic evidence, the erratic and relative sudden period changes—both lengthening and shortening—can be explained by just such ejection, and to date, no other satisfactory explanation has been suggested.

Still, the prospect of a star's losing a large part of its original mass without disturbing interior conditions presents difficulties. Erratic period changes caused by ejection of 10^{-7} stellar mass or less form a phenomenon on an entirely different scale of magnitude. To date, published work trying to solve the problem of evolution by transfer of mass from star to star has not met with conspicuous success. Because of the slowness of evolutionary changes for any but massive stars, it has been necessary to assume large initial masses. But the observed systems showing these anomalies are in general undermassive, and this means that up to 90% of the mass has been lost, with one component still remaining apparently normal. Further puzzles are presented by the fact that it is usually the less massive component which is found near the stability limit, and by the W UMa systems which frequently show mass ratios of 2:1 for components of comparable luminosity. A system like AO Cas may well be explained by normal evolution; here both components are O stars and the primary is near stability limits, but all the difficulties cited above appear when we try to apply this ideas to systems of lower mass.

One possibility is that the less massive component never formed as a normal star in the beginning. We may picture in the initial contraction stages two separate centers of higher than average density around which matter is condensing; each of the two initially is well within the central regions of the huge, tenuous proto-star. Actually, we can imagine more than two such centers, but such a situation would be dynamically unstable, and the additional centers would either combine or escape from the star until only two remained. We can think of these two centers as competing for the material in the proto-star as contraction proceeds, and then try to picture the result.

In the contraction stages, the more massive component probably preceded the secondary in forming as a star. By the time it was well condensed, its gravitational field would prevent material outside the zero-velocity surface from continuing to condense, and an appreciable part of the lighter star's mass would be attracted to the larger star or be lost to the system. In this case, the secondary will have less mass than it would have had, were it not for the presence of the primary, and the observed large mass ratios would result.

Very little is known about the initial process of contraction, so it is not possible to go further on firm evidence. If, however, the process before thermonuclear reactions started were such that the heavier elements tended to condense more rapidly, then the material stolen by the primary would be chiefly hydrogen and this would change the relative abundance of the material remaining to the secondary. The contraction centers themselves might even be chance associations of regions relatively rich in heavier elements and thus slightly denser than the average of the mixture. We can imagine a kind of cosmic race between the contracting secondary and the imaginary zero-velocity surface closing in on it as the primary became more and more condensed. Even if there were no concentration of heavier elements, certain of the atoms near this surface would escape because of their thermal motions, and of these, the lightest and fastest-moving would predominate. In this manner, from the same cloud, two stars with different abundance ratios could develop.

Enough is now known about stellar structure so that the general results can be predicted. The more massive star would settle down on the main sequence in a position appropriate to its mass and the normal composition of the interstellar medium at the time of its birth. The fainter component, with a higher concentration of helium and heavier elements would have a higher central temperature and greater luminosity than it would have had otherwise. It would fill precisely its stability limit because it would have been able to hold only the material within it. This would be a direct result of the conditions at the time it was formed, and not of later evolution.

As an illustration of the order of magnitude which may be expected from varying abundances, Schwarzschild (1958) has given computed changes in various stellar properties of late-type dwarfs based on assumed changes in hydrogen content. For the sun, a change of hydrogen content, from 0.8 to 0.6, leads to an increase in central temperature of ratio of 1.17. This corresponds to an increase of energy generation of nearly 1.9 even if the same nuclear processes prevail. Thus, the loss of any appreciable part of its hydrogen (relative to the other elements) would lead to a star, overluminous for its mass, and this is precisely what is observed in many cases of faint components of this type of eclipsing system.

We can carry the line of speculation a little further. If the original turbulent conditions were such that an appreciable fraction of the hydrogen were lost to the system, both components might be relatively poor in hydrogen and both overluminous. This is precisely what is observed in many cases. If, on the other hand, the primary captured enough hydrogen to alter its own abundance ratio, it would be below the position on the main sequence normal for its mass. It will appear in the general H—R diagram of the subdwarfs, but for quite different reasons, and hence it need not share the other properties or history of single subdwarfs.

More than ten years ago, Struve (1948) pointed out that just such a division did appear to occur for the A stars. Those with weak *Fe* II lines were usually smaller and hence fainter than average A stars, while these with stronger *Fe* II usually were more nearly normal in size. (To prevent any possible misunderstanding, I am not suggesting that weak *Fe* II lines necessarily indicate low iron content; this was simply the ionization feature used by Struve to separate the two groups.)

Thus, the abandonment of the assumption that the components of a double star must form at precisely the same time and be of precisely the same composition, leads to a possible interpretation of many of the problems connected with the strange mass-luminosity relations, and with the evolution, of close double stars. It is, of course, entirely possible that one reason why the interpretation fits so well is that, except for a few very general calculations, the discussion has been entirely qualitative. In particular, the details of the early contraction processes, even for single stars, are still not well known. These suggestions are made, not as answers to the various problems, but as the beginning of a road which may lead to answers.

One further implication is clear. This implies that the majority of eclipsing systems formed after an appreciable fraction of heavy elements existed in the interstellar medium. This in turn implies either that without heavy elements two contraction centers in the same photostar cannot occur, or that continual loss of mass over more than 10^9 years has caused at least one of the components to decrease in size until no detectable eclipse effects are shown. Either of these possibilities agrees with the observational fact that eclipsing systems are certainly very rare, and possibly entirely absent in globular clusters.

In summary, TZ CrA consists of a normal primary of spectral type late A or FO, and a late G or early K secondary which is overluminous for its mass. A radial velocity curve of this system would be extremely useful, but because of the short period it can be obtained only with a large telescope. However, even one spectogram could answer the questions of whether the spectral type obtained from the color measures the correct one.

ACKNOWLEDGMENTS

I am greatly indebted to the entire staff of the Mount Stromlo Observatory of the Australian National University for providing, maintaining, and sharing the equipment with which the observations were made. The work was made possible by a Fulbright award and a sabbatical leave.

I am indebted to Drs. R. H. Koch and L. Binnendijk for critical reading of the first typescript.

REFERENCES

Campbell, L., Popular Astron. **51,** 571 (1943).
Chandrasekhar, S., Monthly Notices Roy. Astron. Soc. **93,** 462 (1933).
Gaposchkin, S., Harvard Ann. **113,** (2) (1953).
Gascoigne, S. C. B. and E. J. Burr, Monthly Notices Roy. Astron. Soc. **116,** 571 (1956).
Gould, N. L., Astron. J. **64,** 136 (1959).
Huang, S. S., Astron. J. **61,** 49 (1956).
Hynek, J. A., *Astrophysics,* (McGraw-Hill Book Company, Inc., New York, 1951), Chap. 10.
Johnson, H. L. and W. W. Morgan, Astrophys. J. **117,** 313 (1953).
Merrill, J. E., Princeton Contr. 23 (1950).
——, Princeton Contr. 24 (1953).
Payne-Gaposchkin, C., Harvard Bull. **917,** 8 (1943).
——, Harvard Ann. **115,** 12 (1950).
Pickering, E. C., Harvard Circular **162,** 2 (1910); Astron. Nachtr. **186,** 317 (1910).
Russell, H. N., Astrophys. J. **102,** 8 (1945).
——, Astrophys. J. **108,** 388 (1948).
Russell, H. N. and J. E. Merrill, Princeton Contr. 26 (1952).
Russell, H. N. and C. E. Moore, *The Masses of the Stars* (University of Chicago Press, Chicago, Illinois, 1940).
Schwarzschild, M., *Structure and Evolution of the Stars* (Princeton University Press, Princeton, New Jersey, 1958), p. 139.
Struve, O., *Harvard Observatory Monograph* No. 7, (1948), pp. 211–230.

THE ASTRONOMICAL JOURNAL VOLUME 65, NUMBER 1276 FEBRUARY, 1960

An Observation Concerning Mean Radiant Paths of Photographic Meteor Showers*

FRANCES W. WRIGHT
Harvard College Observatory, Cambridge, Massachusetts

(Received August 13, 1959)

A survey of twelve meteor showers photographed at Harvard indicates that the sun is never more than a few degrees from the extended great circle through the mean daily path of radiant motion for the corresponding shower. When the earth takes some time in passing through the stream, the daily radiant seems to advance along a great circle path towards the position of the sun at the time of maximum shower activity. This observation can be explained if we assume that, when the earth encounters individual members of a meteor stream, the heliocentric velocity vectors of these individual members are approximately parallel. The observation can prove to be a convenient tool in the future whenever the data for a meteor shower are few or inaccurate.

INTRODUCTION

THE new observation presented in this paper, first reported in Wright (1958), is based on work by Whipple (1947), Whipple and Wright (1948, 1954, and 1957), Wright (1951), Wright and Whipple (1950, 1953), Wright, Jacchia, and Whipple (1954, 1956, and 1957), and is also supported by figures derived from a reanalysis of the Lyrids (Wright, Jacchia, and Boehm, this issue) in press. The pertinent data are presented in summary in Table I (a, b, c).

The first column of Table Ia gives the name of the shower; the second column shows the position of the radiant, corrected for zenith attraction and diurnal motion, of each shower, for the epoch 1950. The position is given in right ascension and declination for the time of maximum activity, for most of the showers. For three showers, which showed no particular maximum, designated by (mid), the table gives the position for the time near the midpoint of the shower. The third column gives the date of maximum activity in Universal Time, with the corresponding longitude of the sun in column (4), while column (5) shows the beginning and ending dates for each shower. Column (6) contains three velocities for each shower. V_∞ signifies the measured velocity corrected for atmospheric resistance; V_G is the geocentric velocity referred to the center of the earth after corrections are applied to V_∞ for the rotational and gravitational attraction of the earth. V_H is the heliocentric velocity after corrections are applied to V_G for the motion of the earth about the sun. In any one shower, each meteor has a velocity characteristic of its shower, and this is one of the criteria used to assign a meteor to its particular shower. Column (7) in Table Ib gives the average elongation for each shower, where elongation (λ) is defined as the angle between the apex of the earth's motion and the corrected radiant. In column (8), $\sin\gamma$ is defined by the relation: $\sin\gamma = (V_G/V_H)\sin\lambda$ (1954). Column (9) shows the duration, in days, of each meteor shower, while column (10) gives the streamwidth that Whipple and Wright (1954) obtained by applying the factor $\sin\gamma$ to the duration in days. Column (11) denotes the average deviation, in degrees, of an extended trail from the moving mean radiant. Column (12) shows the mean daily motion for each shower in minutes of arc, while column (13) gives the average inclination of each shower to the ecliptic. Finally, columns (14), (15), and (16) in Table Ic show the direction cosines λ, μ, ν of the pole of radiant motion for each of the twelve showers which have been completely analyzed.

Figures 1 and 2 picture the orbits of some of the double-station meteors of the twelve showers mentioned above, as well as of the Quadrantids and κ-Cygnids (partially analyzed at Harvard). The earth's orbit is indicated by "⊕", and the "○" on the meteor orbits marks that node which the earth intersects. Inspection of the orbits and of the inclination value "i", written close to the node's position, shows at a glance why the meteor showers of Fig. 1 are in general of shorter duration than those of Fig. 2, whose orbits show a tendency to spread like a fan at the intersection with the earth's orbit.

All of the meteor showers of Fig. 2 are of short period (3–8 years), with aphelia clustering around or near Jupiter's orbit (♃). The Geminids and Quadrantids are also of short period, the Geminids' periods being shortest of all—1.6 years. The Geminids' aphelia lie well within Jupiter's orbit and therefore far from the influence of Jupiter, which has perturbed the orbits shown in Fig. 2 through the years. The large inclination of the Quadrantids has probably kept them freer from perturbations by Jupiter, as compared with the orbits of Fig. 2, which, for the most part, have rather small inclinations. In general, the showers of Fig. 1 tend to lie near the lower end of the "Scatter vs streamwidth" curve of Wright, Jacchia and Whipple (1957).

In the long-period showers, Perseids, Leonids, Orionids, and Lyrids, the few short-period orbits shown in the drawing may be sporadic meteors which really do not belong to these respective showers; or they may be examples of the evolutionary process which over the

---

* These investigations were made possible by the support of a U. S. Air Force Contract, of the U. S. Army Office of Ordnance Research, and also research contracts with the U. S. Naval Bureau of Ordnance (Task I of NOrd 10449), and the U. S. Office of Naval Research.

TABLE Ia. Twelve meteor streams.

(1)	(2)		(3)	(4)	(5)	(6)		
	Corrected radiant (at max or midpoint) 1950					Velocities		
Meteor stream	α	δ	Date at max (UT 1950)	$\lambda_\odot$	Duration dates (U.T. 1950)	V_∞ km/sec	V_G km/sec	V_H km/sec
1. α-Capricornids	308°	−10°	Aug. 1(?)	129°.0	July 16–Aug. 21 (Several streams?)	25.5	23.0	37.4
2. So. δ-Aquarids	339°	−17°	July 30	126°.5	July 20–Aug. 10 or 16	43.0	41.5	37.4
3. No. δ-Aquarids	339°	−1°(mid.)	Aug. 5(mid.)	132°.5	July 14–Aug. 18	42.3	40.6	37.6
4. So. ι-Aquarids	338°	−14°	Aug. 8	135°.3	July 16–Aug. 25 or June 28–Aug. 25	35.8	33.8	37.9
5. No. ι-Aquarids	331°	−5°(mid.)	Aug. 5(mid.)	132°.5	July 16–Aug. 25 or July 16–Sept. 1	31.2	29.5	35.1
6. Perseids	46°	+58°	Aug. 12	139°.0	July 29–Aug. 24	60.4	59.3	41.3
7. Orionids	94°	+16°	Oct. 22	208°	Oct. 16–29	66.5	65.5	40.8
8. So. Taurids	51°	+14°	Nov. 1	218°.0	Oct. 27–Nov. 25	30.2	28.1	37.4
9. No. Taurids	56°	+22°(mid.)	Nov. 8(mid.)	225°.0	Oct. 16–Dec. 1	31.3	29.5	37.0
10. Leonids	152°	+22°	Nov. 17	233°.9	Nov. 15–20	72.0	70.8	41.5
11. Geminids	113°	+32°	Dec. 14	261°	Dec. 10–15	36.5	34.7	34.1
12. Lyrids	271°	+33°	April 22	31°.7	April 7–23	48.6	47.0	41.6

TABLE Ib. Twelve meteor streams.

(1)	(7)	(8)	(9)	(10)	(11)	(12)	(13)
Meteor stream	Elong. (λ)	$\sin \gamma$	Duration (days)	Streamwidth	Av. $\lvert O-C \rvert$	Daily motion	i
1. α-Capricornids	89°.9	0.61	37(?)	$22^{d}.6$	2°.11	52′	4°
2. So. δ-Aquarids	60°.9	0.97	22–28	$21^{d}.3$ or $27^{d}.2$	0°.80	50′	29°
3. No. δ-Aquarids	62°.4	0.96	36	$34^{d}.6$	1°.2	61′	20°
4. So. ι-Aquarids	73°.4	0.85	41–59	$34^{d}.8$ or $50^{d}.2$	1°.8	62′	6°
5. No. ι-Aquarids	73°.0	0.81	41–48	$33^{d}.2$ or $38^{d}.9$	1°.3	63′	5°
6. Perseids	39°.8	0.92	27	$24^{d}.8$	0°.68	44′	114°
7. Orionids	26°.1	0.71	14	$9^{d}.9$	0°.38	43′	164°
8. So. Taurids	80°.0	0.74	32	$23^{d}.7$	0°.57	35′	5°
9. No. Taurids	77°.1	0.78	47	$36^{d}.7$	1°.05	29′	3°
10. Leonids	10°.2	0.30	6	$1^{d}.8$	0°.22	46′	162°
11. Geminids	62°.8	0.90	6	$5^{d}.4$	0°.22	53′	24°
12. Lyrids	60°.4	0.98	17	$16^{d}.8$	0°.38	19′	80°

TABLE Ic. Direction cosines of pole of radiant path (1950 Equinox).

(1)	(14)	(15)	(16)
Meteor stream	λ	μ	ν
1. α-Capricornids	+0.13301	−0.11130	+0.98485
2. So. δ-Aquarids	+0.19225	−0.28882	+0.93788
3. No. δ-Aquarids	−0.06796	−0.20839	+0.97568
4. So. ι-Aquarids	+0.14320	−0.28034	+0.94916
5. No. ι-Aquarids	+0.03212	−0.15023	+0.98813
6. Perseids	−0.45625	−0.71997	+0.52295
7. Orionids	+0.26358	−0.24473	+0.93308
8. So. Taurids	−0.04679	−0.26989	+0.96175
9. No. Taurids	+0.00211	−0.44232	+0.89686
10. Leonids	+0.04021	−0.61660	+0.78625
11. Geminids	+0.17829	−0.50577	+0.84404
12. Lyrids	+0.54557	−0.45362	−0.70469

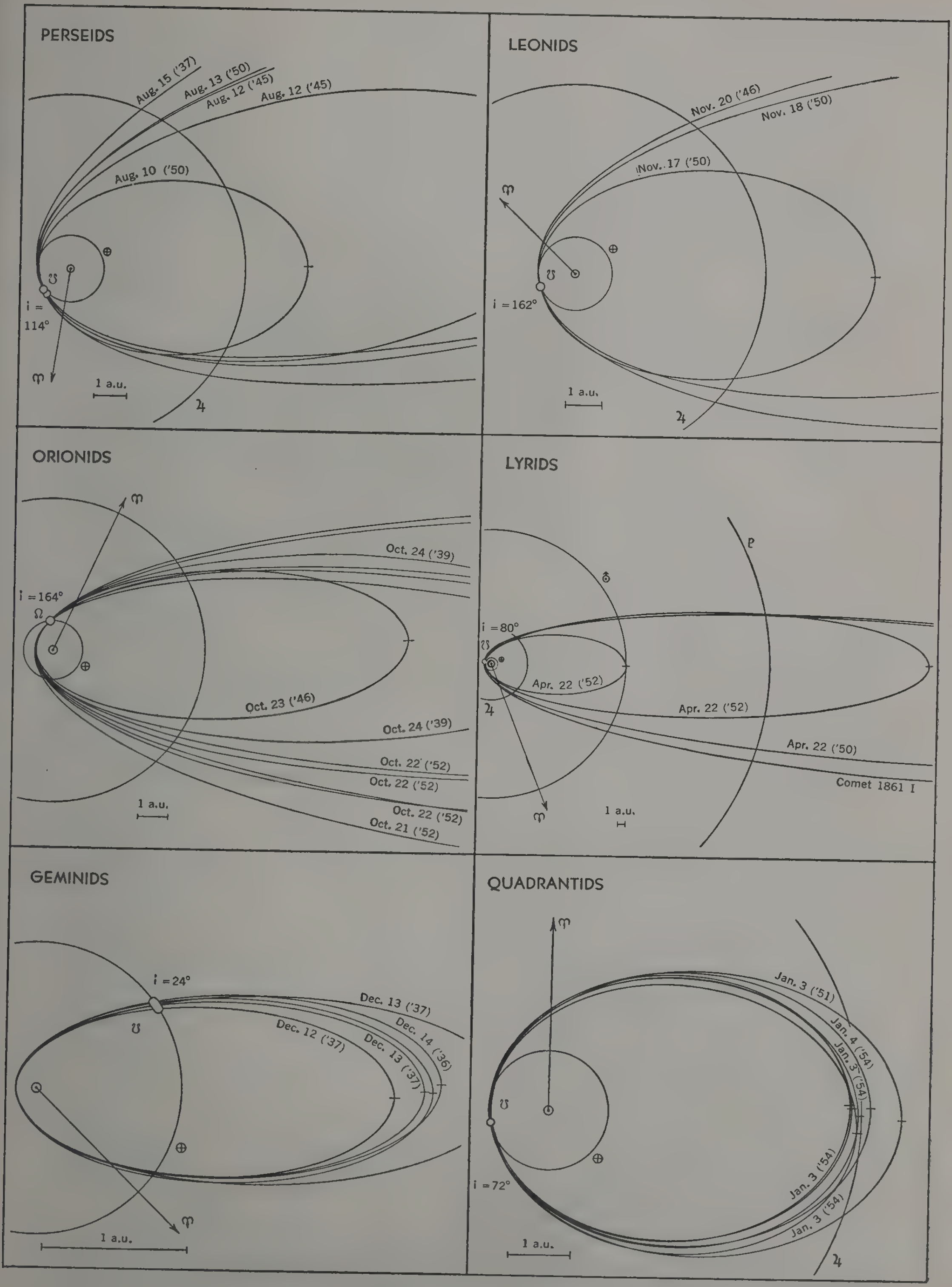

FIG. 1. Meteor orbits of 6 showers.

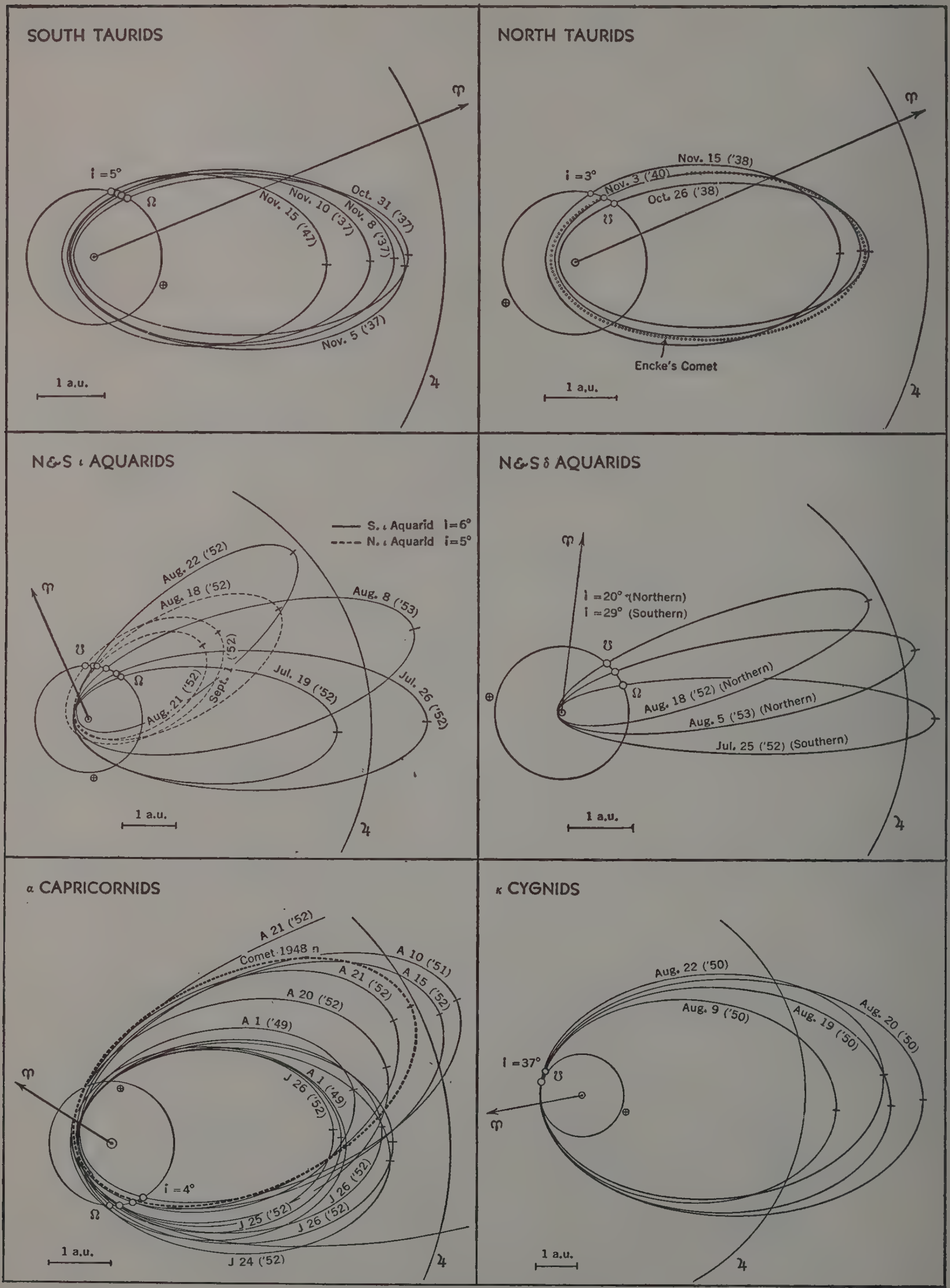

SOUTH TAURIDS

NORTH TAURIDS

N&S ι AQUARIDS

N&S δ AQUARIDS

α CAPRICORNIDS

κ CYGNIDS

Fig. 2. Meteor orbits of 8 showers.

years tends to reduce long-period to short-period orbits, with aphelia close to Jupiter, since the latter planet, the largest in the solar system, plays the greatest role in perturbing meteors.

As shown in Fig. 3, the fourteen meteor showers of Figs. 1 and 2 also fit very well the "cometary-meteor" branch of the velocity-elongation diagram of Whipple and Hughes (1955). It is also evident, from Fig. 3, that with the exception of the Leonids, Orionids, and Perseids, the apparent elongation (or the angle between the apex of the earth's motion and the corrected radiant) for any of the above shower meteors lies between the range 60°–94°, a conclusion that agrees with the results of Whipple and Hughes (1955), Astapovich (1939), and Levin (1950) for meteors in general. The Perseids, Orionids, and Leonids have smaller apparent elongations because of their much greater values of V_∞, as shown in Table Ia.

For all fourteen showers, with the exception of some of the Geminids, the author has measured and reduced all the single-station meteor trails and all the double-station trails that have not been used for orbit determination. The investigation has included a special study of the daily motion of the mean radiant for each of the twelve showers completely analyzed and of the "scatter" for each shower—the distance of each extended meteor trail from the mean radiant of the instant.

The techniques used are those described by Whipple and Wright (1957) which were developed for the rapid analysis of single-station photographs of meteor trails used in determining the nature of shower radiants. The measurements were made graphically on Durchmusterung star charts, and were reduced with the use of direction cosines. For each meteor trail, the computations included the direction cosines of the pole of the great circle path through four or five points on the meteor trail. Finally, the mean radiant path for each meteor shower was obtained.

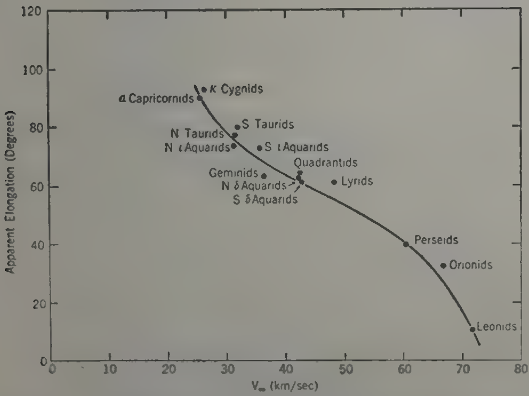

Fig. 3. Correlation between velocity and elongation for 14 meteor showers.

Table II. Best radiant paths.

Shower	Distance ⊙ to rad. path	$\lambda_\odot$	Dur. (days)	No. of meteors Dbl.	No. of meteors Single
So. δ-Aquarids	1°	122°		5	26
	0°	126°(max)	22–28		
	3°	132°			
So. ι-Aquarids	3°	115°	41–59		
	1°	135°(max)		6	15
	4°	150°			
Perseids	3°	130°	27	9	49
	2°	139°(max)			
	6°	144°			
So. Taurids	3°	218°(max)	32	8	31
	4°	226°			
	5°	238°			
No. Taurids	1°	203°	47	3	19
	2°	228°(near middle)			
	3°	248°			
Geminids	5°	256°	6	5	38
	6°	261°(max)			
	8°	271°			

DIRECTION OF MEAN DAILY RADIANT PATH

A survey of the twelve mean daily paths of the radiants which were plotted on a 10-in. radius globe suggested that the mean radiant path for each shower seemed to lie in the direction of the position of the sun on the globe at time of maximum shower activity. In order to test this apparent correlation the author selected three points on the mean radiant path of each shower, one point near the time of maximum activity, a second at a time preceeding, and the third at a time following the more exact point of maximum activity. Direction cosines were used to compute the distance of the sun from the mean radiant path for these three times in each shower.

Table II gives the best radiant paths, derived for the best-determined showers, while Table III gives radiant paths which may be less accurate, or only approximate, for showers that may be less well determined. In both tables, showers are listed in order of increasing longitude of the sun.

The first column designates the shower; the second column shows the angular distances of the sun from the extended great-circle path of the mean radiant for three different times in each shower, while the third column gives the longitude of the sun at the time of the corresponding distance. The time of maximum activity is indicated for each shower, except for three showers without definite maximum activity, for which the sun's longitude near the midpoint of the shower appears. The duration in days is repeated in the fourth column for comparison purposes. The last column for each shower indicates the number of double-station ("dbl.") meteors, and also the number of single-station

TABLE III. Approximate radiant paths.

Shower	Distance ⊙ to rad. path	$\lambda_\odot$	Dur. (days)	No. of meteors Dbl.	Single
Lyrids	19°	17°	17	6	14
	7°	30°			
	6°	31° (max)			
No. δ-Aquarids	12°	112°	36	11	2
	11°	132° (near middle)			
	10°	146°			
No. ι-Aquarids	12°	118°	41–48	3	24
	9°	135° (near middle)			
	5°	152°			
α-Capricornids	10°	121°	37?	12	50
	8°	129° (max)			
		several streams (?)			
	2°	148°			
Orionids	17°	202°	14	3	22
	18°	207° (max)			
	18°	210°			
Leonids	10°	233.5°	6	6	20
	10°	234° (max)			
	11°	238°			

("single") meteors upon which the analysis of each shower was based.

The approximate radiant paths of Table III may not be as well determined as the radiant paths in Table II for two reasons: (1) the determinations of the radiant path either depended on fewer meteors, or the duration of each shower was shorter. The North δ-Aquarids, for instance, depended for their solution on only thirteen meteors, and this fact might well explain the greater distances of the sun from the extended mean radiant path. Both the North δ-Aquarids and the North ι-Aquarids have no pronounced maximum activity at all, and the maximum activity of the North ι-Aquarids may well be past the middle of the shower, as shown in Table III. If any maximum activity exists at all for the North ι-Aquarids, the time near the end of the shower is indicated. Analysis of the α-Capricornids was based upon many meteors, but this is an "impure" shower and there is uncertainty as to whether we have one big meteor shower here or two or three smaller showers instead. If the latter is true, the durations of the individual showers are shorter, and the two or three radiant paths may be poorly determined. For the Orionids, the scarcity of double-station meteors combined with the shorter duration could explain the greater distance of 18°. In the case of the Leonids, the extremely short duration, compared with the durations of most of the other showers, could cause the fairly large distance of 10°. There is some uncertainty in the duration of the Lyrids. The Quadrantids have such a short duration that probably no daily radiant motion will be derived. For all of the twelve photographic meteor showers completely analyzed, and also for the Quadrantids and the κ-Cygnids, the distance of the sun from the radiant path ranges from about 80°–170°.

The following explanation for the motion of the radiant was suggested by Richard B. Southworth.

It can be shown that when the earth encounters some members of a meteor stream, if the heliocentric velocity vectors of the individual shower-members are parallel, then the radiant moves toward the position of the sun.

Let $\mathbf{V}_H$ be the heliocentric velocity of an individual meteor encountered by the earth at the time, and let $\mathbf{V}_G$ be its geocentric velocity, if we neglect the earth's attraction. Let $\mathbf{V}_E$ represent the velocity of the earth. Let the braces $\{\ \}$ denote a unit vector, and hence let $\{R\}$ denote the unit vector in the direction of the radiant. Let $\{S\}$ represent a unit vector directed from the earth to the sun.

Take

$$d\mathbf{V}_H/dt=0. \tag{1}$$

We wish to show that $d\{R\}/dt$ is directed toward the sun.

Let the unit of time be $365\frac{1}{4}/2\pi$ days, and the unit of absolute magnitude of velocity be V_E. Then,

$$d\mathbf{V}_E/dt=\{S\} \tag{2}$$

and Fig. 4,

$$\mathbf{V}_G=\mathbf{V}_H-\mathbf{V}_E. \tag{3}$$

Hence, if we take derivatives with respect to the time t,

$$d\mathbf{V}_G/dt=-\{S\}, \tag{4}$$

from (1) and (2).

Now,

$$\{R\}=-\mathbf{V}_G/V_G \tag{5}$$

from definition of $\{R\}$, the radiant being, of course, the direction from which the meteors approach the earth.

If we take the derivative of (5) with respect to t,

$$d\{R\}/dt=[V_G\{S\}+\mathbf{V}_G(dV_G/dt)]/V_G^2 \tag{6}$$

$$=[\{S\}/V_G]+[\mathbf{V}_G(dV_G/dt)/V_G^2] \tag{7}$$

$$=[\{S\}/V_G]-[\{R\}(dV_G/dt)/V_G] \tag{8}$$

from (5).

The last term in this expression (8) does not alter the direction of the radiant and therefore the direction of motion of the radiant is toward the position of the sun at the time.

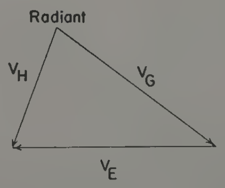

FIG. 4. Vector diagram of meteor velocities.

As a corollary of this theorem, if the heliocentric velocity vectors of individual meteors of a stream are nearly parallel, then the radiant moves in a direction *close* to that of the sun at the time.

It seems to follow quite logically, then, that the mean radiant paths of the twelve meteor showers of Table I lie in a direction approximately towards the position of the sun, since the velocity vectors of the individual members seem to be nearly parallel. Divergence from parallelism could, of course, be the cause of the larger distances, of the sun from the radiant path, which are given in Table III.

This newly observed relation of the sun to the extended mean daily radiant path of a meteor shower may well prove a most convenient tool in the future. If the time of maximum of any shower is known, and if one has at hand some accurately determined radiants at time of maximum (from double-station meteors), the mean radiant path can be determined quickly and fairly accurately as the great circle through the position of the sun at this time, and through an accurate determination of the radiant at maximum. Finally, in cases of uncertain maximum activity as with both streams of ι-Aquarids, the Northern Taurids, and the Northern δ-Aquarids, this new criterion aids in fixing the time of a possible maximum. Already this new method has helped to clarify the problem of the mean daily path for the κ-Cygnids and for another meteor shower—the η-Eridanids, discovered by Whipple (1947, unpublished). At the time of discovery, the more north-south direction indicated for the mean daily radiant path was quite at variance with the daily path which we had obtained for other meteor showers. By chance, these ran more parallel to the ecliptic. Since we had no double-station meteors to support the results, and no known certain velocities of this new shower, the results for the daily path were laid aside temporarily. Now, with this recently observed relation between the position of the sun and the mean radiant of the shower at maximum activity, we feel much more certain that the mean radiant path obtained in 1947 was correct. This new relationship will be useful also in radio astronomy, as applied to meteors, where the accuracy of radiant determination cannot be as great as in photographic work.

TABLE IV. Daytime η-Arietids.

1951	Weighted mean radiant R.A.	Dec.	Shower maximum June 12, 1951
May 30	39.8°	+21.4°	
June 8	43.7°	+24.5°	R.A. Sun 79.4°
June 18	47.6°	+27.3°	Dec. Sun +23.1°

An example appears with the η-Arietids (Hawkins and Almond, 1952). Table IV shows the predicted mean radiant as determined from radio observations. Since the sun is almost due east of the radiant path near the maximum of the shower, an easterly direction for the mean radiant path rather than a northeast direction is indicated.

Many more and fainter meteor showers will doubtless be discovered through radio astronomy techniques. To identify members of a single shower, the velocity must be known, and the extended meteor trail must be near the mean radiant path at the moment. We may now add the criterion that the mean radiant path should be directed towards the position of the sun at the time of maximum activity for the relevant shower, or to within a few degrees of this position.

REFERENCES

Astapovich, I. S., Astron. J. Soviet Union, **16**, 6 (1939).
Hawkins, G. S. and M. Almond, Astron. Contr. Univ. Manchester, Series 1, (1952); Jodrell Bank Ann. **1**, No. 1.
Levin, B. U., Meteoritika **7**, 113 (1950).
Whipple, F. L., Proc. Am. Phil. Soc. **91**, No. 2 (1947).
——, and R. F. Hughes, J. Atmosph. Terr. Phys., Special Supplement **2** (1955).
Whipple, F. L. and F. W. Wright, Astron. J. **54**, 54 (1948).
——, Monthly Notices Roy. Astron. Soc. **114**, 229 (1954).
——, Smithsonian Contr. Astrophys. **1**, 239 (1957).
Wright, F. W., Harvard Reprint Ser. **II-38** (1951).
——, 1958, Ph.D. Thesis, Radcliffe College.
Wright, Jacchia, and Whipple, Astron. J. **59**, 400 (1954).
——, Astron. J. **61**, 61 (1956).
——, Astron. J. **62**, 225 (1957).
Wright, Jacchia, and Boehm, Astron. J. (in press).
——, and Whipple, F. L. 1950, Harvard Reprint Ser. **II-35** (1950).
——, *ibid.* No. **47** (1953).

THE ASTRONOMICAL JOURNAL VOLUME 65, NUMBER 1276 FEBRUARY, 1960

Photographic Lyrid Meteors

FRANCES W. WRIGHT, LUIGI G. JACCHIA, AND BARRY W. BOEHM
Harvard College Observatory, Cambridge, Massachusetts

(Received September 1, 1959)

This analysis shows that the mean radiant path of the photographic Lyrids has a daily motion of 16′ eastward and 10′ northward with respect to the equator in the interval from April 7 through April 23 UT The mean deviation of an extended meteor trail from the mean moving radiant is ±23′. This value is in general agreement with the relation between meteor stream widths and radiant deviations which was derived for eleven other photographic streams.

At the time of maximum activity of the Lyrids, on April 22 UT, the sun is only 6° from the extended mean radiant path. This agrees with a recent observation by one of us that the sun is never more than a few degrees from the extended mean radiant path of a meteor shower near the time of maximum activity.

THIS paper gives an analysis of all possible photographic Lyrid meteors found on Harvard plates during the interval from April 7 through April 23 for the years 1940–1955.

THE ORBITS

We have made complete reductions for six doubly-photographed Lyrids, and the data are presented in Table I. The arguments of this table are in large measure self-explanatory and follow previous usage (Wright and Whipple 1953; Wright, Jacchia and Whipple 1956; Wright, Jacchia, and Whipple 1957). V_∞ is the meteor velocity outside the earth's atmosphere; V_G the geocentric velocity; and V_H the heliocentric velocity. Angle Q is the apparent dihedral angle between the great circles of the two photographs, while Z_R is the zenith-distance of the radiant. The length of the trail is that from the Doña Ana station and, in parenthesis, from the Soledad station. The perihelion distance is indicated by q, and aphelion distance by q'. The elongation is that of the corrected radiant from the apex of the earth's motion at the time. The quality classification, *A*, *B*, or *C*, for the older meteors, indicates the degree of known or suspected errors. *A* denotes the most perfect examples, with minimum errors. *B* determinations are somewhat less certain, and *C* is a poor determination. For the meteors photographed more recently, quality 1 corresponds approximately to *A*, 2 to *B*, and 3 to *C*. Meteor No. 1922, however, has a well determined radiant.

Figure 1 shows the orbits of five Lyrids, and of Comet 1861 I. The orbits are drawn on the plane of the ecliptic without correction for foreshortening. The close relationship between the Lyrids and Comet 1861 I, as established by Pape (1861), Weiss (1867), and Galle (1867) is well brought out by a comparison of Oppolzer's (1864) orbital elements of the comet, as shown in Table II, with the mean of the elements of the Lyrids from Table I.

MEAN RADIANT AND ITS MOTION (FIRST SOLUTION)

The methods used to determine the mean radiant and its motion are essentially those described by Whipple and Wright (1957). Most of the 424 meteor trails photographed in this region at Harvard were at once eliminated from the Lyrids after a plot on a globe showed that they were further than 10° from the tentative radiant at the corresponding instant. We also rejected meteors with a velocity which differed by more than 15% from that indicated by the accurate double-station meteors.

The position $\alpha=270°12'$, $\delta=+33°06'$ (equinox 1950.0) was adopted as the assumed radiant. We applied the usual corrections for zenith attraction and diurnal motion, using techniques discussed in detail by Whipple and Wright (1957). We adopted 48.6 as the mean V_∞. In the rectangular coordinate system with origin at the assumed radiant, we used the formula: $\Delta x=\Delta\alpha\cos\delta$ and $\Delta y=\Delta\delta$.

Our final least-squares solution included the six double-station meteors of Table I, and only those other meteors which were most certainly Lyrids, with $X \sin\psi<3°$. These 14 meteor trails were listed in Table III as "probable members." Four double-station meteors, in rows 2 and 3, 6 and 7, 8 and 9, and 12 and 13, were treated as single-station meteors; hence there are ten distinct meteors in the first part of this list. The entries of Table III are the same as those of Table III in Wright, Jacchia, and Whipple (1956). The two "possible members" are undoubtedly Lyrids, but were not included in the least-squares solution. The velocity of the first one is not known.

The first solution for the mean corrected radiant motion, in terms of x and y coordinates referred to the assumed radiant path, gave the following results, where t is the longitude of the sun.

$$x=+41'.9+16'.1(t-30^\circ.68),$$
$$\pm 1'.6$$
$$y=+13'.6\pm 10'.0(t-30^\circ.68)$$
$$\pm 1'.6.$$

Hence, the total daily motion of the radiant is 19′ The probable deviation of a single extended great circle from the mean radiant at the instant is 22′. The path

TABLE I. Double-Station Lyrids.

eteor No.	10531	1922	1998	3271	3217	1065
r., Mo.	'54 Apr.	'50 Apr.	'50 Apr.	'52 Apr.	'52 Apr.	'41 Apr.
T	7.46231	21.37	22.37	22.35236	22.43214	23.32
un's Longitude	17°.0	30°.7	31°.7	32°.1	32°.2	32°.9
pp. Rad. α (1950.0)	267.4	270.4	272.8	271.7	271.6	273.6
pp. Rad. δ (1950.0)	31.0	+32.9	+33.2	+33.4	+33.2	+33.6
orr. α (1950.0)	267.0	270.4	272.2	271.9	271.3	273.3
orr. δ (1950.0)	+31.0	+33.0	+33.4	+33.5	+33.3	+33.5
uality Class	1	C	A	1.5	2	A
$_\infty$ (km/sec)	51.07	47.8	48.7	47.37	48.04	48.8
$_G$ (km/sec)	49.78	46.3	47.2	45.83	46.67	47.4
$_H$ (km/sec)	41.80	41.2	41.8	40.93	41.65	41.9
beg. (km)	108.9	103.6	102.5	105.7	106.7	110.8
mag. (km)	99.5	84.6	84.6	92.1	100.2	86.5
end (km)	85.0	80.4	83.1	85.3	92.5	67.6
in Q	0.333	0.265	0.179	0.330	0.451	0.774
os Z_R	0.982	0.858	0.862	0.824	0.983	0.956
ength of Trail	8°.0 (8°.2)	9°.6	7°.5 (7°.7)	10°.7 (11°.7)	4°.2 (3°.8)	4°.0
o. Breaks	29–27	16–20	17–25	28–29	16–17	10–19
uration (sec)	0.48	0.57	0.47	0.52	0.30	0.95
ass (gm)	0.0174	0.27	0.27	0.032	0.010	4.1
bs. pg. mag. (max)	−0.9	−3.3	−3.4	−1.5	−0.6	−7.3
	208°.3	216°.3	213°.1	215°.0	215°.2	212°.2
1950.0	17.0	30.7	31.7	32.1	32.2	32.9
	86.1	79.0	80.2	78.5	79.1	80.4
$=\omega+\Omega$	225.3	247.0	244.8	247.1	247.4	245.1
/(1/a) (a.u.)	39.3	12.7	56.2	10.12	31.64	207
	0.976	0.928	0.983	0.909	0.971	0.996
	0.942	0.911	0.985	0.919	0.915	0.928
	77.7	24.5	111.	19.32	62.36	413
longation	56°.9	61°.1	61°.0	61°.3	61°.5	60°.8
esidual	9′.8	23′.3	27′.9	12′.7	12′.9	50′.3
(corrected)	−162′.8	+11′.7	+101′.1	+85′.1	+53′.5	+155′.9
x Residual ($O-C$)	+15′.4	−30′.3	+43′.4	+20′.0	−12′.9	+78′.5
(corrected)	−123′.5	−6′.9	+17′.0	+26′.7	+13′.3	+26′.3
y Residual ($O-C$)	−0′.9	−20′.6	−06′.4	−01′.3	−15′.5	−09′.3

f this mean radiant is about 56° north of the ecliptic, nd the plane of the path has an inclination of about 0°. Table IV lists the data for the Lyrid moving rad- ant.

The mean length of trail for nine other photographic eteor showers was 6°.5, and the ratio "mean length/ istance" was 0.15. The corresponding figures for the yrids are in close agreement.

The residuals of individual meteors from the moving adiant are indicated graphically in Fig. 2, where the rdinate is declination, and the abscissa, right ascen- ion. A point represents the nearest point of the ex- ended great circle of each meteor trail to the calculated ean radiant of the instant. A line joins this nearest oint to the mean radiant; hence the great circle for ach trail is perpendicular to this joining line. Double ircles represent the radiants of the double-station eteors of Table I, while lines connect each of these ouble circles to the mean moving radiant of the nstant. The lengths of all lines from the points to the orresponding radiant of the instant represent graphi- ally the $O-C$ residuals obtained from the least-squares solution. The deviation of ±23′ (average $O-C$) of an extended meteor for the Lyrids, and the corresponding values of 17 days for duration and 16.8 days for streamwidth is in general agreement with the relation between meteor streamwidths and radiant deviations which was derived for eleven other photographic streams (Whipple and Wright 1954).

Figure 3 shows the daily frequency of the Lyrids. The predicted mean radiant as a function of date, for this first solution, is given in Table V. The theoretical values of δ are explained under "Discussion."

Some question may arise as to the identification of the April 7 double-station meteor as a Lyrid. As stated above, we included it on the basis of its velocity and orbit. Unfortunately, no certain photographic Lyrids appeared between April 7 and April 20. One of the "possible Lyrids" in Table III might fall in this interval. It is our opinion that an outlying member of a meteor stream, such as the April 7 meteor, may sometimes be photographed even when similar early members are not observed visually. Far from maximum activity, identity is more difficult to establish visually.

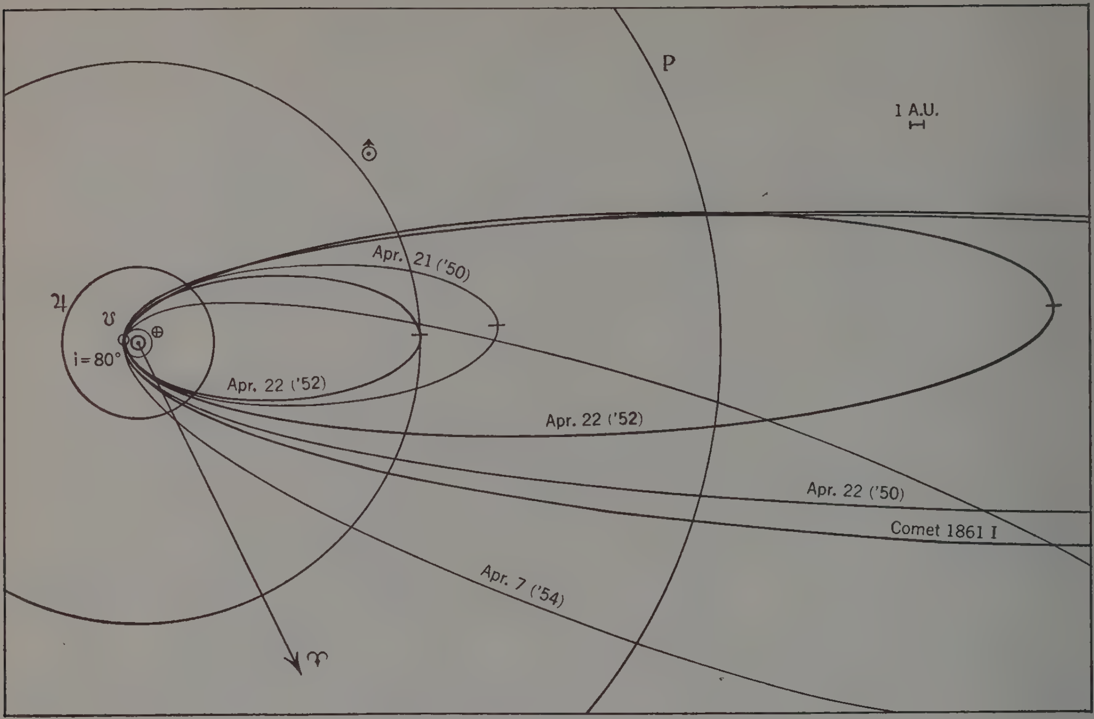

Fig. 1. Orbits of 4 Lyrids and Comet 1861 I.

Some of the earliest visual observations of the Lyrids are around April 12. Hoffmeister (1948) gave April 12–24, (1903–38) as the duration of the Lyrids. Bakharev (1953) reported an hourly rate of 3 meteors on April 15 and 7 on April 18. Olivier (1929) has reported observations of the Lyrids between April 18–26. Both R. Rigollet (1949) and Lovell (1954) have described the past history of the Lyrids. According to the latter, Prentice (1930) refers to the discrepancy between observations of the 1922 Lyrids in Britain and in Greece. The hourly rate in Great Britain was 0.5 to 3, while in Greece, H. N. Russell reported an hourly rate of 96 on April 21, 1922. These figures echo some of the ancient displays of the Lyrids, including the last great shower in 1803, when Herrick's count gives an hourly rate of 668. Prentice concludes that the rich portion of the shower must be extremely narrow. Certainly the poor visual displays since 1803, with the one exception of observations in Greece in 1922, account for the small number of Lyrids photographed in this century.

Table II. Comparison of orbital elements.

T	Comet 1861 I (Oppolzer) June 3.3899		Lyrids (mean)	
V_∞ km/sec	48.6		48.6	
ω	213°.4		213°.4	
Ω	29.9	1861	29.4	1950
i	79.8		80.6	
π	243°.4		242°.8	
1/(1/a) (a.u.)	55.7		23.3	
e	0.983		0.96	
q	0.921		0.933	
q'	111.		118.	

MEAN RADIANT AND ITS MOTION (SECOND SOLUTION)

A second least-squares solution, with the same assumed radiant, but without the April 7 meteor, gave the following results:

$$x=+18'.9+40'.8(t-30^\circ.68),$$
$$\pm 6'.6$$
$$y=+17'.5+6'.0(t-30^\circ.68).$$
$$\pm 6'.9.$$

The corrected radiant here is $\alpha=270°34'.5$, $\delta=+33°23'.5$, and the daily motion of the mean radiant for this solution is 44′. The probable errors for the daily motion in this second solution are larger, because of the smaller interval considered. The probable deviation of a single extended great circle from the mean radiant at the instant is 20′.

Since most of these meteors occur in a 3-day interval, the motion of the radiant remains poorly determined unless we assume that the April 7 Lyrid is genuine, and has its radiant near the mean radiant path.

TABLE III. Lyrids, positions and residuals for single-station meteors.

Plate ser.	Year	Date UT April	Long. ⊙	La.	Lc	l	Dist.	Pole of trail (1950.0) λ	μ	ν	cosχ	X sinχ	Δx	Δy	Δ	O—C
								Probable members								
FA	50	20.18	29°53	F	F	5°	43°	+0.93671	+0.17400	+0.30381	+0.348	−0.023	+75′	−33′	−20′	−42′
SL	50	21.36	30.40	F	f+	3°	24°	−0.15008	+0.53832	+0.82927	−0.989	+0.001	+5	+5	+1	+6
SK	50	21.36	30.40	F	f+	5°	43°	−0.10855	+0.54139	+0.83374	−0.994	+0.107	+5	+5	+1	+8
FA	55	21.30	30.62	M	M	10°	29°	+0.89592	+0.24767	+0.36877	+0.442	+0.003	+26	+1	+36	−7
KF	50	21.36	30.68	B	B	10°	33°	−0.77313	+0.34321	+0.53337	−0.636	+0.002	+3	+5	+5	−19
SL	53	21.41	30.95	M	f	2°	33°	−0.02953	+0.54466	+0.83814	−1.000	+0.001	−13	+4	0	+15
ST	53	21.41	30.95	M	f	2°	30°	−0.54211	+0.46896	+0.69728	−0.841	−0.014	−13	+4	−57	−69
SL	53	21.43	30.97	M	f	2°	29°	+0.49696	+0.49357	+0.71375	+0.867	+0.022	−19	+3	+69	+32
ST	53	21.43	30.97	M	f	2°	18°	+0.09916	+0.55021	+0.82911	+0.995	+0.008	−19	+3	+28	+7
ST	52	22.22	31.98	B	F	*15°	85°	+0.37393	+0.52106	+0.76725	+0.927	−0.016	+60	−17	+63	+15
ST	52	22.28	32.05	B	F	8°	52°	−0.36373	+0.49974	+0.78610	−0.932	+0.010	+35	+1	+45	+47
FA	52	22.40	32.16	M	M	6°	48°	−0.84553	+0.28792	+0.44965	−0.536	+0.002	−10	+5	−4	−44
AI	52	22.40	32.16	M	M	5°	52°	−0.92837	+0.18988	+0.31950	−0.373	+0.013	−9	+5	+34	−16
ST	52	22.44	32.21	B	F	4°	27°	+0.83675	+0.32109	+0.44357	+0.545	+0.024	−23	+2	+65	−6
								Possible members								
BM[a]	40	15.28	25°29	F	F	7°	35°	−0.45836	+0.44413	+0.76984	−0.888	+0.047	+5′	+5′	+160′	−188′
AI	41	22.35	31.94	F	F	4°	52°	+0.98988	+0.10861	+0.09141	+0.134	+0.038	−23	+2	+108	+43

[a] Velocity unkown.

DISCUSSION

For eleven other photographic meteor showers, Wright (in press) observed that at time of maximum activity for a shower, the sun is never more than a few degrees from the extended great circle through the mean daily path of radiant motion. Computed distances of the sun, by use of direction cosines, show that on April 21.0 UT, for our first solution above, the sun is 6°8 from the extended mean radiant path for the Lyrids. On April 22 the solar distance is 6°. Thus, the Lyrids provide supporting evidence for the observation, which holds for eleven other photographic meteor streams; the observation itself provides evidence that our first solution is more probable than our second.

In accordance with the theory of this observation, we next derived the pole of the great circle through the Lyrid radiant at shower maximum (approximately the same for both solutions) and the position of the sun at this time ($\lambda_{\odot}=31.7°$). This pole is at $\alpha=132°58'$; $\delta=+48°29'$. The equation of the great circle of radiant motion, in terms of the direction cosines of its pole, is convenient for the determination of theoretical values of the declination of the mean radiant as given numerically in Table V, and indicated by Δ in Fig. 2. These theoretical values seem to give the best mean radiant path. This path is close to the one derived from the first solution, and further from the radiant path derived from the second solution. For this second solution, on April 21.0, the sun is 15.5° from the mean extended path of this solution, and on April 22.0, the solar distance is 16.3°.

CONCLUSION

Either solution gives general agreement with the relation between meteor streamwidths and radiant deviations, and good agreement with the recent observation in regard to the position of the sun with respect to the mean radiant path near the time of maximum shower activity. The latter observation favors the first solution presented in the foregoing and can improve the first solution because of the scarcity of early Lyrids.

TABLE IV. Corrected radiant (1950.0) at maximum.

Mean long. of sun (1950)	31°7
Corr. α	271° 21′
Corr. δ	+33° 30′
Δα cosδ (per day)	+16′±1.6′
Δδ (per day)	+10′±1.6′
Total motion (per day)	+19′
P.E. residual (O—C)	22′
Mean length of trail	6°4
Mean dist. from radiant	40°
Mean length/distance	0.16

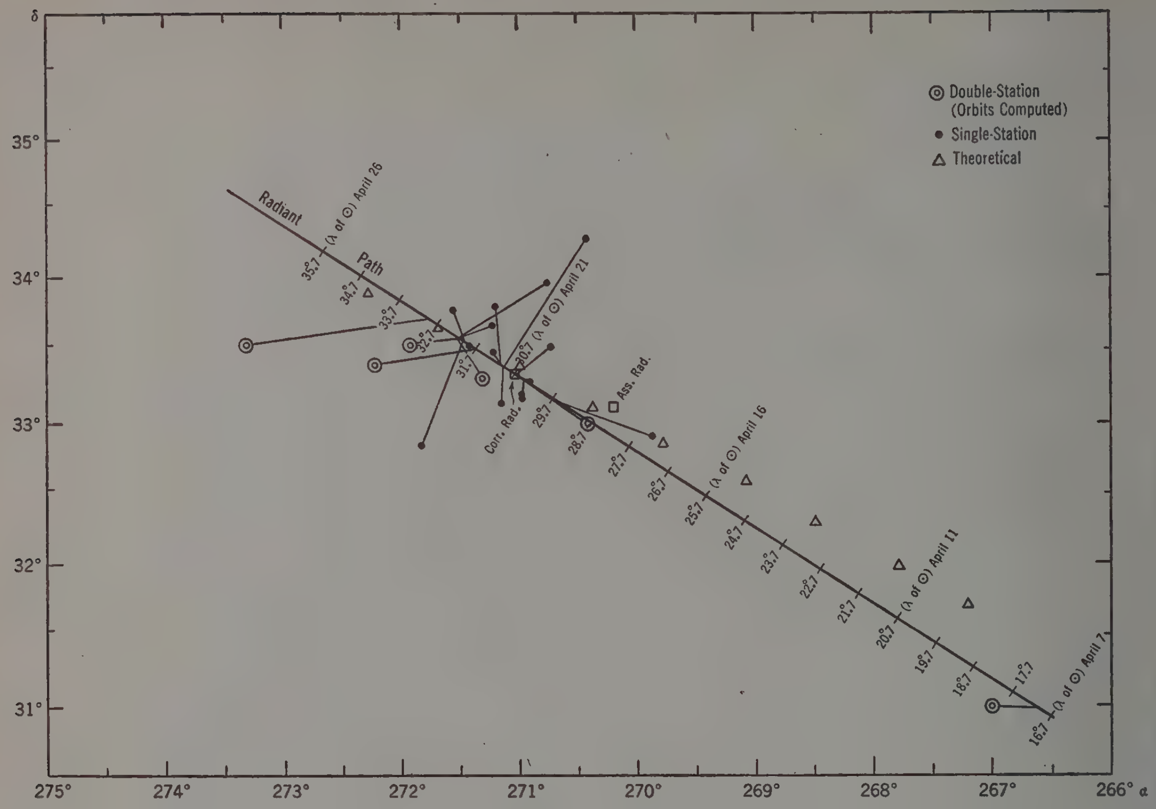

FIG. 2. Photographic radiant path.

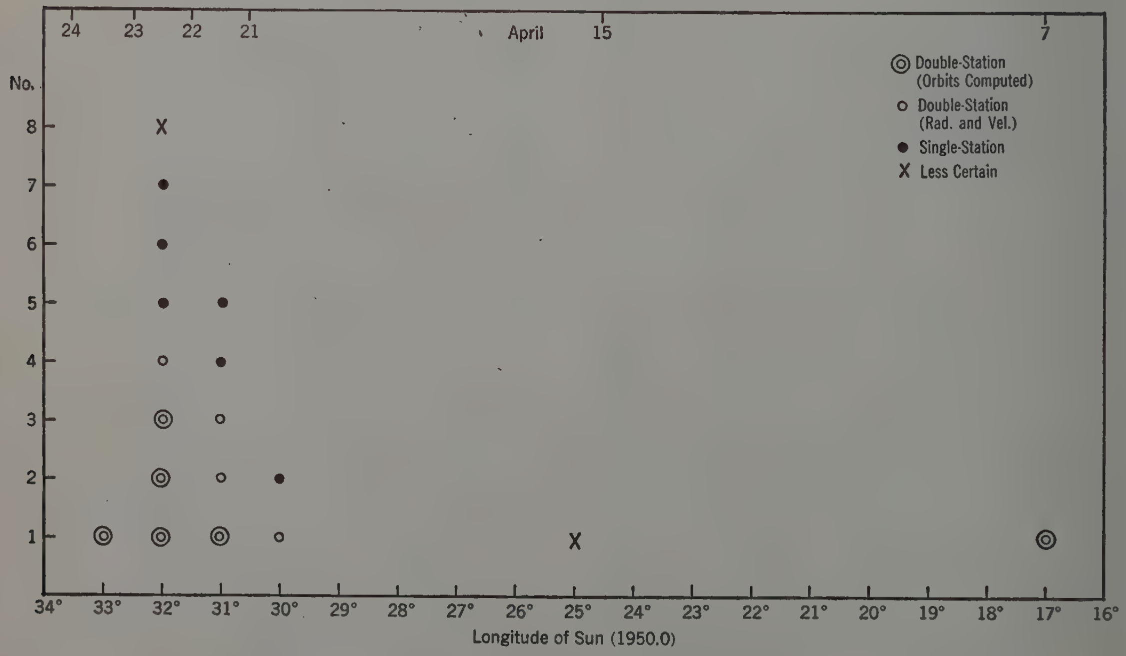

FIG. 3. Frequency of Lyrids.

TABLE V. Predicted corrected mean radiant of the Lyrids. (1950.0)

Date UT	Long.	α (1950)	δ (Obs.)	δ (Theoret.)
April 9	18°.7	267° 12′	+31° 20′	+31° 42′
April 11	20.7	267 50	+31 40	+31 59
April 13	22.7	268 28	+32 00	+32 16
April 15	24.7	269 06	+32 20	+32 33
April 17	26.7	269 45	+32 40	+32 50
April 19	28.7	270 23	+33 00	+33 06
April 21	30.7	271 02	+33 20	+33 22
April 23	32.7	271 40	+33 40	+33 38
April 25	34.7	272 19	+34 00	+33 53

This investigation was supported by a U. S. Air Force contract, and by the U. S. Army Office of Ordnance Research. The double-station meteors were photographed by Harry J. Emerson, Edward A. Horine, Elmore D. Mayhew, Gunther Schwartz and Robert C. Wells. Hai Rhee assisted with general computing. The computers for the double-station orbits were Robert E. Briggs, Jeannie R. B. Carmichael, Gilbert F. Davoren, Patricia Y. Dettmer, Elaine M. Guinee, John J. Murphy, Richard B. Southworth, and June R. Wessel under the direction of Jacchia. Boehm did the preliminary work and search for all possible Lyrids. Wright measured and reduced the meteors of Table III, and made the final analysis.

REFERENCES

Bakharev, A. M., Astron. Tsirk, Acad. Sci. Tajik S.S.R. No. 138 (1953).

Galle, J. G., Astron. Nachr. **69**, 34 (1867).

Hoffmeister, C. *Meteorströme* (Verlag Werden und Wirken, Weimar, Germany, 1948).

Lovell, A. C. B., *Meteor Astronomy* (Clarendon Press, Oxford, England, 1954).

Olivier, C. P., Publication of the Leander McCormick Obs. of the University of Virginia V, (1929), Part I.

Oppolzer, T., Astron. Nachr. **62**, 187 (1864).

Pape, C. F., Astron. Nachr. **55**, 253 (1861).

Prentice, J. P. M., J. Brit. Astron. Assoc. **40**, 137 (1930).

Rigollet, R., *Documentation of Observers* (Institut. d'Astrophysique de Paris, 1949), Bull. No. 5.

Weiss, E., Astron. Nachr. **68**, 381 (1867).

Whipple, F. L. and F. W. Wright, Monthly Notices Roy. Astron. Soc. **114**, 230 (1954).

Whipple, F. L. and F. W. Wright, Smithsonian Contrib. Astrophys. **1**, 239 (1957).

Wright, F. W., Astron. J. **65**, 33 (1960).

Wright, Jacchia, and Whipple, Astron. J. **61**, 61 (1956).

Wright, Jacchia, and Whipple, Astron. J. **62**, 225 (1957).

Wright, F. W., and F. L. Whipple, Harvard Reprint Ser. **II-47**, 33 (1953).

THE ASTRONOMICAL JOURNAL VOLUME 65, NUMBER 1276 FEBRUARY, 1960

Time Derivatives of the Components of Proper Motions of Stars

PAUL KUSTAANHEIMO

Astronomical Observatory, Helsinki, Finland

(Received August 10, 1959)

The rates of change with time in the spherical components of the constant motion of a star are deduced by means of direct projection on the local coordinate base vectors. In many textbooks on spherical astronomy these formulae are given incorrectly.

BEMPORAD (1937) has called attention to a certain inconsistency occurring in the textbooks on spherical astronomy of Newcomb (1906) and Smart (1931) for the case where the difference is deduced between the components of the proper motion of a star at different epochs, but referred to the same equatorial system. In these deductions, the influence of the radial velocity of the star is neglected. However, this influence is of the same order as the whole change of the components.

The deduction of Newcomb (1906) and Smart (1931) is repeated in the books of Andoyer (1911), de Ball (1912), Becker (1934), Schaub, (1950) and Smart (1956). However, in exercise 7 on p. 276 of Smart (1956), the correct formulae are given. The other textbooks on spherical astronomy, e.g., those of Åkesson, Brünnow, Campbell, Chauvenet, Heiskanen, Herr and Tinter, Ivanov, Nassau, and Schalén, do not treat the time derivatives of the components of proper motion.

The general error mentioned in the foregoing seems to be caused by a paper of Bessel (1844) in which, on p. 147, the term $\dot{r}r^{-1}$ is omitted because "eine Änderung von r ein unbedeutendes Verhältniss zu r selbst hat." Already Seeliger (1900), p. 70, has called attention to this omission.

By using vector methods (cf. Kustaanheimo 1959), the time derivatives of the components of proper motion can be deduced very simply in the following way.

Let $\mathbf{R}$ be the vector from the observer to the star. We assume that the space-velocity $\partial\mathbf{R}/\partial t$ is constant; $\partial^2\mathbf{R}/\partial t^2=0$. Let further $\mathbf{P}$ be the unit vector pointing from the observer towards the celestial north pole. The equatorial reference system is assumed to be at rest; $\partial\mathbf{P}/\partial t=0$. Thus, the equatorial spherical coordinates of the star, α and δ, are changed by the proper motion caused by $\partial\mathbf{R}/\partial t$ only.

Now we have

$$\mathbf{P}\cdot\mathbf{R}=r\sin\delta \tag{1}$$

$$|\,\mathbf{P}\times\mathbf{R}\,|=r\cos\delta, \tag{2}$$

where $r=|\,\mathbf{R}\,|$ is the distance of the star. Thus,

$$\mathbf{e}_r=\mathbf{R}r^{-1} \tag{3}$$

$$\mathbf{e}_\alpha=\mathbf{P}\times\mathbf{R}r^{-1}\sec\delta \tag{4}$$

$$\mathbf{e}_\delta=\mathbf{e}_r\times\mathbf{e}_\alpha=\mathbf{P}\sec\delta-\mathbf{R}r^{-1}\tan\delta \tag{5}$$

are those three mutually orthogonal unit vectors that form the local coordinate basis belonging to the apparent position of the star on the celestial unit sphere.

The linear components of $\partial\mathbf{R}/\partial t$ with reference to (3)–(5) are

$$(\partial\mathbf{R}/\partial t)\cdot\mathbf{e}_r=\dot{r}=\mathbf{R}\cdot(\partial\mathbf{R}/\partial t)r^{-1} \tag{6}$$

$$(\partial\mathbf{R}/\partial t)\cdot\mathbf{e}_\alpha=\dot{\alpha}r\cos\delta=\mathbf{P}\cdot\mathbf{R}\times(\partial\mathbf{R}/\partial t)r^{-1}\sec\delta \tag{7}$$

$$(\partial\mathbf{R}/\partial t)\cdot\mathbf{e}_\delta=\dot{\delta}r=\mathbf{P}\cdot(\partial\mathbf{R}/\partial t)\sec\delta-\dot{r}\tan\delta \tag{8}$$

where $\dot{\alpha}$ and $\dot{\delta}$ are the spherical components of the proper motion (generally denoted by μ_α and μ_δ, but here expressed in radians per time), and $\dot{r}$ is the radial velocity.

The components (6)–(8) satisfy

$$\dot{r}^2+\dot{\alpha}^2r^2\cos^2\delta+\dot{\delta}^2r^2=(\partial\mathbf{R}/\partial t)\cdot(\partial\mathbf{R}/\partial t)=\text{const.} \tag{9}$$

The variations of $\dot{r}$, $\dot{\alpha}$, and $\dot{\delta}$ with the time, i.e., $\ddot{r}$, $\ddot{\alpha}$, and $\partial^2\delta/\partial t^2$, are obtained when differentiating (6)–(8):

$$\begin{aligned}\ddot{r}&=(\partial\mathbf{R}/\partial t)\cdot(\partial\mathbf{R}/\partial t)r^{-1}-\mathbf{R}\cdot(\partial\mathbf{R}/\partial t)r^{-2}\dot{r}\\&=\dot{\alpha}^2r\cos^2\delta+\dot{\delta}^2r\end{aligned} \tag{10}$$

$$\begin{aligned}&\ddot{\alpha}r\cos\delta+\dot{\alpha}\dot{r}\cos\delta-\dot{\alpha}\dot{\delta}r\sin\delta\\&\quad=-\mathbf{P}\cdot\mathbf{R}\times(\partial\mathbf{R}/\partial t)r^{-2}\dot{r}\sec\delta\\&\quad+\mathbf{P}\cdot\mathbf{R}\times(\partial\mathbf{R}/\partial t)\dot{\delta}r^{-1}\sec^2\delta\sin\delta\\&\quad=-\dot{\alpha}\dot{r}\cos\delta+\dot{\alpha}\dot{\delta}r\sin\delta\end{aligned} \tag{11}$$

$$\begin{aligned}&(\partial^2\delta/\partial t^2)r+\dot{\delta}\dot{r}\\&\quad=\mathbf{P}\cdot(\partial\mathbf{R}/\partial t)\dot{\delta}\sec^2\delta\sin\delta-\ddot{r}\tan\delta-\dot{r}\dot{\delta}-\dot{r}\dot{\delta}\tan^2\delta\\&\quad=-\dot{\alpha}^2r\sin\delta\cos\delta-\dot{r}\dot{\delta}.\end{aligned} \tag{12}$$

Thus we have finally

$$\ddot{r}=\dot{\alpha}^2r\cos^2\delta+\dot{\delta}^2r \tag{13}$$

$$\ddot{\alpha}=2\dot{\alpha}\dot{\delta}\tan\delta-2\dot{\alpha}\dot{r}r^{-1} \tag{14}$$

$$\partial^2\delta/\partial t^2=-\dot{\alpha}^2\sin\delta\cos\delta-2\dot{\delta}\dot{r}r^{-1}. \tag{15}$$

The differentiation of (9) gives a certain check: (13)–(15) must satisfy

$$\dot{r}\ddot{r}+\dot{\alpha}\ddot{\alpha}r^2\cos^2\delta+\dot{\delta}(\partial^2\delta/\partial t^2)r^2+\dot{\alpha}^2r\dot{r}\cos^2\delta$$
$$+\dot{\delta}^2r\dot{r}-\dot{\alpha}^2r^2\dot{\delta}\sin\delta\cos\delta=0. \quad (16)$$

REFERENCES

Andoyer, H., *Cours d'astronomie* I (Hermann et Fils, Paris, France, 1911), 2nd ed.

Ball, L. de, *Lehrbuch der sphärischen Astronomie* (Engelmann, Leipzig, Germany, 1912).

Becker, F., *Grundriss der sphärischen und praktischen Astronomie* (Dümmler, Berlin, Germany, 1934).

Bemporad, G., *Pub. Oss. Astron. Torino* **32**, (1937).

Bessel, F. W., *A. N.* **22**, 145 (1844).

Kustaanheimo, P. "On vector methods in spherical astronomy", reprint Astron. Obs. Helsinki, 1959.

Newcomb, S., *A Compendium of Spherical Astronomy* (Macmillan and Company, New York, 1906).

Schaub, W., *Vorlesungen über sphärische Astronomie* (Geest & Portig, Leipzig, Germany, 1950).

Seeliger, H., A. N. **154**, 65 (1900).

Smart, W. M., *Text-book on Spherical Astronomy* (Cambridge University Press, England, 1931).

Smart, W. M., *Text-book on Spherical Astronomy* (Cambridge University Press, England, 1956), 4th ed.